

Current Status in the Utilization of Biobased Polymers for 3D Printing Process: A Systematic Review of the Materials, Processes, and Challenges

Mahdiyar Shahbazi* and Henry Jäger*



Cite This: <https://dx.doi.org/10.1021/acsabm.0c01379>



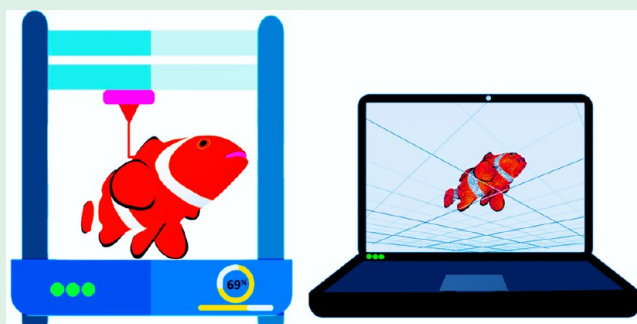
Read Online

ACCESS |

Metrics & More

Article Recommendations

ABSTRACT: Three-dimensional (3D) printing is a revolutionary additive manufacturing technique that allows rapid prototyping of objects with intricate architectures. This Review covers the recent state-of-the-art of biopolymers (protein and carbohydrate-based materials) application in pharmaceutical, bioengineering, and food printing and main reinforcement approaches of biomacromolecular structure for the development of 3D constructs. Some perspectives and main important limitations with the biomaterials utilization for advanced 3D printing procedures are also provided. Because of the improved the ink's flow behavior and enhance the mechanical strength of resulting printed architectures, biopolymers are the most used materials for 3D printing applications. Biobased polymers by taking advantage of modifying the ink viscosity could improve the resolution of deposited layers, printing precision, and consequently, develop well-defined geometries. In this regard, the rheological properties of printable biopolymeric-based inks and factors affecting ink flow behavior related to structural properties of printed constructs are discussed. On the basis of successful applications of biopolymers in 3D printing, it is suggested that other biomacromolecules and nanoparticles combined with the matrix can be introduced into the ink dispersions to enhance the multifunctionality of 3D structures. Furthermore, tuning the biopolymer's structural properties offers the most common and essential approach to attain the printed architectures with precisely tailored geometry. We finish the Review by giving a viewpoint of the upcoming 3D printing process and recognize some of the existing bottlenecks facing the blossoming 3D pharmaceutical, bioengineering, and food printing applications.



KEYWORDS: biomaterials, additive manufacturing, bioengineering, food printing, printability, rheological properties, shape fidelity, chemical cross-linking

1. INTRODUCTION

There is increased attention to fabricate robust smart objects aimed at a variety of pharmaceutical, food, and bioengineering sectors. Three-dimensional (3D) printing is a revolutionary and cutting-edge additive manufacturing method for the fabrication of complex architectures with unique structures and diverse properties.^{1–4} The 3D printing process with using CAD software, generating an STL (stereolithography, entitled after Charles Hull's SLA method) file format that offers for the design of virtual constructs and the control of the nozzle and stage of 3D printer.^{5–7} The 3D printing technique is commonly more cost-efficient and faster than traditional formative techniques. Developments in the 3D printing process enable manufacturing companies to enlarge from design the 3D printed prototypes to the quick manufacturing of end-products. The 3D printing offers exclusive features for industry including minimized decentralized manufacturing and inventories, in which the custom-designed objects are developed when and where they are required. Some of the printing machines present in the market

are included fused direct ink write (DIW) and deposition modeling (FDM) for extrusion processes. Powder bed fusion (PBF) and selective laser sintering (SLS) are applied for processing, which requires a laser to treat or fuse polymeric materials. Inkjet printers also use irradiation to photopolymerize ink solution/suspension into complex objects.^{3,8}

This technique is extensively utilized in pharmaceutical, bioengineering, and food applications because of numerous benefits, including the production of small batches of medicines with customized designs, simplifying the supply chain, and widening of the available product.^{1,2,7,9} The production of 3D

Received: October 24, 2020

Accepted: December 8, 2020

Table 1. Examples of 3D Printing Methods Employed for Pharmaceutical and Bioengineering Applications

technology	biodegradable polymer	other excipients (binder, stabilizer, etc.)	active ingredients/cells	application	ref
SLS	β -cyclodextrin/mannitol	candurin; kollidon VA64; Gold Sheen	ondansetron	personalized medicine	39
	hydroxypropyl methylcellulose	candurin; Gold Sheen	paracetamol	personalized medicine	40
	polycaprolactone		progesterone	drug delivery system	41
	polycaprolactone		ibuprofen	bone regeneration	42
FDM	polyvinyl alcohol	triethyl citrate; talc	budesonide; eudragit L100	controlled-release dosage	43
	hydroxypropyl cellulose	barium sulfate	domperidone	drug delivery system	44
	polyvinyl alcohol		aminosalicylate (5-ASA, 4-ASA)	personalized medicine	45
	microcrystalline cellulose	eudragit EPO; talc; tricalcium phosphate	5-ASA; captopril; theophylline; prednisolone	personalized medicine	46
extrusion (room temperature)	hydroxypropyl methylcellulose	microcrystalline cellulose; lactose; polyvinylpyrrolidone	dipyridamole	drug delivery system	47
binder jet	hydroxypropyl cellulose/ethylcellulose	polyvinylpyrrolidone K30	acetaminophen	controlled-release dosage	48
	polycaprolactone	polyethylene glycol	methylene blue; alizarin yellow	drug delivery system	49
(laser) bioprinting	sodium alginate	gelatin	NIH 3T3 mouse fibroblast	cell printing	50
	hyaluronic acid	hydroxyapatite	adipose-derived mesenchymal stem cells	tissue engineering	51
	collagen	alginate	osteoblast-like cells; human adipose-derived stem cells	tissue engineering	52

printed medicines and printed functional organs may finally result in the theory of personalized medicines and the reconstructing of an entire organ becoming a reality. Although additive manufacturing is extremely favorable to improve the patient-centered dosage forms, some challenges, such as printability, resolution, cost of the techniques, etc., must be addressed before application for personalized medicine. Regarding the food industry, it has started a revolution in food processing, where 3D printed food products are manufactured by a specific printer to tailor a healthy diet for population groups with specific needs.^{5,8,10}

The effective uses of additive manufacturing to create the 3D structures are mainly reliant on the improvement of printable ink dispersions. A biopolymeric ink must show shear-thinning, viscoelastic, and thixotropic features to avoid rising difficulty in the printing process with a large degree of cross-linking capacities permitting for the tuned polymeric ink to maintain the 3D architectures after printing.^{11,12} When polymeric inks are exposed to constant stress, their bonds can be depolymerized, resulting in a weak mechanical property and losing structural integrity. Most inks intrinsically do not possess suitable flow behavior to print. Then, it is essential to attain appropriate rheological properties by introducing specific biobased polymers to widen the scope of 3D printing applications.^{13,14} Supramolecular polymers dramatically affect the flow behavior of ink-based dispersion even though present at low concentrations. The primary purpose behind the extensive use of biopolymers in 3D printing is their ability to improve the dispersion stability and flow behavior of inks, as well as thermal, mechanical, and structural properties of printed constructs.^{7,15–18} Biomacromolecules are commonly a heterogeneous group of high-molecular-weight biopolymers (proteins and polysaccharides) obtained from animal, bacterial, plants, and algae-based sources. The existence of a large number of hydrophilic groups remarkably enhances their affinity for water binding, producing viscous dispersions and forming hydrogels. The flow behavior of ink

usually changes with concentration, temperature, and deformation rate in a complex way dependent on the specific biopolymer and the existence of other components in the systems. Therefore, the introduction of supramolecular biopolymers potentially increases the fabrication speed of printable inks, contributing to a tunable surface structure, and imparts desired mechanical features of 3D printed constructs through reinforcement of interlayer adhesion and inducing self-assembled supramolecular structures.^{7,19–22} The neat biopolymers, however, have commonly poorer rheological features and weak mechanical strength than those of synthetic polymers, which consequently limit their printability.^{17,23–25} Nevertheless, tuning the functional properties of biopolymers remains challenging, needing modifications to attain the desired tailored geometries after the printing process. To make biobased polymers more suitable to apply in the printing process, they can be modified through photo-cross-linking,¹² chemical,²³ enzymatic,²⁶ and ionic cross-linking treatments²⁷ to allow the biomaterials to be cured upon the 3D printing process. Hence, the reinforcement of biopolymeric structure followed by a 3D printing process is poised to open innovative prospects in additive manufacturing by producing well-defined 3D constructs with improved functionalities and precise geometries.

Several sets of criteria for biobased polymeric ink properties have been stated in the past.^{28–31} Most of these criteria are broad requirements for the material to fulfill instead of applied engineering specifications and procedures. Careful attention is imperative once selecting a material to print a particular object. While there are a variety of commercially available biobased polymers, not one biopolymer inclusive and will give one the functional properties needed for a particular printing application. Besides, a distinct printing technique is not capable of printing any one individual biopolymer available in the literature or marketplace. When designing a biopolymeric ink, the flow properties and extrudability of inks are essential for their successful 3D printing process.^{17,32–34} Surprisingly, the role of

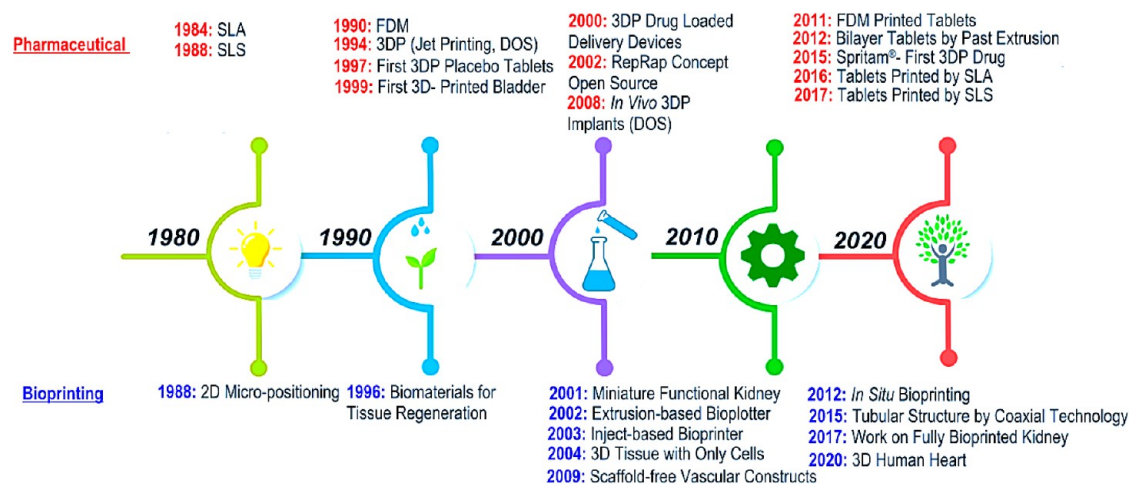


Figure 1. Principal progress in 3D printing achieved in the biomedical and pharmaceutical sectors.

rheological properties in ink formulations linked to geometries and spatial resolution of the final printed objects remains poorly understood during ink development and evaluation. Moreover, there are a few reviews regarding the materials utilization and modification techniques to enhance the quality attributes and functional features of the 3D structures.³⁵

Because biomaterials are the most promising biodegradable materials for the 3D printing process, this Review intends to provide a comprehensive review of 3D printing techniques in terms of the main materials utilized and a perspective on current important limitations of the 3D printing technique. We also review the main procedures for biobased ink reinforcement in the 3D printing process, as well as provide an in-depth insight into the recent progress and advanced biomaterials for 3D printing applications. Additionally, selected applications prove how printable biopolymeric inks are being applied in pharmaceutical, bioengineering, and food processing, as well as personalized and customized constructs designs. We also highlight the profitable introduction of 3D printing technology in the bioengineering and food industries based on critical studies of the material's functional features and the most effective use of multicomponent systems including proteins and carbohydrates.

2. HISTORICAL DEVELOPMENT, KEY MOTIVATION, AND CLASSIFICATION

2.1. Pharmaceutical and Bioengineering Application.

Numerous additive manufacturing technologies have recently been adopted to construct 3D printed architectures with consideration of material varieties. Similar to conventional synthetic polymers, the effective applications of biomaterials are reliant on the proper selection of a printing method. Some printing approaches are more appropriate for particular biopolymers varieties since they utilize diverse physicochemical approaches aimed at layered solidification of building biomaterials. Among the printing techniques dedicated to printing biomaterials, FDM, SLS, and binder jet technologies are extensively utilized for pharmaceutical and medicine applications (Table 1). Although at its infancy, 3D printing technology is paving its way toward the assembly of customized and personalized medicines from the ongoing “one-size-fits-all” manner. Complex dosage forms can be developed through these approaches and additional programming these dosage forms to show tailored impacts or to the target-specific organs. The

motivations for research in pharmaceutical printing are designing personalized and customized medicine to offer utmost therapeutic effects for different disorders, and decreasing the time and cost of operation and the necessary supplies of the conventional processes.^{36–38} At present, it is also quite impracticable to attain 3D bioprinting of fully functional organs. However, it is a fact that cannot be denied that 3D bioprinting techniques have considerably progressed.^{53,54} While it may be realistic that the economic considerations suggest that 3D printing technology does not seem to achieve the potential of overcoming the global health challenges.

The application of additive manufacturing in personalized medicine and controlled-release dosage serves as a promising technology to develop a customized product. Among almost 40 years of the 3D printing process history in the medical application, numerous different techniques have been emerged and developed with technological progress. Decades ago Pierre A. L. Ciraud stated the technique of powdered component application and following solidification of each layer through a high-energy beam, where meltable metals or plastics could be hypothetically utilized for the preparation of 3D constructs.³⁷ In the early 1980s, Ross Housholder proposed a concept for the sand binding using several components, and Carl Deckard established a technique for the solidification of the powdered bed using the SLS method. At the end of the 1980s, the FDM printing technique was filed by Scott Crump for the first time. In the 1990s, Emanuel Sachs and co-workers in their “Three-Dimensional Printing Techniques” patent applied a binder to linking the particular areas of powdery materials.³⁷ The central attainments in additive manufacturing for pharmaceutical and bioengineering applications are illustrated in Figure 1.

The additive manufacturing technologies gain importance in pharmaceutical and bioengineering fields because of the opportunity of quick fabrication of customized printed constructs utilized in controlled-release dosage or tissue engineering. The application of additive manufacturing in the biomedical sector principally intends to the improvement of patient-centered printed dosage forms according to the 3D structure. The 3D printing is still considered an emerging technique in biomedical fields with the potential to construct the sustained release drug delivery systems with a precisely tailored geometry. Numerous scientific works are performed to design and develop the 3D printed dosage forms, as the oral administration way remains the most favorite route relating to

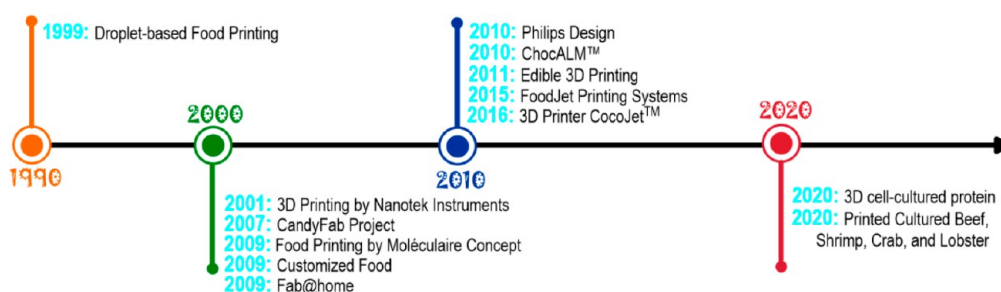


Figure 2. Pivotal achievements in food additive manufacturing.

Table 2. Examples of Printing Systems Used to Fabricate Custom-Designed Foods

system type	method	mechanism	ingredient range	critical parameters	ref
extrusion process	soft material extrusion	binding based on rheological properties only (phase changes do not occur)	meat purees; chocolate; syrups; frosting; processed cheese; dough batters	viscosity	68–71
	melting	solidification upon cooling	chocolate; sugar; confection	temperature	72, 73
	hydrogel-forming	ionic or enzymatic cross-linking	biopolymeric hydrogels (including starch, xanthan, gelatin, alginate, etc.)	viscoelastic behavior	74
air sintering	sintering and melting	powder binding; hot air	sugar	temperature	58
inkjet printing	drop-on-demand deposition	accommodation of layers adjusted with flow behavior	chocolate; sugar icing, liquid dough; meat paste; cheese; biopolymeric hydrogels	viscosity	75–78
liquid binding	drop-on-demand deposition; powder binding	chemical procedures; adhesive interactions	chocolate; gels; fondant; sugar	temperature	79–81
SLS		laser; powder binding	sintered and melted sugar/lipid	viscoelastic	82, 83
bioprinting		self-assembly of cells	cultures of living cells and biological materials	viscoelastic, temperature	84, 85

drug usage. The instances of printing objects prove the increasing attention to the designing drug with multitarget activity through various printing methods (Table 1). Note that standardization of equipment is mandatory along with verifying the protection of accessories. Likewise, the progress in the formulation of printable biopolymeric ink aimed at use in the 3D printing process must comply with the physicochemical standards for effective printed medicine manufacture.^{36,37}

Since the 3D printing process shows the capacity to develop personalized medicines to cure specific diseases, it can offer end-users customized therapeutic strategies among target populations. Therefore, additive manufacturing as an efficient medical approach can be considered to curing a wide range of clinical disorders, including Alzheimer's disease, different types of cancer, and respiratory diseases, as well as pediatric and geriatric populations.³⁶ The idea of end-users having tailor-made medicines supports the fact that the precise dose delivered at the proper time to a patient, therefore supplying the greatest advantages of drug treatment to show appropriate pharmacokinetic and pharmacodynamic responses. Furthermore, such treatment offers other parameters, including genotype, gender, health conditions, nutrition, physical activity, and weight, to design and develop the dosage forms. In contrast, the common dosage forms are only relied on certain strengths to support the main part of the patient population. Additionally, additive manufacturing offers versatility for in-place assembling, while common treatment depends on the formation of a wide-ranging constructing system with advanced technologies. Therefore, additive manufacturing could manage therapy to an individual-centric rather than a group-centric method.³⁷

2.2. Food Application. One of the first methods used for 3D food printing was using droplet-based printing systems and demand on rheological features of inks applied for drop-on-demand approaches has led to the development of direct inkjet

printing and hot melt printing process (Figure 2). Another attempt to use 3D printing technology in food processing was patented in 2001 by Nanotek Instruments, Inc., stating the additive construction of a 3D structured birthday cake. However, no prototype was fabricated. After a few years, an affordable open-source 3D printer was introduced in 3D food printing with some technical improvements.^{55,56} Nico Kläber⁵⁷ designed an idea in the Electrolux Design Lab (2009) competition, printing a customized complex food product through a mini robotic arm. One of the first experimental implementations was reported in the CandyFab project, which used a low-velocity hot air stream sintering and melting sugar to reduce the thermal distortion and simplify the fusion among layers.⁵⁸ The method's low cost, using nonproprietary resources and its open-source nature, allowed processes by innovative preparations like producing the recipes in the common food products. Philips Design⁵⁹ also offered to generate a customized meal through the cartridges with a cooperating graphical operator interface for choosing components, amounts, geometries, and textures.

Over the past few years, different additive manufacturing techniques were launched in food science and improved to address the request for resource processing and food design (Table 2). Considerable scientific research has been stated in recent studies aiming to differentiate 3D printed foods from traditional products.^{7,10,11,60–65} The research work evaluates the important motivations for printing adjustment in the industry, which compares various 3D printing processes and resources and address possible areas of application. Conventional industrial food manufacturing purposes to develop domestic food in an economic large-scale production that guarantees the constant product quality and features expected by end-users from former consumption. On the other hand, 3D printing allows the fabrication of innovative food structures with

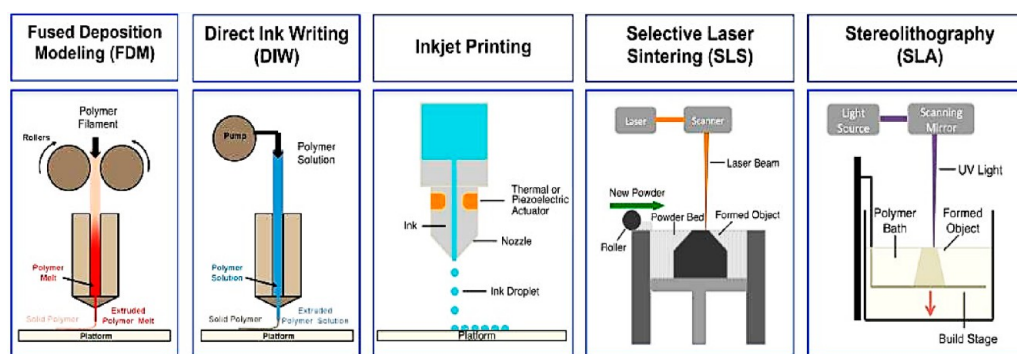


Figure 3. Graphics representing different additive manufacturing systems. Reproduced with permission from ref 93. Copyright 2016 American Chemical Society.

acceptable sensory attributes and offers end-users customized foods and innovative sensory properties.^{1–3,7,64,66,67}

Concerning food science and technology, 3D printing techniques are generally included in extrusion-based methods (FDM and DIW), SLS, SLA, and inkjet printing (Figure 3). Explanations of each 3D food printing system were previously reviewed in detail.^{3,8,60,77} The extruder systems are the attractive 3D printing process in the food sector, allowing deposition of molten material. For the extrusion process, the biobased polymeric inks need to be obtained such that the *pseudoplastic* properties during extrusion conditions to offer high printability and resolution. This technique is frequently applied in the extrusion of hot-melt chocolate,^{5,68,69} dough,^{86,87} mashed potatoes,^{88,89} meat puree,^{68,70} and cheese.^{90,91} Examples comprise printing through Fab@home and ChocALM to manufacture custom-designed food products prepared by different types of edible components. Periard et al.⁷¹ and Lipton et al.⁷⁰ fabricated cookies and frosting through an extruder-based 3D system.⁹²

Powder binding technology is another widest method in food additive manufacturing. The process is based on the powder binding using sintering sugar and lipids of food components.^{82,83} By applying laser sintering, several fascinating complicated 3D objects were fabricated by CandyFab, which could not be developed via traditional methods.⁵⁸ The liquid binding technique has been originally introduced by Brecht and Anderson⁵⁵ as a 3D printing method. Using this technique, 3D System's Chefjet printer used the Z-Corp inkjet method to fabricate different customized 3D architectures in diverse flavors-sculptural.⁸¹

Binder jetting technology (or inkjet printer), gives the rapid prototyping, development of 3D custom-designed architectures with relatively low-cost components (Figure 3). Binder jetting commonly employs components with a low consistency index; therefore, it can be mostly applied to create the image decoration and surface filling.^{94–96} Grood and Grood⁷⁸ developed a binder jetting system to distribute food ink on top of product surfaces to produce attractive figures. On the basis of the binder jetting technique, Southerland et al.⁹⁷ attempted to develop edible printed objects through sugars and starch blends. Sugar-based materials were handled using an inkjet printer technique like the 3D printing process. Holland et al.⁹⁸ applied a ball mill to modify the functional properties of amorphous cellulose and xanthan gum to produce a 3D structure through 3D binder jetting. Izdebska and Zolek-Tryznowska⁹⁹ fabricated numerous attractive edible constructs with different colors and flavor binders. In another study,¹⁰⁰ a printable food ink was developed by inkjet

printing generating a high image quality of edible substrates to use in the confectionary field. The FDM technology was used in food printing as an approach for the development of edible components, mimicking a wide range of mouthfeels.⁷⁴ Zhang et al.¹⁸ used an FDM printer to print wheat dough, in which printed dough showed good printability and adequate stability upon the printing process.

The 3D printing process as a cutting-edge technology offers a cost-effective customization alternative to conventional food processing methods. Inspired by research personalized nutrition and customized decorative accessories represent, the 3D printing technique can be considered as an influential approach to offer healthy products with custom-designed shapes, allowing personalized foods with healthy edible features and attractive structures.^{96,101–106} The personalized nutrition promoted by the printing process can address the requirements of functional products, especially healthy foods. With introducing printing technology to the food application, the edible components are easily customized and can be converted into complicated attractive shapes. The customized and personalized printed products content customer prospects of diverse lifestyles obtaining tailored features of texture, color, sensory properties, and nutrition. In the wider outlook, to fabricate customized printed products, digital gastronomy and 3D printing methods are necessary to minimize human involvement.^{1,2,8,77} Despite fabricating 3D objects with complex shapes and exclusive mechanical properties, the sensory properties could also be improved through additive manufacturing. Moreover, it is likely to develop custom-designed personalized constructs containing a great number of components with antioxidant activity with acceptable sensory sensations.⁶⁶

3. BIOBASED MATERIALS FOR 3D PRINTING

Many ingredients and additives can be utilized to enhance the quality attributes, rheological, mechanical, and structural characteristics of 3D printed objects, but biobased polymers are used as the most important printable materials to regulate the flow properties of the ink system, improving the geometries and spatial resolution of resulting printed constructs.^{13,14,21} Supramolecular biomaterials, as high-molecular-weight compounds, are frequently applied to fabricate a printable biopolymeric ink-based dispersion for controlling flow behavior, mechanical, and microstructural properties owing to their hydrophilic nature, gelation, and aggregation features. They can offer crucial chain entanglements for printable inks, and therefore develop a well-defined geometry for the 3D printed objects.^{7,16–18,107} Numerous biopolymers belong to the

Table 3. List of Proteins to Use As a Material in the Blend of Different Biomaterials along with Printer Type, Advantage, Disadvantage, and Application

protein	blended with	printer type	advantage	disadvantage	application	ref
gelatin		FDM; extrusion	homogeneous structure; high-fidelity parts	weak mechanical strength	biomedical engineering; food products	74, 116–118
	Kappa-carrageenan	FDM	increased gelling temperature	poor 3D structure	food printing	119
	agar	jet extruder	jelly-like texture	low hardness	soft food	101
	egg-white protein/starch	melt extrusion	improved viscosity; formation of single-helix structure	increasing the particle size	food printing	109
	alginate	extrusion	shear-thinning behavior	increase in deformation	drug delivery systems	120
	zinc oxide/clove oil	melt extrusion	antimicrobial features; good shape-fidelity	rough surface	tissues regeneration; packaging	121
	soy protein isolate/alginate	extrusion	shear-thinning behavior; good geometries	weak mechanical strength	food printing	7
collagen	polyethylene glycol diacrylate (PEGDA)	SLA	improve mechanical stability	low collagen loadings	tissue engineering	122
	agarose/mesenchymal stem cells	bioprinting	enhancing the cell spreading	poor printability by lower agarose ratio	bone tissue engineering	123
	alginate/agarose/chondrocytes	bioprinting	facilitating cell adhesion; accelerating cell proliferation	lower swelling ratio	cartilage tissue engineering	15
	hyaluronic acid	extrusion bioprinting	facilitating cell viability	some extent of phase separation	liver tissue constructs	16
soy		extrusion bioplotter	enhancing geometric accuracy	limited cell proliferation	tissue regeneration	124
	alginate/gelatin	extrusion	shear-thinning behavior; proper flow properties	low hardness	food printing	7
zein	xanthan	extrusion	improving the printability	low cohesiveness	food printing	115
	lipid	FDM	improving the printability	lower mechanical properties	biomedical printing	125
	poly(ϵ -caprolactone)	electrohydrodynamic	enhancing the mechanical strength	some extent of macroscopic contraction	drug delivery systems/tissue engineering	29
	acrylonitrile butadiene styrene	extrusion	improved convexity index	slow sintering kinetics	material printing	126
casein	magnesium silicate/poly(caprolactone)	extrusion bioplotter	porous structures; enhancing proliferation		bone regeneration	127
	whey protein	extrusion	thermally stable gels	some extent of aggregation	food printing	9
	milk protein concentrate (MPC)	extrusion	improving the thixotropy; high-fidelity parts	some extent of aggregation	food printing	110
wheat flour	pectin/sucrose/starch	FDM	improved rheological properties	low printability due to low gelation temperature	food printing	17
	wheat flour	FDM	good printing stability	some extent of heterogeneous matrix	food printing	18
	egg-white	extrusion	improved printability	collapsing the uppermost layer	food printing	128
	nonfat milk/sugar	extrusion	enhanced flow properties	some extent of thermal instability	food printing	87
gliadin	magnesium calcium silicate/polycaprolactone	bioprinter	improved structural strength		bone regeneration	129
gluten	potato granules/sugar	extrusion	improved rheological properties	weakened mechanical strength	food and biomedical printing	130
whey	starch/canola oil	extrusion	desired shape fidelity	low hardness	food printing	13
	milk protein concentrate	extrusion	inducing homogeneous matrix	low hardness	food printing	131
	gellan	extrusion	shear-thinning behavior; high fidelity	solid-gel structure due to the increase in particle size	food and biomedical printing	30
egg proteins		extrusion	desired shape fidelity	thermal instability	food printing	132
	rice flour	extrusion	good printing accuracy	thermal instability	food printing	133
	gelatin/starch/alginate/sucrose	extrusion	desired shape fidelity	increasing particle size	food printing	109
peanut protein	starch	extrusion	improved mechanical stability	thermal instability	food printing	134
	hydrolysate/xylose	extrusion	improved printability; thermal stability	low cohesiveness	material printing	135
faba- and oat bean	starch/cellulose nanofiber/milk powder	extrusion	good printing accuracy	spreading after printing	food printing	11
silk		extrusion	biocompatibility; biodegradability	sparse nanoholes	tissue engineering	136, 137
	chitosan/human fibroblast cells	extrusion	improved printing accuracy		soft tissue engineering	138
	xanthan/trimetaphosphate	extrusion	self-healing property	low swelling ratio	tissue engineering	139

category of permitted printed pharmaceutical, bioengineering, and food additives in many countries throughout the world. The selection of biomaterials for the 3D printing process depends on

the application and the customers' needs, as well as the suitable selection of a printing method.^{3,8,108} While it is likely to construct identical 3D structures with diverse 3D printing

methods, the ink formulations vary considerably in their proportions and compositions depending on printed objects.^{5,17,34,109,110} Generally, a printable biopolymeric ink must show a well-defined shear-thinning, viscoelastic, and thixotropic characters to simply extrude out from the nozzle tip. The flow property of inks is usually related to quality indicators of end-products and offers the main information for printing processes, allowing the suitable selection of materials to optimize the final product.^{12,13,109,110} The biobased polymeric inks must also develop stable polymeric networks, resisting stresses from capillary forces with restricted shrinkage upon drying; preventing 3D printed constructs deformation and/or crack development.^{111,112} Extensive reviews on these processing and 3D printing technologies have been published elsewhere.^{3,8,108,113,114}

3.1. Printing of Protein-Based Materials. The biomaterials employed in additive manufacturing can be categorized according to their supramolecular functionality suitable for printing processing. Proteins utilized in the 3D printing application experience processing in the natural form owing to organizational states, high-molecular-weight nature, and supramolecular functionality.^{2,8,77} The flexibility in the molecular geometry and facility in the mixing, gelation, aggregation, and deposition related to the printing applications allow proteins to develop extremely efficient 3D printed architectures.^{7,16,115} This reality can be commonly linked with organizational situations and unique hierarchical architectures resulted from self-assembly, influencing by 3D printing. This complexity and sometimes intricacy seldom occur in the nondegradable polymers. The information on protein printing is in the early stages and is mostly devoted to the progressing of the ink composition approaches to attain desired printed structures. Table 3 covers an outline of utilized proteins in additive manufacturing. In the subsequent sections, the applications of different proteins in the 3D printing process are described.

3.1.1. Gelatin and Collagen. Gelatin is a complex polypeptide used in different areas, including pharmaceuticals, bioengineering, cosmetics, and widely in the food industry. It has been widely applied to produce functional printable inks due to biodegradability, biocompatibility, substantial cross-linking site, and thermal stability in the environment.^{74,116–118} Gelatin can be processed in the native state to create printed constructs with an even and uniform structure, producing high-fidelity architectures. Nijdam et al.¹¹⁸ printed gelatin solutions (5–20 wt %) as cylinder shape and found that gelatin experiences initial instantaneous and height deformations, which was especially obvious at the lower concentrations. Stevenson et al.¹¹⁷ combined indirect additive manufacturing and freeze-drying techniques to generate gelatin-based open-channeled objects with dimensional stability. They specified that the indirect 3D printing process of molds together with freeze-drying were hopeful manufacturing approaches to quickly fabricate customized gelatin products with controlled shapes, in which the printed samples preparation procedure did not rely on either the freeze-drying process or the heating process. In another relevant study, Gholamipour-Shirazi et al.¹⁴⁰ printed gelatin with different concentrations and found that gelatin at the level of 0.5% created a well-defined hydrogel, but it was not able to preserve its shape. They also demonstrated that only a concentration of 2% gelatin was printable self-supportive. Tamura et al.¹⁴¹ used a microelectrical discharge machine for the microfabrication of gelatin hydrogel, mainly from the outlook of its application in the food sector. They showed that

the application of safflower oil on the printed gelatin-based objects was applicable with slight taste altering.

The developments of triple-helix networks are related to the aggregation and/or gelation of gelatin, preventing its printing process. Therefore, combinations of solvents and other ingredients, as well as environmental factors disrupting the triple-helix creation are suitable.⁷⁴ The 3D printing of gelatin in combination with other biopolymers through a syringe-based FDM process was stated by Cohen et al.⁷⁴ They reported that the pure gelatin fitted only with a poor to the rigid range and moved to granularity form after introducing xanthan gum into the gelatin matrix. In another related work, Warner et al.¹¹⁹ applied a custom-made FDM printer to print a blend based on gelatin and carrageenan for the printing process. The results showed that the printed square-shaped objects processed with neat gelatin showed an even and homogeneous width. They assumed that the greater printer temperature and slight development of the elastic network caused the system to show a viscoelastic behavior. In contrast, introducing carrageenan allowed regulating the printing process, which gelled just above ambient temperature. A relevant study was performed on printing a blend of gelatin and agar by using a jet extruder at different concentrations for the elderly. The incorporation of gelatin into the system demolished the mechanical strength of agar hydrogel, characterized by a reduction in the firmness of the 3D printed sample.¹⁰¹ In contrast to the above-mentioned study, it is reported that gelatin addition is helpful for the printing of most important proteins such as soy protein isolate⁷ and egg-white protein¹⁰⁹ to extruding out from the nozzle tip and preserving the deposited layers. Chen et al.⁷ reported that a blend of gelatin and soy protein isolate printed with a stable shape and precise geometry. Liu et al.¹⁰⁹ also produced a printable ink based on gelatin and egg-white protein to process through a melt extrusion printer, in which gelatin formed single-helix networks beneath the gelation temperature. Gelatin can be also applied for the fabrication of a 3D printed scaffold in a single form or with a combination of other biobased materials. In this regard, Park et al.¹⁴² used gelatin to suspend hydrogels for 3D lattice scaffolds through a 3D extrusion printer. The 3D printed scaffold was fabricated with dispersing gelatin in the culture medium including CaCl₂. Kuo et al.¹²⁰ also fabricated bioscaffold based on gelatin and alginate as an effective delivery system using extrusion-based 3D printing. They determined optimum printing performance with a ratio of gelatin to alginate of 1:1.

Collagen, as an abundant structural protein, is one of the most frequently used biopolymers in additive manufacturing, especially, upon working with cells.^{5,8,52,122,123} Collagen is an important element of connective tissue acting as a structural protein. It can be printed as a gel, after the extrusion printing process and enzymatic digestion. However, the neat collagen suffers the required strength to develop the printed architectures, thus it should be blended with different biomaterials.¹⁴³ Collagen has also reported that has a low consistency index and is slow to polymerize, in which it is hard to maintain the collagen functionality in liquid form as a printable bioink. In this regard, extrusion, inkjet, and SLS printing methods can be applied to processing the difficult-to-print collagen-based dispersions.^{123,143} Moreover, temperature and pH should be controlled during the printing process. The extrusion printing method coupled with a multiprint head can perform along with an in situ cross-linking printing system.^{16,143} Nevertheless, the main challenges with using collagen as an

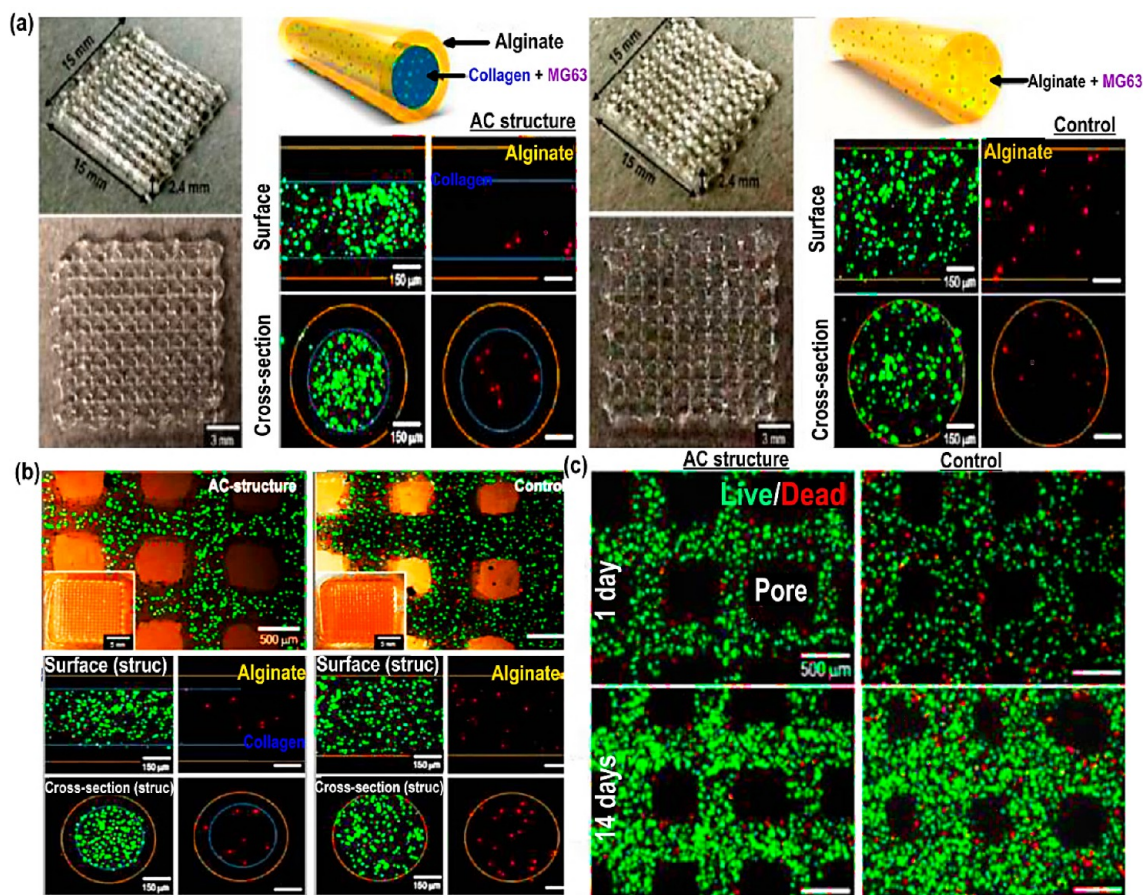


Figure 4. (a) Micrographs of (left) AC structure (cell-laden system) and (right) alginate with human adipose tissue-derived stromal cells (hASCs). (b) AC structure (hASCs-laden) including cell-laden collagen (core)–alginate structure (pod), where control is alginate with hASCs. (c) AC structure and control. Reprinted with permission from ref 52. Copyright 2016 American Chemical Society.

extrudable polymer are a long gelling time and swelling, which was also flagged up. One strategy for processing collagen with other biopolymers is the freeform reversible embedding of the dispersed gels.¹⁴³ In this regard, PEGDA/collagen blend hydrogel could be printed through SLA to light-assisted producing 3D collagen networks.¹²² Collagen was also utilized in the biopolymeric blend form with sodium alginate to gene expression and proliferating chondrocytes using in tissue engineering.¹⁰⁷ According to the literature, collagen can be used with gelatin methacrylate system, collagen/agarose for spreading, feasibility, and variation of osteocytes of mesenchymal stem cells;¹²³ and collagen blending with hyaluronan using in liver microenvironments including primary liver stellate cells and human hepatocytes.¹⁶ Yeo et al.⁵² prepared a cell-embedded mesh structure based on collagen blended with alginate for tissue engineering, fabricating through a cell-printing system enhanced via the core–pod nozzle and cross-linking technique. Considering diverse pressure and ionic conditions, the cell-laden support was fabricated, including cell-laden collagen as core zone covered with neat alginate as pod area (Figure 4).

3.1.2. Soy. Soy protein as a source of essential and nonessential amino acids shows the proper nutritional quality and physicochemical features to be applied as a biopolymeric ink for the 3D printing process.^{144,145} The popularity of soy is among other proteins triggered by its application in pharmaceutical, bioengineering, and healthy food products, along with the fact that it is a cost-effective product and

promising sustainable plant protein sources with an extensive range of usages. It can improve the flow behavior of the system and can be extruded out through the nozzle tip and deposited for the fabrication of different 3D printed constructs. However, soy protein cannot be printed alone and needs a carrier biopolymer with the purpose of involving in 3D printed networks. Chen et al.⁷ printed a blend of soy protein isolate, alginate, and gelatin by an extrusion printing system. They showed that soy protein ink exhibited a shear-thinning character, in which gelatin and alginate caused the substantial rise of consistency index and mechanical properties. Moreover, resilience, firmness, and chewiness parameters of printed samples were improved in the printed soy protein/gelatin blend, supporting the customized 3D matrix upon printing technique. The results also showed that soy protein blended with alginate and gelatin was printed with a precisely tailored shape, and the inclusion of more gelatin amount provided a shape with finer resolution. In another work, Phuhongsung et al.¹¹⁵ fabricated soy protein isolate blended by xanthan in the presence of NaCl solution. The prepared ink was well printed with proper resolution and precise geometries. They proposed that soy protein isolate/xanthan ink in the presence of 1 g/100 mL NaCl solution was the optimum ink for the printing application. Chien and Shah¹⁴⁶ successfully synthesized a porous soy protein-based scaffold using 3D printing techniques. The porous soy protein-containing scaffold comprised a variety of layers configured in a vertical stack, each layer comprising a variety of strands comprising denatured soy proteins. The same work was accomplished by Chien et al.,¹²⁴

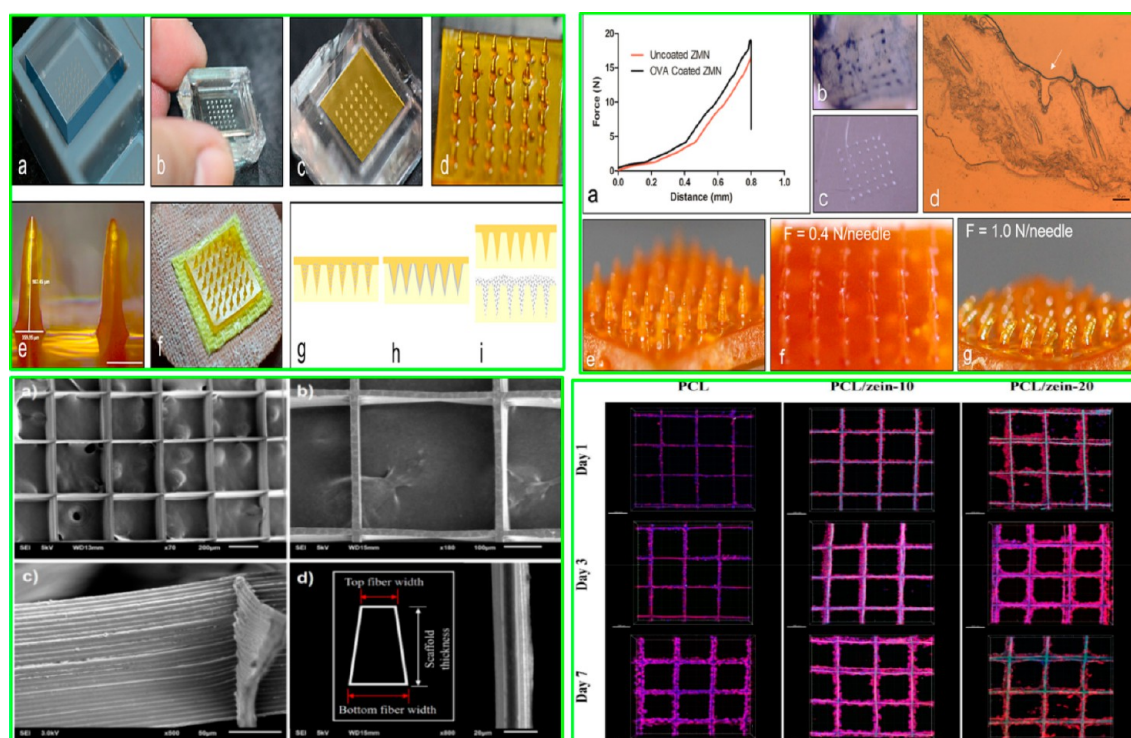


Figure 5. (Top-left) Fabrication of zein microneedles (ZMNs). (a) Casting PDMS mold, (b) obtained PDMS mold, (c) ZMNs casting, (d) ZMNs array, (e) images of ZMNs, and (f) microneedle array. Micrographs of (g) ovalbumin (OVA)-entrapped ZMNs, (h) OVA-coated ZMNs, and (i) OVA use upon pretreatment of ZMN. (Top-right) (a) Mechanical strength of ZMNs, (b,c) stained skin upon insertion of ZMN, and (d) schematic representation of skin cryosection upon ZMNs treatment. ZMNs before (e) and after insertion in the skin with 0.4 (f) and 1.0 N/needle (g). Reproduced with permission from ref 147. Copyright 2017 American Chemical Society. (Bottom-left) SEM micrographs of printed PCL/zein scaffold: (a) top view, (b) back view, (c) side view, and (d) magnified top view of the fibers. (Bottom-right) Confocal images of cell seeding on PCL and blend of PCL/zein scaffolds. Reproduced with permission from ref 29. Copyright 2018 American Chemical Society.

who printed reproducible printed scaffolds based on soy protein through a bioplotting system. The ink flow rate was found to be a vital factor that could be used to predict the printability of biomaterials, as well as help as an indicator for quality control purposes. They stated that the printability of soy protein was mainly beneficial as the printing process could be performed at room temperature, which is suitable for drug delivery systems or growth parameters. Further to the studies of raw components, there are some recent research works to improve the 3D printing of products by using soy protein. In this regard, Fan et al.²⁸ examined the impacts of microwave pretreatment and salt incorporation on printability and self-supporting performance of printable ink based on soy protein isolate including strawberry (in powdery shape). Functional properties of the printable ink showed that microwave process and salt addition importantly enhanced printability and self-supporting behavior of blend ink.

3.1.3. Zein. Zein is a type of alcohol-soluble prolamine storage proteins in corn, which is rather rich in hydrophobic and neutral amino acids, along with some polar amino acid residues. It can be applied as a hydrophobic printable ink for different 3D printing applications, including drug delivery systems, bioengineering, and food application.^{29,125–127} Since zein is an expensive protein, therefore extraction of zein and production of 3D printed objects from it would produce an important economic benefit. Moreover, the classical brittleness and flexibility drawbacks of objects produced by zein are an essential problem for their use as a free-standing 3D printed construct and more widespread application as a printable ink. In the study performed by Chaunier et al.,¹²⁵ they revealed that plasticized zein could be processed by 3D printing using an FDM printer.

No molecular orientation was found in the deposited filament at the outlet of the printer nozzle and the amorphous structure of zein was cross-linked upon the extrusion printing process. They assumed that such results can be used to evaluate more precisely the rheological behavior of zein-based structures in the molten form and their hot fusing features. Furthermore, the possible interactions of zein with different plasticizing compounds (e.g., polar, apolar, or ionic materials) could lead to an improvement of 3D printing abilities.¹²⁵ It is shown that some biopolymers can be introduced into zein-containing ink to improve the flexibility, flow behavior, and consequently mechanical stability of printed constructs. Bhatnagar et al.¹⁴⁷ investigated the possibility of fabrication of antigen delivery using a micromolding technique made by a blend of zein and corn protein. It was shown that zein could be molded to achieve a microneedle array, showing adequate mechanical strength to enter the skin. Their results also showed that zein could be easily cast using the micromolding technique with the potential for scale-up (Figure 5). Jing et al.²⁹ developed a blended ink formulated with poly(ϵ -caprolactone)(PCL) and zein and examined the printing performance for scaffold fabrication. The enzyme-accelerated *in vitro* degradation experiment revealed the scaffolds including zein showed a dose-responsive behavior against degradation in the presence of protease and cell culture. Furthermore, the blend biocompatibility was evaluated in human lung cancer cells (H1299) and mice embryonic fibroblast (NIH/3T3), which displayed well cell affinity. The elastic modulus and yield stress of the PCL/zein blend scaffold were remarkably enhanced in comparison with the neat PCL scaffold. These results offered an effective method for modification of mechanical strength of 3D

scaffold without application of toxic cross-linking compounds, where the PCL/zein blend scaffold manufactured by the solution-based electrohydrodynamic printer can be used in drug delivery system and bioengineering. Similar work was accomplished by Ru et al.,¹²⁷ who developed bioactive and degradable scaffolds based on magnesium silicate/zein/PCL ternary system through the 3D printing method. They reported that the *in vitro* apatite mineralization behavior and the scaffolds degradability were prominently enhanced upon increasing zein level. The scaffolds containing zein also considerably improved the proliferation and initial differentiation of osteoblastic cell line that was dependent on the zein level. Moreover, an enhancement was detected regarding *in vivo* osteogenesis of printed scaffolds, which also depends on the zein level.

3.1.4. Casein. Caseins are the main phosphoproteins of mammalian milk as micelles involving polypeptides called as α -, β -, and κ -caseins. They are commonly applied in the 3D printing process due to their textural, sensory, and nutritional features. Caseins have been electrospun/printed using some carrier biopolymers, including pullulan,¹⁴⁸ whey protein,⁹ pectin/sucrose/starch,¹⁷ and PVA.¹⁴⁹ Numerous published studies address the effective application of casein with consideration of different printing factors principally in the 3D food printing application. Daffner et al.⁹ tested an edible suspension formulated with casein and whey protein for tailored nutrition application through an extrusion-based 3D printer. The results revealed that rigid hydrogels were obtained at a pH of 4.8–5.0. Liu et al.¹¹⁰ prepared a milk protein blend hydrogel by introducing milk protein concentrate to the casein system and the obtained ink was printed by an extrusion-based 3D printer. Reportedly, calcium ions might enable forming an attractive force with casein and alter the isotropic behavior of casein dispersion; thus, the development of a stiff 3D printed network could be facilitated in the presence of calcium ions. Kern et al.⁹⁰ produced a model cheese in the presence of calcium ions by a hot-melt extrusion printing. The printed cheese including calcium ions (pH 6.3) provided a protein structure with improved firmness, decreasing the dry content. The increment in the shear force caused the improved association of para-casein “backbone” among, needing additional cross-linking reorganization.⁹⁰ In another work, the printability of calcium caseinate and wheat dough using an FDM printer was evaluated by Zhang et al.,¹⁸ who reported that printability was dependent on the composition of wheat dough with consideration of moisture content and flour kind, along with casein level. The dough printability was considerably improved upon the addition of calcium caseinate at 3% (w/w). It is also interesting to characterize casein conjugated with polysaccharide via the Maillard reaction as a printable ink for food additive manufacturing. In this case, Schutyser et al.¹⁷ successfully prepared sodium caseinate structures using an FDM approach, thanks to the reversible gelation behavior of sodium caseinate. They assumed that the incorporation of sucrose, pectin, and starch compounds was essential to achieve well-defined 3D printed constructs.

3.1.5. Whole wheat, Gluten, and Gliadin. The application of whole wheat for 3D printing is more and more popular.^{1,2,18,150} Whole wheat flour is a blend of wheat bran and flour at adaptable mixed amounts to attain a preferred nutritional value and taste, leading to different functionality. The Netherlands Organisation for Applied Scientific Research (TNO) and an Italian Pasta Company (Barilla) were shown improvement of printed pasta with durum wheat semolina and water.^{1,2,150} Natural Machines

Co. also extruded fresh food ingredients through the Foodini printer to fabricate 3D printed foods.⁹⁶ The extruded components can be applied to image decoration and surface filling.^{68,69} Zhang et al.¹⁸ printed dough with various amounts of water, flour types, and casein content upon the FDM technique. They argued printing performance of dough correlated to the ink flow behavior and its microstructure, in which formulation with greater loss factor, yield stress, and complex viscosity showed proper printability and good stability upon extrusion. In another work, the impact of printing parameters on the printing performance of wheat-made object was studied.¹⁰² It is reported there was a positive correlation between infill amount and a solid portion of 3D printed uncooked and cooked products and their firmness parameters. It was also shown that the interior printed matrix preserved the designed shape, where the irregular layer deposition resulted in the unsystematic filling of the void area. It was concluded that a suitable adjustment of the printing variables must be achieved regarding the mechanical properties to the real utilization of additive manufacturing for cereal-based foods. Similar work was conducted by Severini et al.,¹⁴⁵ who used additive manufacturing for the fabrication of snacks prepared from wheat flour containing edible insects (Yellow mealworm) as a sustainable protein source. Their results indicated that the milled insects could be considered as an appropriate nutritious component for the development of 3D printed constructs with precisely tailored shapes without negative influence on the technical feature. In another work by Keerthana et al.,¹⁵¹ they evaluated the printing performance of the mushroom powder mixing with the wheat flour. The printing process of freeze-dried mushroom was failed, while the addition of wheat flour notably improved the system printability. Fahmy et al.¹²⁸ used two material systems involving wheat dough and a blend of starch and egg-white to evaluate printability and shape fidelity. The quality features and dimensional properties of printed morphologies were evaluated through in-place depicting. It was found that the formation of the gluten network could stabilize the printed structure and induce a well-defined geometry. Pulatsu et al.⁸⁷ also prepared dough with different formulations including fat, flour variants, nonfat milk, and sugar, where the obtained dough was printed via an extrusion-based printer. The obtained data showed the dough prepared by low-level sugar was the optimum formulation in terms of printability. The existence of the gluten network during the 3D printing process induced higher-order impact, stabilizing the geometries, and enhancing the spatial resolution of the deposited layer of the printed architectures.⁸⁷ Krishnaraj et al.¹⁵² printed a healthy high-fiber high-protein product formulated with a blend of flour variants and specific seeds to assess the printing performance. Liu et al.¹³⁰ used an extruder printer type to fabricate dough based on gluten prepared from wheat flour, potato granules, and sugar. Zhang et al.¹²⁹ constructed a printed scaffold based on gliadin mesoporous bioglass fibers and PCL along with magnesium calcium silicate through a bioprinting system. The data demonstrated that introducing gliadin and calcium silicate into the PCL led to an enhancement in mechanical parameters and degradability of 3D printed scaffolds.

3.1.6. Whey Proteins. Whey protein is widely used as an ingredient in foods because of its excellent nutritional profile quality and exclusive functional features, that is, emulsification, thickening, gelation, and water-holding ability. They are also extensively applied as a functional ink owing to hydrogel-forming ability and printability features.^{13,131,153} Considering the role of whey proteins in the adjustment of the flow behavior

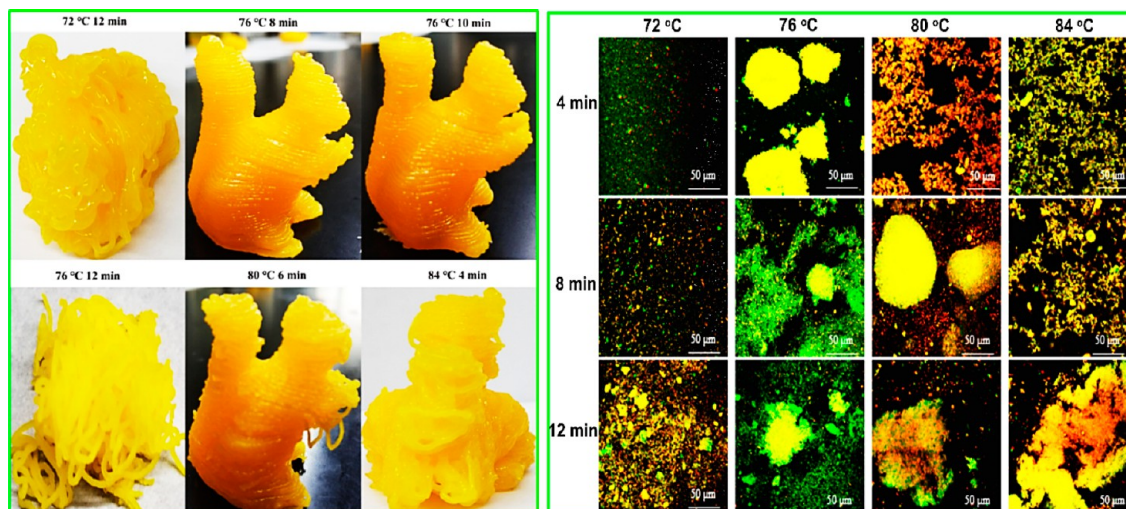


Figure 6. (Left) Images of 3D printed architectures prepared with heat-induced egg yolk paste. (Right) Confocal micrographs of egg yolk after heating treatment. (Red color represents lipids, and green color shows proteins.) Reproduced with permission from ref 132. Copyright 2019. Published by Elsevier Ltd.

of ink formulations and printed constructs improvement, numerous investigations were performed in additive manufacturing using whey proteins either individually or in blending with other biopolymers. Liu and Ciftci¹³ used whey protein isolate, canola oil, and corn starch for the printing process. The consistency index and loss tangent values specified all ink samples were *pseudoplastic* fluids and displayed predominantly elastic behavior. Liu et al.¹³¹ printed milk protein and evaluated the impact the whey protein addition on the printability of milk protein. The data presented the milk blend paste obtained from the mixture of milk protein concentrate (5 wt %) and whey protein isolate (2 wt %) was the optimum ink formulation, which was effectively processed via extrusion printer and obtained a well-designed printed structure. Oliveira et al.³⁰ produced multiscale inks by segregative phase separation of whey protein isolate and gellan gum. They stated that the printing performance of inks with a low consistency index might be amended thru ion cross-linking via calcium ions. The data offered the ink with minimum whey protein isolate (1%) and supreme viscous character (10% whey protein isolate) was effectively printed by using gentle extrusion forces and shear stresses. In this regard, they adjusted the printing variables to efficiently obtain the precise geometries, where the optimum printing parameters enhanced the interlayer adhesion, consequently improving the shape retention and integrity of resulting printed architectures.³⁰

3.1.7. Egg Proteins. Egg proteins are a favorable material for the fabrication of 3D objects with different shapes as they form heat-induced edible hydrogels, which conduce to further thermal processing treatment. Xu et al.¹³² developed printed architecture with heat-induced egg yolk. Reportedly, the egg yolk processed with a temperature of about 76 °C for 8 min showed well printability as the 3D constructs had finer resolution and precise geometries. The authors assumed the β -sheets intermolecular development might adversely affect the 3D printing process. They concluded that individual forms of the egg yolk could barely content the request for the development of customized products with functional properties and nutritional profiles and it should print with some other biobased polymers and binders¹³² (Figure 6). In another work, Anukiruthika et al.¹³³ studied the printing performance of egg

yolk and its blend with rice flour, aiming to adjust different printing variables such as diameter and height of nozzle, printing, and extrusion motor speed, as well as extrusion rate. The results presented the rice flour introducing with levels of 1:1 and 1:2 w/w showed an important impact on the stability enhancement and strength improvement of 3D printed egg yolk and egg white. They reported the printing process yielded the 3D constructs with precise geometry and finer resolution with sufficient adhesion between deposited layers. Liu et al.¹⁵⁴ demonstrated the printability of composite bioink consists of egg-white (albumen) and sodium alginate. The *in vitro* tests showed that HUVECs (umbilical vein endothelial cells) could effectively attach to the printed scaffold and preserve high viability. The vascular sprouting and neovascular network development were observed in-between fibers within the 3D printed scaffold. The results also demonstrated that 3D printed albumen/alginate composite bioinks with favorable biological functionality hold promising potential in tissue and organ engineering application. In a relevant study by Liu et al.,¹⁰⁹ the experimental situations essential for 3D printing blend bioink were optimized by changing different concentration ratios of albumen/alginate. This formulation was also comprised of egg-white protein, corn starch, gelatin, and sucrose. The rheological and tribological data showed the egg-white protein mixture system (5.0% (w/w)) was the best formulation to apply for the printing process. Furthermore, a specific ratio of egg-white protein enhanced the springiness and firmness of printed hydrogel. These enhancements facilitated the easily extruded out through the nozzle tip and improved the structural strength of 3D objects. Charbonneau et al.¹⁵⁵ successfully printed egg yolk plasma with controlled geometries. They manually extruded egg yolk plasma bioink containing the fluorescence cells in the 3D-Cryo well inserts and displayed the positioning of the cell. This 3D-Cryo insert exposed some data on cells embedded in the egg yolk plasma, representative it would be suitable for cultures of living cells via additive manufacturing.

3.1.8. Other Plant-Based Proteins. Some other plant-based proteins are also shown a great promising resource for additive manufacturing. Lille et al.¹¹ evaluated the printability of a blend ink based on oat- and faba bean proteins by evaluating the regularity of extrusion-based printing systems, in addition to the

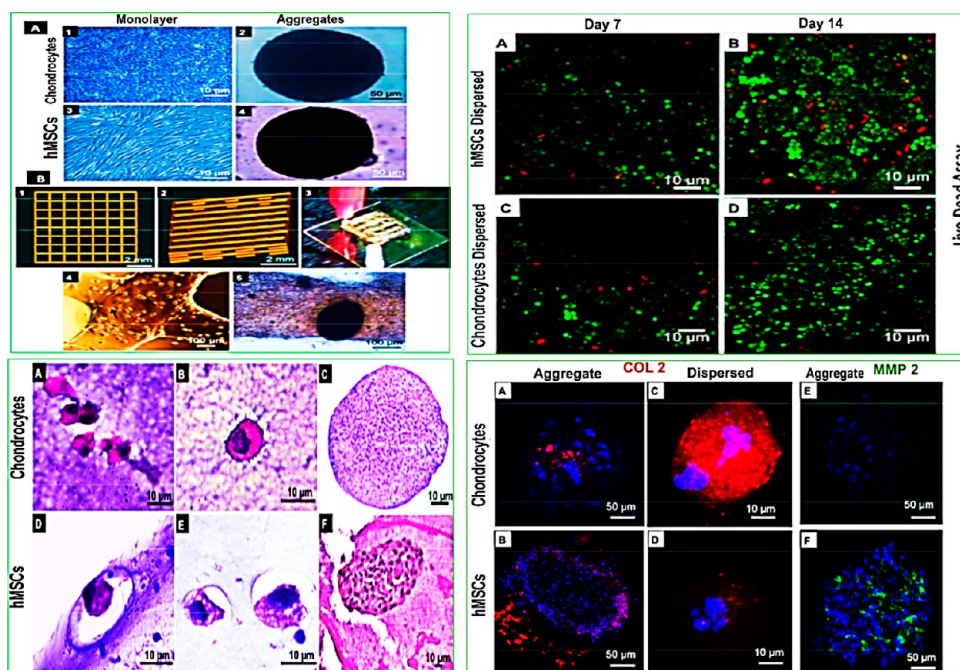


Figure 7. (Top-left) (A) Illustrative micrographs of chondrocytes and mesenchymal stem cells in monolayer (A1 and A3) and aggregates (A2 and A4) before bioprinting and (B) virtual construct by CAD (B1 and B2). 3D printed constructs of cell-laden silk and gelatin blend (B3) dispersed state (B4) and aggregated (B5). (Top-right) (A–D) Live/dead fluorescent of chondrocytes and hMSCs bioprinted blend. (Bottom-left) Cell-laden blend divided and stained with hematoxylin and eosin. A strong indication of the pericellular system in the dispersed bioprinted chondrocytes and hMSCs cells (A, B, D, and E). Evidence of aggregation (C and F) after 14 days. (Bottom-right) Immunohistochemistry of dispersed and aggregated architectures of the cell-laden blend at day 14. Complete architectures stained by anti-collagen2A1 antibody–AF 546 (red) (A–D), anti-MMP2-FITC (green) (E and F), and counterstained by DAPI (blue). Reproduced with permission from ref 14. Copyright 2016 American Chemical Society.

resolution and shape stability of 3D objects. The oat protein concentrate (35% solid content) was practically well printed with precise geometry, though the 3D structures did not show suitable shape retention upon the process. There were considerable variances regarding the protein ratios required to produce a desired printable plant-based ink with an appropriate flow behavior for the printing process. It is shown that the best ratios for printing were 35% for protein concentrate and 45% for faba bean.¹¹ In another study, Chuanxing et al.¹³⁴ assessed the printability of a starch system blended with pea protein by developing a printable food ink for 3D printing application. They indicated the printing quality improved by increasing the pea protein content to a level of 1%. Zhou et al.¹³⁵ also investigated the printability of 3D printed pea protein objects with consideration of enzymatic hydrolysate–xylose Maillard reaction. They found that compared to enzymatic hydrolysate addition, the objects including Maillard products noticeably enhanced the printing performance of the 3D printed objects.

Silk fibroin produced by *Bombyx mori cocoons* is a common fibrous protein, which has been used to develop the 3D printed hydrogel objects showing unique flow behavior, structural strength, and good biocompatibility. Mu et al.¹³⁶ printed the 3D silk structures with different architectures and a diverse range of functional components. The printing performance was demonstrated through single-step manufacturing a perfusable microfluidic chip was fabricated with reducing the application of supporting and sacrificial components. They also assumed that the 3D printed shaping capability of silk fibroin could be potentially used in the drug delivery system, surgical implants, and tissue engineering. In another study, Du et al.¹⁵⁶ extracted silk fibroin from *Bombyx mori cocoons* and fabricated a 3D printed composite scaffold containing mesoporous bioactive

glass. The results illustrated that the silk-based scaffolds showed greater compressive strength and improved biocompatibility and stimulated bone development capacity. Zhao et al.¹³⁷ developed a 3D printed hydrogel based on silk protein including a microalgal strain by an extrusion-based printer to host the living microalgae. Chameettachal et al.¹⁴ evaluated the hypertrophic suppression and chondrogenic differentiations in a cross-linked blend bioink based on silk and gelatin containing dispersed and aggregated cells for chondrocytes and mesenchymal stem cells (hMSCs). The hMSC spheroids chondrogenic differentiation (without the protein-based blend) revealed an increment in the hypertrophy. In contrast, the dispersed and aggregates hMSC-laden bioink objects exposed an upregulated hypoxia. The results showed that gelatin promoted the MMP2 action, degrading the fabricated system, and producing pericellular area to accumulate the growth factors and newly fabricated systems (Figure 7).

3.2. Printing of Polysaccharide-Based Materials.

Numerous published investigations are focusing on the utilization of polysaccharide-based materials for 3D printing applications.^{88,157–159} Typically, the resolution of the deposited layers and printing precision offered by polysaccharides are reliant on the degree of chain entanglements. Consequently, the polysaccharide levels, chemical structure, and flow behavior affect the printing condition.^{8,160} Moreover, the ratios of covalent or ionic linkages of carbohydrate-based materials are associated with the cross-linking degree; therefore the structural strength of 3D printed constructs. The concentration needed for substantial entanglements of polysaccharide-based ink dispersions shows a point where the entangled polymeric strands are developed. This point presents the coil-overlap of polysaccharides at which point the compact globular-like strands

Table 4. List of Printable Polysaccharide Blended with Different Biomaterials along with Printer Type Advantage, Disadvantage, and Application

polysaccharide	blended with	printer type	advantage	disadvantage	application	ref
chitosan		extrusion	self-healing properties	filament shrinkage	tissue engineering	162, 163
	silk	extrusion	improved printing accuracy		human fibroblast cells	138
	gelatin	bioprinting; bioplotter	high shape-fidelity; biocompatibility	low structural strength	skin tissue engineering	164, 165
	carboxymethyl cellulose (CMC)	bioprinter	stable structure; high biocompatibility	low swelling ratio	tissue engineering	166
	gellan	FDM	enhancing mechanical strength		biomedical printing	167
	PLA	extrusion; FFF	improved cell viability	high water solubility; low tensile strength	tissue engineering	168, 169
starch		extrusion	shear-thinning behavior; good geometries	low structural strength	food printing	19, 20, 22, 161
	cellulose acetate	FDM	good structural homogeneity and deposition	low adhesion between layers	biomedical printing	63
	oat- and faba beans carrageenan/xanthan	extrusion	good printing accuracy	spreading after printing	food printing	11
		extrusion	increased the gelation temperature; thixotropic behavior	some extent of thermal instability	food printing	33
alginate	plant cell	extrusion	enhanced cell viability	some extent of poor resolution	plant tissue simulation	142
	soy protein isolate/gelatin	extrusion	stable and precise geometries	weak mechanical strength	food printing	7
	pea protein	extrusion	suitable textural properties	collapsing the object	food printing	65
	taro/CMC/xanthan/guar/whey protein	extrusion	desired printability	low textural parameters	food printing	10
	gelatin	extrusion	shear-thinning behavior; stronger printed gel	increasing the deformation rate	drug delivery systems	120
cellulose	starch/milk powder/rye bran/oat and faba beans	extrusion	good printing accuracy	spreading after printing	food printing	11
	xanthan	binder jetting	good resolution	limitation of layer number	food printing	31, 98
	lignosulfonate	extrusion	shear-thinning behavior; high yield stress	continuous deformation until spreading	biosourced precursor	111
	gelatin/cellulose	extrusion	porous structure; improved cytocompatibility		artificial tissue	170
pectin		extrusion	desired printability	some extent of shrinking behavior	food printing	171
	bovine serum albumin/sugar	extrusion	appropriate flowability	a higher pectin ratio hampered printability	food printing	172
	chitosan	extrusion	good printability; self-adhesion to skin	recommended only for fresh epidermal wounds	wound dressings	173
	sucrose/starch/sodium caseinate	FDM	improved rheological properties	low printability due to low gelation temperature	food printing	17
	TEMPO-oxidized cellulose	extrusion bioprinting	shear-thinning property; improving the printability	partial filaments instability	tissue engineering	174
xanthan	gelatin	FDM	desired printability	granularity structure	food printing	74
	taro/alginate/CMC/guar/whey protein	extrusion	shear-thinning behavior	some level of printing deviation	food printing	10
	methylcellulose	extrusion	high structural retention; high shear modulus	poor 3D printing performance	food printing	86
	konjac gum	extrusion	desired rheological parameters	formation of weaker gels	food printing	175
	starch	extrusion	desired printability	high adhesiveness	food printing	176
	pureed carrot/guar/gelatin	extrusion	increasing the hardness	some level of printing deviation	food printing	177
	silk fibroin/trimetaphosphate	extrusion	self-healing property	low swelling ratio	tissue engineering	139
	guar	extrusion	less dense microstructure	some level of printing deviation	food printing	178
carrageenan		extrusion	desired rheological parameters		biofilter designs	179
	gelatin	FDM	increased gelling temperature	poor structural strength	food printing	119
	epoxy amine	extrusion	enhanced mechanical performance		tissue engineering; soft robotics	180
cyclodextrin	pectin/honey	extrusion bioprinter	good releasing rate	precipitation the inclusion complex; thermal instability	drug delivery systems	181
	cellulose/carbamazepine	extrusion	shear-thinning behavior; desired drug-releasing profile	existence of the brittle objects	drug delivery systems	182
	mannitol/ondansetron	SLS	improved drug releasing rate	some amount of drug was inaccessible	drug delivery systems	183
maltodextrin	PVA	not defined	good architectural accuracy	random shapes and sizes in pores	bone regeneration	184

Table 4. continued

polysaccharide	blended with	printer type	advantage	disadvantage	application	ref
	paracetamol/glycerine TiO ₂ /span	filament extrusion	desired drug loading	generating inhomogeneous spot	drug delivery systems	185
	sorbitol/hydroxyethyl cellulose	SLS	quick melting	low structural strength	food printing	82, 83
hyaluronic acid	cyclodextrin	FDM	supporting cell adhesion	losing the printed filament	tissue engineering	186
	gelatin/CMPCs cell	bioscaffolder tissue printer	improving myocardial viability; preservation of cardiac performance		regenerative medicine	187
	polylactic acid/polyethylene glycol	SLA	enhanced survival human adipose stem cells	limited matrix deposition	degenerative joint diseases	188
	methacrylated gelatin	bioscaffolder pneumatic system	improved shape fidelity and cell survival	limited connectivity of newly formed extracellular matrix	cartilage tissue engineering	189
	dextran	bioscaffolder pneumatic system	good cytocompatibility; high porosity		tissue engineering	190
	polybutylene terephthalate/CNT	digital light processing	good cytocompatibility		some level of deformation	cartilage tissue engineering

produce fewer entanglement chains compared to random walk-coil-like strands at a similar concentration.^{8,160} In this sense, a shear thickening behavior offers an increased extensional viscosity, which simply blocks the nozzle tip causing a failure in the printing application.¹⁶⁰ To overcome this challenge, a printable ink with a suitable shear-thinning character and an improved viscoelastic behavior is essential as it could be simply extruded out through the nozzle tip. Thus, *pseudoplasticity* and shear-thinning behaviors are crucial for the printing process of polysaccharide-based inks.^{14,33,159,161} A summary of individual printable inks containing polysaccharides blended with other biopolymers, as well as the printer type is shown in Table 4. The following sections introduce examples of utilizations of 3D printed materials formulated with polysaccharides are described.

3.2.1. Chitosan. Chitosan can readily be obtained by the process of alkaline N-deacetylation of chitin, mostly extracting from shellfish. The functionality of chitosan is dependent on acetylation degree and molecular weight, affecting the printability, biodegradability, shape fidelity, mechanical strength, and more importantly, flow properties.^{192–195} It is also distinguished as a natural polymer with wide applications in the printing process.^{162–165} However, the pure printed chitosan construct suffers from poor precise geometries and weak structural stability due to their hydrophilic character and the shrinking tendency of the 3D structure, which raises difficulties to process into the 3D printed architectures. Numerous efforts were carried out to develop printable chitosan-based ink for different potential applications with a combination of PLA,^{168,169} silk protein,¹³⁸ gelatin,¹⁶⁵ CMC,¹⁶⁶ and gellan.¹⁶⁷ In an investigation performed with Wu et al.,¹⁶² they offered a 3D printing system for hydrogel construction based on chitosan with great functional features and ordered microfiber structures. The microstructured hydrogel scaffold was made with a neutralization process. The failure strain of 3D printed hydrogel scaffolds reached ~400% and maximum strength was ~7.5 MPa. In another study performed by Zhang et al.,¹³⁸ the printed chitosan hydrogel strengthened with physically ground silk powders developed through an extrusion printing system. Compared to the neat chitosan, introducing the silk powders led to a notable enhancement of compressive modulus and also considerably better printing precision with improved construct stability. Wu et al.¹⁶³ evaluated the printability of chitosan inks directly in the air at ambient temperature and fabricated a 3D scaffold with intricate geometries. They stated that extrusion bioprinted chitosan scaffolds with improved printing perform-

ance and feature sizes of ~50 μm. Zolfagharian et al.¹⁶⁵ optimized the printing adjustment and printing variables to create a polyelectrolyte complex hydrogel based on chitosan and gelatin upon severe printing conditions. The results revealed that the printing process enhanced the maximum deflection compared to both cast films based on neat gelatin and intact chitosan.

Chitosan colloidal dispersion can also be used as bioinks for 3D bioprinting. Detailed research studies into the 3D printing processing variables of chitosan-based bioinks including flow behavior, structural strength, biocompatibility, and solvent evaporation are recently published.^{38,196,197} Jiankang et al.¹⁹⁶ used the SLA technique to process chitosan ink to fabricate a printed scaffold; in which a laser-induced μ-SLA system and two-photon polymerization technique were applied on the grafted chitosan-g-oligolactide copolymer. They argued that the molecular weight of chitosan and oligolactide strands could affect the functionality of 3D printed hydrogels. In another study, an ear-shape scaffold based on a mixture of chitosan and PEGDA was fabricated through SLA. Using adjusting the chitosan molecular weight and the ratio of chitosan, PEGDA, and photosensitizer, mechanical strength, printing performance, and cell adhesion were improved.¹⁹⁸ It is reported that chitosan addition to PEGDA increased the flow behavior of the system, and the lowest level of PEGDA for the printing process from 30 decreased to 6.5% w/v. The change in the feed ratios of chitosan to PEGDA from 1:5 to 1:10 led to swelling dropped from 8.4 to 8.1%, respectively, whereas an increase in the ratio from 1:5 to 1:15 raised the elastic modulus.¹⁹⁸

3.2.2. Starch. Starch macromolecule shows an extensive application range in pharmaceuticals, bioengineering, and food since it is considered as a cost-effective biopolymer with excellent functionality. Starch originated from diverse sources, that is, cassava,²⁰ corn,¹⁶¹ potato,¹⁰⁷ rice,²² and wheat,¹⁹ has been utilized in the printing process to improve the flow properties and extrudability. Starch either in the granular state or gelatinized form can be incorporated into the biopolymeric system to create a printed construct with enhanced printability, improved biodegradability, precise geometries, and structural characteristics.^{11,80,158} Numerous attempts have been focused on the starch blending with other biopolymers including cellulose,⁸⁰ oat- and faba bean proteins,¹¹ and carrageenan-xanthan,⁸⁸ which shows desired processability and adequate structural strength to attain fine resolutions and improved shape retention. Chen et al.¹⁶¹ recognized a relationship between flow

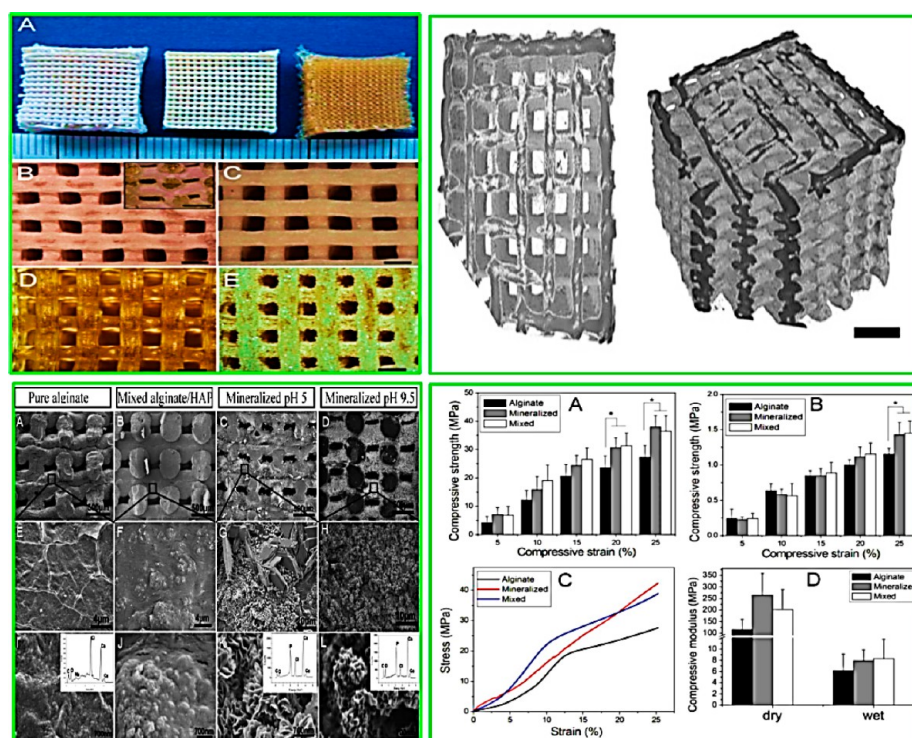


Figure 8. (Top-left) (A) Images of printed samples, from right to left: intact alginate, HAP, and alginate blend, mineralized alginate. Micrographs of (B) treated alginate in pH 9.5, (C) HAP and alginate blend, (D) intact alginate, and (E) treated alginate in pH 5. (Top-right) The μ -CT image of the treated scaffold in pH 9.5; (left) cross-sectional vision and (right) overview. (Bottom-left) Micrographs of (A, E, and I) intact alginate, (B, F, and J) HAP and alginate blend, and treated scaffold in (C, G, and K) pH 5 and (D, H, and L) pH 9.5. (A–D) Cross-sectional and (E–L) surface views. (Bottom-right) Mechanical properties of bioplotted scaffold at (A) dry form and (B) wet states. (C) Tensile strength plots at the dry form and (D) the scaffolds' elastic modulus. Reproduced from ref 4. Copyright 2015 American Chemical Society.

behavior and printing performance of 3D printed starches. The rheological data showed the shear-thinning behavior and strain-responsiveness character were obtained by using concentrated starches, which were printable to 3D constructs. Their results also specified that rice starch (15–25% (w/w)) gelatinized at 80 °C, corn starch (20–25% (w/w)) processed at 75 °C, and potato starch (15–20% (w/w)) treated at 70 °C had proper flow stress (140–722 Pa), yield stress (32–455 Pa), and elastic modulus (1150–6909 Pa), respectively. Yang et al.¹⁰⁷ investigated the change in the flow behavior and mechanical parameters of lemon juice hydrogels as affected by potato starch addition. The data showed that it was proper to adjust the nozzle height size similar to the nozzle diameter that could not be associated as important parameters affecting the printability. Regarding this printer, it was found that the nozzle diameter of 1 mm, extrusion rate of 24 mm³ s⁻¹, and nozzle movement with the speed of 30 mm s⁻¹ were determined to be optimum variables for the fabrication of the 3D objects quite similar to the design geometry with high resolution and a smoother edge.

In another study performed by Zheng et al.,¹⁹ it was revealed the starch hydrogel presented a reduced consistency index with improved extrudability, along with enhanced storage properties. The 3D printed objects showed a smoother surface, where 3D structures were more even with a compact matrix compared to the common gelatinization process. This proved printing process resulted in the cross-linked amylose decreased the empty areas, consequently altering the hydrogel matrix to a well-occupied chains gel network. Maniglia et al.²⁰ also demonstrated that the simple and efficient technique of dry heating treatment could expand the application of cassava starch, in particular for

3D printing. They assumed that hydrogel firmness was consistent with the profile of gelling printability. In this work, dry heating treatment could modify the molecular and granular characteristics of cassava starch, which resulted in a decrease in peak viscosity and increasing hydrogel hardness. The temperature used to induce gelatinization and the storage period were factors affecting each starch treatment. Azam et al.¹⁹⁹ characterized the printability of orange leather by adding varying ratios of wheat starch. The 3D printed matrix offered the optimum mastication feature with a starch ratio of 20%. The optimum printing performance for the printing process of orange leather was also set at 1.5 mm nozzle diameter, 1.5 mm nozzle-bed height, 245 mm³ s⁻¹ extrusion rate, and 35 mm s⁻¹ nozzle movement speed. Liu et al.¹³⁰ also showed controlling the starch level and process temperature were critical factors to adjust the starch printing performance. They showed that shear stress, shear strain, and elastic modulus parameters of potato starch, as well as the printing temperature, were important parameters to ensure successful printability during the printing process. Theagarajan et al.²² printed rice starch to construct 3D structures through an extrusion printing system. It was reported that the printing by a nozzle diameter of 1.5 mm at 150 cm min⁻¹ with a speed of 180 rpm provided an optimum printed architecture.

3.2.3. Alginate. Alginate has gained widespread interest in the printing context.^{3,12,125} As an anionic linear polysaccharide, it contains repeating units of β -D-mannuronic acid and α -L-glucuronic acid that occurs in a large number of species in brown seaweed.¹⁹⁴ Most of the prepared inks and bioinks formulations used in the 3D printing application include alginate as most

important constitute contributing to shaping retention, mechanical strength, and multifunctionalities of 3D printed constructs owing to the fast-ionic cross-linking ability and improved rheological properties.^{3,7,10,12,67,200,201} Alginate can also be mixed with other biopolymers to produce innovative oriented printed objects with enhanced printability. Chen et al.⁷ attempted to print a blend ink based on soy protein isolate, alginate, and gelatin via an extrusion-based printing system. They reported that the soy protein isolate blended by alginate and gelatin (2–10%) was well printed with a precise shape structure, in which introducing more gelatin levels (6–10%) induced more attractive objects.⁷ In a relevant work, Dankar et al.⁶⁷ attempted to construct the intricate geometries of potato puree through extrusion 3D printing. They evaluated the effect of alginate at three concentrations (0.5–1.5%) on construct stability, mechanical parameters, surface morphology, and optical properties of the 3D structures. Optimum printing variable was obtained at 4 mm nozzle size with 0.5 cm nozzle height, where a printing substrate based on potato puree/alginate blend offered stable end-shape 3D objects with high resolution and several built-up layers. Oyinloye and Yoon⁶⁵ found the optimum formulation prepared by alginate-based ink (80%) blended with pea protein (20%) for the 3D printing process. The blend system showed gelation temperature of about 43 and 38 °C with a heating rate of 5 and 2 °C min⁻¹, respectively. This implied a good 3D structure in the term of mechanical properties upon blending of alginate and pea protein as printable ink. This blending system also preserved its shape during printing and offered an improved structure after the printing process. Liu et al.²⁰² printed cross-linked alginate hydrogel scaffolds via an extrusion-based printer and assessed the impact of different printing factors on obtained cross-linked alginate 3D scaffolds. It was reported the alginate level had a critical impact on geometrical features and shape stability of 3D printed scaffolds. In another study, Park et al.¹⁴² assessed the possible mimicking the plant tissues through the printing process. The data showed that increasing alginate content resulted in an enhancement of printing performance. Luo et al.⁴ printed a scaffold based on alginate containing nanohydroxyapatite (HAP) through a bioplotting system along with in situ mineralization method. The physicochemical and structural features, as well as the ability of scaffolds for sustained protein releasing, were assessed. Additionally, the culturing of hBMSC (human bone-marrow-derived mesenchymal stem cells) was performed through the reaction of the cell to the 3D printed scaffolds. Results indicated the proposed technique was appropriate for manufacturing the blend scaffold comprising the nano-HAP layer, covering the surface of alginate chains evenly and entirely. Moreover, the surface mineralization method improved the structural strength, enhancing attachment of cells, where homogeneously dispersed in the system. Furthermore, the sustained protein releasing of the 3D blend scaffold was improved in comparison with neat 3D printed scaffolds without nano-HAP (Figure 8).

3.2.4. Cellulose. Cellulose, as the most abundant linear polysaccharides on earth, is a promising renewable resource able to address the demand for minimizing the environmental footprint, proposing a large number of advantages in manufacturing cost with desirable physicochemical and chemical features. However, the neat cellulose application in the 3D printing process is suffered from poor processability, low solubility, and lacks the stability required to construct a 3D structure.^{27,31,98,111,203,204} Therefore, native cellulose without

physicochemical and mechanical modifications is normally offered impractical for the 3D printing process as it can be degraded upon heating or severe extrusion shear force during extrusion. With proper physical, mechanical, and chemical modifications, cellulose can be applied to fabricating well-defined 3D constructs with enhanced functionalities and high-quality 3D structures. The modified cellulose-based hydrogel can be considered as a printable ink to produce the support objects since it can thermally liquefy and simply dissolve in water because of its thermal gelation feature (see section 4.4). Lille et al.¹¹ reported the applicability of cellulose from dried bleached birch Kraft pulp blended with the milk powder, cold swelling starch, oat, and faba bean proteins, rye bran for customized 3D printed products. In this regard, cellulose was mechanically modified by passing it once through an ultrafine friction mill. Then, the hydrogel was produced using a microfluidizer with an application of 185 MPa pressure to obtain an amorphous cellulose powder. After that, xanthan gum was incorporated into the cellulose ink media to obtain a cohesive 3D cellulose matrix. The optimum printability was found in the ink formulated with semiskimmed milk at a ratio of 60%, skimmed milk with a level of 15%, starch with an amount of 10%, oat protein concentrate in the level of 35%, or faba bean protein at the ratio of 45%, and rye bran with a ratio of 30%.¹¹ In another study, Holland et al.³¹ applied a mixture of amorphous cellulose powder and xanthan gum in the printing application. The improved processability and printability of the cellulose blended by lignosulfonate were per the investigation of Shao et al.¹¹¹ They stated that once cellulose/lignosulfonate blend ink showing a higher consistency index, it could be well printed, where the 3D structure, as square cuboids, was simply constructed without deformations.

3.2.5. Pectin. Pectins involve a diverse group of acidic polysaccharides characterized by the existence of D-galacturonic acid residues. They can produce an independent polymeric structure that is coextensive with that developed by cellulose and cross-linking glycans. It is necessary to blend pectin with other biobased materials to facilitate the printability, which has been approved and used in the culinary fields,^{74,174} wound dressing,¹⁷³ and cell culture.²⁰⁵ Low-methoxylated pectin has been widely utilized as a gelling agent for printing applications.¹⁷² The gelation of low-methoxylated pectin-based sol can be progressed by the development of calcium ions cross-linking among carboxyl groups.¹⁷² Vancauwenberghe et al.¹⁷² investigated the printing performance of a 3D hydrogel structure based on pectin, calcium ions, bovine serum albumin, and sugar upon extrusion 3D printing. In this work, an innovative printer head was designed and pectin stimulant was printed as an interior layer, and calcium ions were considered as an outer layer. The pectin levels were showed a positives impact on the hardness and elasticity of printed constructs. They also stated that the incorporation of sugar allowed an improvement in the ink consistency index, which affected printability and shapes fidelity. In another study, Vancauwenberghe et al.¹⁷¹ revealed the printability of pectin ink simulant via a coaxial print-head system. The coextrusion printer offered pectin gelation with enhanced functional properties and stable geometry, which did not need postprinting treatment. Vancauwenberghe et al.²⁰⁵ also presented land-plant-based cells were effectively embedded in 3D printable ink with great density, where the printed ink showed improved printability and high resolution. They supposed that ink formulation prepared with diverse contents of pectin did not change the cell viability. Long et al.¹⁷³ developed 3D printed biodegradable thermosensitive scaffolds

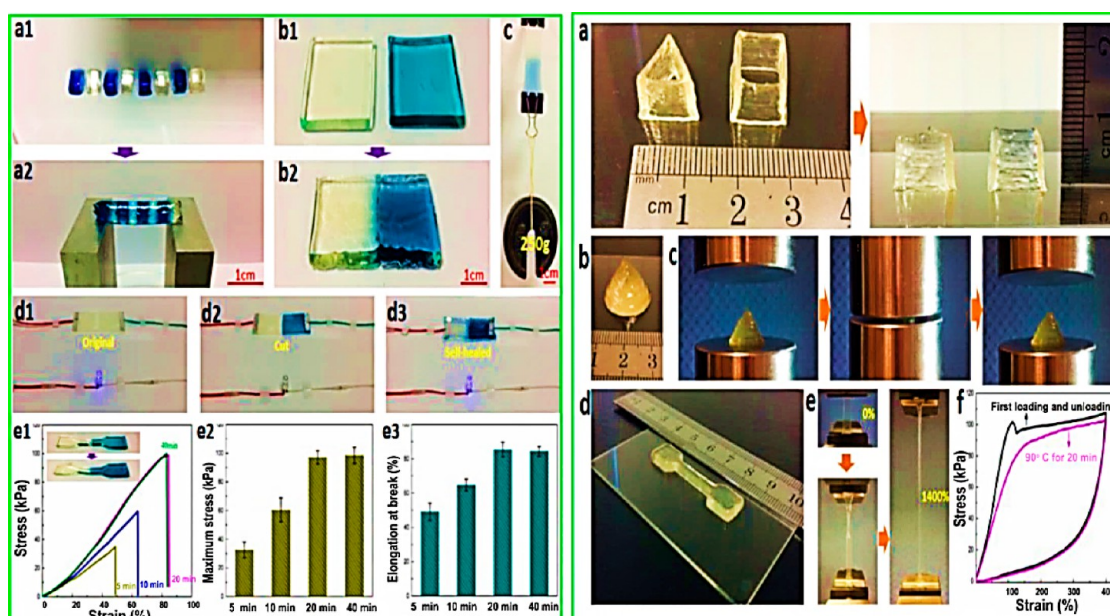


Figure 9. (Left) Freshly cut double network (DN) objects with tiny column-shaped (a_1). Self-healed cylinder links two “piers” supporting self-weight (a_2). Freshly cut DN objects with sheet shape (b_1). Self-healed sheet-shaped object (b_2). (c) Self-healed object (2.4×0.25) cm^2 maintains 0.25 kg weight. The current includes an LED joint with intact (d_1), cut (d_2), and self-healed DN object (d_3). Impact of storage time on stress–strain plot of the self-healed object (e_1). Storage time dependences of maximum stress (e_2); elongation at break (e_3). (Right) 3D printing DN constructs (a) 3D structures of the cube and hollow character and (b) cone shape. (c) Ability of printing cone object to recover its structure under 90% deformation rate and relaxation. (d) Printing a dumbbell-formed construct and its mechanical assay (e). (f) Stress–strain hysteresis regarding freshly printing object (black line) upon treating for 60 min and recovered object (pink line). Reproduced with permission from ref 206. Copyright 2017 American Chemical Society.

based on pectin and chitosan for wound dressing applications. The blend showed good printing performance, and the resulting lyophilized wound dressings displayed improved shape stability and flexibility. Cernencu et al.¹⁷⁴ designed novel bio-based ink formulations by using a blend of pectin and TEMPO-oxidized cellulose nanofibrils solution for printing application. The rheological assay exposed pectin content influenced flow properties of blend dispersion, maintaining the *pseudoplasticity* behavior with improving yield stress parameter and enhanced ink printability. Schutyser et al.¹⁷ stated that fabrication of a blend ink based on pectin, starch, and sucrose simplified the printing of caseinate dispersions, in which the 3D printing process of sodium caseinate dispersions was improved via an enzymatic cross-linking method even at a low sodium caseinate ratio.

3.2.6. Xanthan. Xanthan is an anionic microbial heteropolysaccharide obtained from aerobic fermentation of the bacterium *Xanthomonas campestris*. It is commonly incorporated into the flowable materials to modify the flow behavior of the material in tissue engineering and food printing.^{70,139} Xanthan is widely and more extensively used for printing application with gelatin,⁷⁴ carrageenan,³³ taro paste,¹⁰ amorphous cellulose powder,^{31,98} methylcellulose,⁸⁶ konjac gum,¹⁷⁵ and starch.^{110,176} Cohen et al.⁷⁴ assembled a 3D nonprintable meal construct with Fab@Home printer using a mixture of xanthan and gelatin with diverse flavoring agents. According to their results, neat gelatin and intact xanthan fitted with a poor structure to a firm character, whereas the blend of xanthan/gelatin was moved to a more granular character. As a rule, the higher level of xanthan and gelatin led to a stiffer hydrogel matrix with more granularities. Lipton et al.⁷⁰ stated the application of transglutaminase and xanthan gum could considerably maintain the resolution and geometrical stability of 3D structures through the

cooking process. Kim et al.⁸⁶ evaluated the impact of xanthan gum/methylcellulose blend on geometrical and structural features of dough to overcome the 3D shape instability of printing cookie constructs upon postprocessing. Their results revealed that the proportion of xanthan below 0.5 g/100 g in ink formulation led to drop suppression in structural strength and increased processability and extrudability. García-Segovia et al.¹⁷⁵ investigated the printability of hydrogel based on xanthan and konjac gum. They reported that konjac gum could be introduced into xanthan ink to enhance the flexibility and mechanical stability of 3D printed objects. Rheological data exposed that the printed hydrogel processed via the temperature of 50 °C showed decreased elastic character with more fluidity behavior. Higher dynamic rheological parameters were also achieved with a greater amount of xanthan gum and konjac gum. In another work, Huang¹⁷⁶ used a room temperature extrusion-based printer to fabricate a 3D structure of xanthan gum and starch. The results proposed that 5% xanthan paste slide off the spoon with the lowest deposit and most spreading, indicating low adhesiveness. Strother et al.¹⁷⁷ studied the impact of xanthan, guar, and gelatin on mechanical parameters and sensory features of pureed carrot. According to the texture profile analysis, the object comprising xanthan (2%) presented considerably greater hardness, cohesiveness, springiness, and gumminess parameters compared to other formulations. Holland et al.⁹⁸ modified amorphous cellulose through a ball mill and added it to xanthan gum to create 3D structures via binder jetting. They concluded these mechanically modified porous components can be considered as a dietary fiber to create low-calorie 3D printed food products. Zhang et al.¹³⁹ fabricated trimetaphosphate (STMP) chemically cross-linked printable and self-healing hydrogel ink based on silk fibroin and xanthan. Rheological data demonstrated that incorporation of the silk

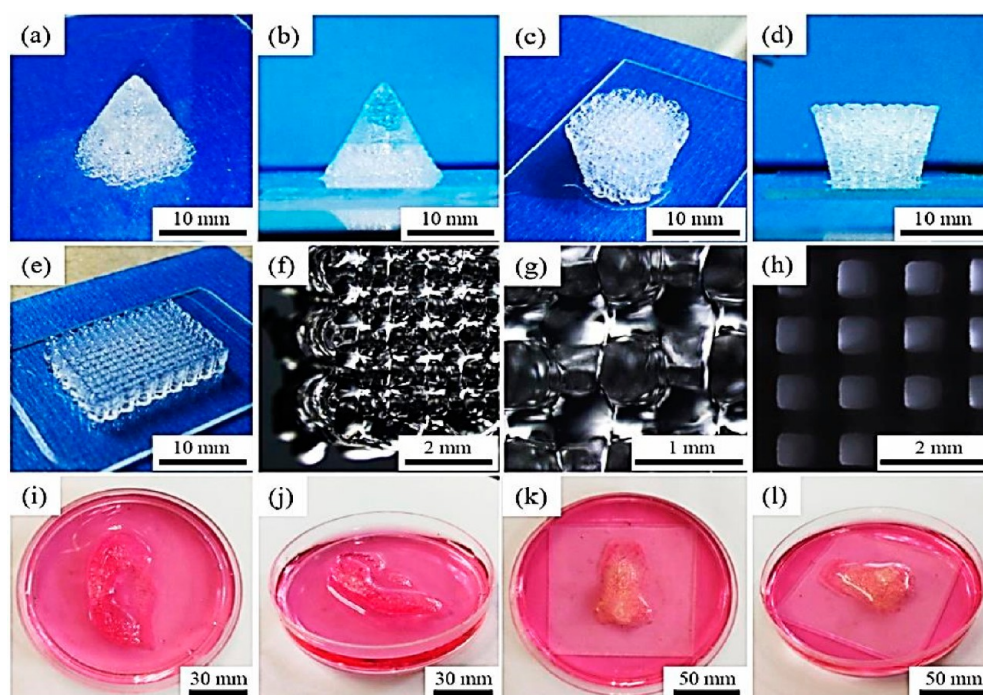


Figure 10. Images of 3D printed models prepared by gellan (1.5 wt %)/PEGDA (10 wt %) ink. Aerial view (a) and left view (b) photos of a sharp cone object. Aerial view (c) and left view (d) photos of a reverse square prism construct. (e) Aerial view photos of a cuboid object. Partially enlarged photos by stereoscope are also shown in panels f–h (upon treating by liquid nitrogen). Top view (i) and aerial view (j) photos of a 3D printed hydrogel human ear. Top view (k) and aerial view (l) photos of a 3D printed hydrogel human nose. Reproduced with permission from ref 218. Copyright 2018. Published by Elsevier Ltd.

fibroin microparticles into the STMP cross-linked xanthan hydrogel could be contributed to improving storage modulus and viscosity. It also indicated that xanthan/silk fibroin/STMP ink was more applicable to use as an injectable material for fiber development or 3D printing with high shape retention than the xanthan/STMP hydrogel. Dick et al.¹⁷⁸ recently evaluated the effect of xanthan and guar incorporation on flow behavior, mechanical, as well as morphological features of printed cooked pork objects. Upon freezing and heating as postprocessing treatment, introducing xanthan/guar into printable cooked paste caused improved mechanical features with potential utilizing in the common meals.

3.2.7. Carrageenan. Carrageenan is linear sulfated D-galactan extracted mainly from the red algae,^{206,207} containing repetitive units of D-galactose, as well (3,6)-anhydro-D-galactose joint with α -(1,3) and β -(1,4) glycosidic bonds. It is widely used for the development of the 3D printed constructs, where the flow behavior and physicochemical features of obtained printing structures are amended using carrageenan.^{33,119,179,180} A 3D printed composite construct has been developed based on carrageenan blending with gelatin,¹¹⁹ epoxy amine,¹⁸⁰ and xanthan gum/starch.³³ Caroway et al.¹⁷⁹ designed a special printing system equipped with a pneumatic pump to fabricate a well 3D printed carrageenan hydrogel. They stated that lengthy polymeric carrageenan strands are promoted by gelation mechanism, allowing the hydrogel well-formed in a three-dimensional fashion. Liu et al.³³ prepared multicomponent kappa-carrageenan/xanthan/starch hydrogel ink and the blend was printed via a 3D extrusion system. They showed that an increase in the amount of kappa-carrageenan considerably increased the complex modulus. This was predictable as a high amount of kappa-carrageenan could simply convert to a denser hydrogel because of developing a 3D structural matrix formed

with an aggregation of double helices. Liangliang et al.²⁰⁸ studied 3D printing of complex alumina parts via direct ink writing using thermally induced solidification by carrageenan swelling. The paste consisting of 0.4 wt % carrageenan with a temperature of 55 °C could be rapidly solidified on the 3D printing with good printability. Liu and Li²⁰⁶ synthesized an elastic double system gel with biodegradable and self-healing characters. In this way, the printable ink was cross-linked with mixing carrageenan by polyacrylamide (PAAm). Stiffness and toughness of cross-linked hydrogel system even with fracture were recovered to ~90% and ~85%, respectively. The author argued that this behavior was assigned to the thermoreversible property of the sol–gel transition of carrageenan. Moreover, this feature was accountable for self-healing character in carrageenan/PAAm double network, in which gel–sol–gel transition behavior upon the heating–cooling cycle led to healing the cut surfaces, displaying outstanding self-healing yield. The 3D printed double network hydrogels also established great tensile strength upon exposure to UV irradiation. Besides, double network hydrogel included deformation sensitivity, offering the 3D printed carrageenan/PAAm hydrogel was able to serve as a wearable sensor for detecting diverse body movements (Figure 9).

3.2.8. Gellan, Locust Bean, and Guar Gums. Some papers are dealing with the application of other promising biopolymers, including guar gum and locust bean gum for the 3D printing process.^{140,209–212} Guar gum is originated from the seeds of the *Cyamopsis tetragonoloba* plant. It is used as a thickening and viscosity control, texture, and body improver in the pharmaceutical and food industries, which obtains a high viscosity value in water within a few minutes.²¹³ The potential application of guar gum in the printed vitamin-D-fortified orange concentrate,²¹⁴ mashed potato,⁸⁸ printed packaging,²¹⁵ antifreezing, injectable, strain-sensitive hydrogel,²¹⁶ wound

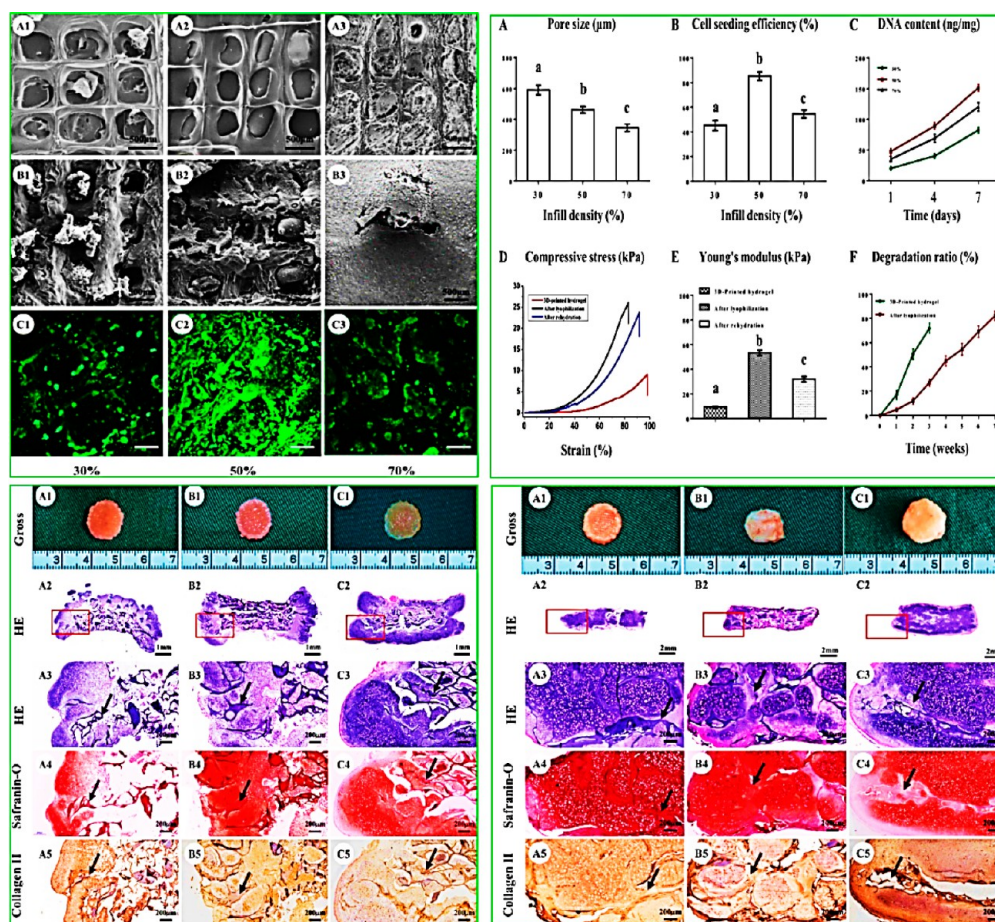


Figure 11. (Top-left) Images present the size of pore in 3D scaffold reducing by incremented infill density (A1–A3). In vitro culture after 4 days, pore matrix in the 50% and 70% clusters could be well-filled through cartilage extracellular matrix (ECM) and chondrocytes (B1–B3) and their relevant confocal micrographs (C1–C3). (Top-right) Size of the pore is reduced by incremented infill density (A). The 50% cluster attains maximum cell-seeding effectiveness after 1 day among all clusters (B). DNA measure displays an identical rising tendency (C). Compressive strength (D), Elastic modulus (E), 3D objects preserve greater mechanical parameters compared to printing gel (D, E). In vitro degradation scaffold period was extended to 56 days upon lyophilization, whereas printing gel was preserved to 28 days (F). (Bottom-left) All objects at 14, 28, and 56 days reserved initial structure developing cartilage-like tissues (A1–C1). Histologically, manufactured cartilage was developed in 14 days with characteristic lacunae matrices and cartilage-particular ECM structures at 2 weeks (A2–A5), at 4 weeks (B2–B5), at 8 weeks (C2–C5) and matures by incremented in vitro culture period along with increasing 3D printed scaffold degradation (A–C). (Bottom-right) Upon 56 days after in vivo implantation, objects from days 14, 28, and 56 in vitro homogeneously regenerated the mature cartilage having characteristic lacunae matrices and cartilage-specific extracellular structures (A₁–C₁). Structures at 2 weeks (A₂–A₅), at 4 weeks (B₂–B₅), and at 8 weeks (C₂–C₅). Reproduced with permission from ref 224. Copyright 2018 American Chemical Society.

dressings,²¹⁷ drug delivery system,²¹³ and human-scale nose architectures²¹⁸ has been recently demonstrated. Liu et al.⁸⁸ evaluated the flow behavior, morphological, as well as printability of mashed potatoes formulated with various biopolymers, including guar gum. They proposed that mashed potatoes showed a shear-thinning character where guar considerably influenced its flow behavior, water mobility, surface morphology, and printability. In another study, Kim et al.²¹⁰ studied the application of different biopolymers containing gellan, guar, and locust bean gum for food additive manufacturing. Gholamipour-Shirazi et al.¹⁴⁰ designed a printable biopolymeric functional ink aimed at use in the printing application. It was reported that locust bean (4%) and guar gum (4%) were recovered as 80% and 100% in the recovery index against the phase angle plot. Pan et al.²¹⁶ prepared multifunction guar gum–glycerol ionic hydrogel in the glycerol/water solution system, which showed the potential to be used in the printing process to develop wearable, flexible, and 3D printable skin.

The polysaccharide gellan gum includes a repeating unit containing β -D-glucose, L-rhamnose, and D-glucuronic acid with wide ranges of application in food and pharmaceutical as a thickening agent, structuring, and gelling agent, which promoted a hydrogel matrix with a rigid and brittle texture to a liquid form.²¹³ It is reported that gellan can develop easy-to-swallow dosage form, including 3D printed hydrogels and covered pills, where gellan could improve the releasing rate of active components from 3D printed medicines. Then, the potential application of gellan gum for the printing process has already been considered in the pharmaceutical and bioengineering rather than the food sector. Wu et al.²¹⁸ formulated a binary hydrogel system based on gellan/PEGDA and printed the obtained double network hydrogel by extrusion printing. This system combined greater shear-thinning character and recovery features of gellan with photo-cross-linking capability of PEGDA suitable for the fabrication of 3D human-scale nose architectures with high-fidelity (Figure 10). Lozano et al.²¹⁹ established an innovative process for the creation of a 3D brain-like construct

based on gellan gum. They established effective microencapsulation, survival, as well as produced a network based on primary cortical neurons and glia in modified printing gellan 3D structure. In another study, Yu et al.²²⁰ studied the potential application of gellan gum for wound dressing and cartilage by using the 3D printing process. Akkineni et al.²²¹ prepared blends of highly concentrated gellan gum and alginate to enhanced functionalities and printability for the printing process.

3.2.9. Hyaluronic Acid. Hyaluronan is a functional linear polyelectrolyte-based polysaccharide, occurring in the acid form. It comprises the repetitive unit of β -(1–4) D-glucuronic acid linked with β -(1–3) N-acetyl-D-glucosamine. This biopolymer is essential for controlling diverse cellular actions and tissue functionalities, covering proliferation, migration of cells, and differentiation, as well as angiogenesis.²²² According to these functionalities, hyaluronic acid is of interest in the 3D printing process, where it can be efficiently blended with other biopolymers based on methacrylated gelatin,¹⁸⁹ photocurable dextran,¹⁹⁰ and as a conjugate with thermos responsive poly(*N*-isopropylacrylamide) to promote cross-linking.²²³ The excellent cross-linking ability allows hyaluronic acid to develop a functional hydrogel maintaining its 3D geometrical structures upon printing. Moreover, the capabilities of hyaluronic acid to blend with human cells can produce promising printable bioinks for tissue engineering. Ouyang et al.¹⁸⁶ used hyaluronic acid as printable ink for 3D printing applications and reported that cross-linking reaction caused changes in produced 3D printing filament constructs and some differences in shape fidelity. Their results showed that the dual-cross-linking approach did not need the application of any common supporting component, including alginate and gelatin. This approach allowed the hyaluronic acid hydrogel to be considered for a particular process with the taking advantage of the elimination of secondary supporting system.¹⁸⁶ Shie et al.¹⁹¹ reported on an innovative liquid resin fabrication process of polyurethane-based photosensitive components linked with hyaluronic acid for 3D printing of customized cartilage scaffolds. Gaetani et al.¹⁸⁷ showed that the hyaluronic acid/gelatin matrix could be applied with the tissue printing process, which allowed human cell attachment and proliferation. After printing, the cells retained their cardiogenic phenotype in vitro for up to one month. Similar work was carried out by Sun et al.,¹⁸⁸ who printed a multicomponent system based on hyaluronic acid/PLA acid/PEG blend through the SLA technique. The printed constructs showed a compressive strength of about 780 kPa, which is appropriate for use in cartilage tissue engineering. Xia et al.²²⁴ fabricated an ink based on hyaluronic acid mixed with gelatin for scaffold printing. The methacrylic anhydrides along with photosensitizer were incorporated into a blend of hyaluronic acid and gelatin system, making the printable photocurable ink. Then, lyophilization was applied to additional improvement of mechanical features and delay scaffold degradation time. The 3D scaffold object designing by an infill density of 50% attained an appropriate interior pore construct proper for proliferation, distribution of cell, as well as adhesion. Also, freeze-drying notably increased the 3D printed object's mechanical properties, reducing the degradation degree matching to cartilage regeneration. Above all, 3D printing architectures included chondrocytes effectively renewed matured cartilage with characteristic lacunae matrix and cartilage-particular extracellular deposition (Figure 11).

3.2.10. Cyclodextrin and Maltodextrin. Cyclodextrin is shortened cone form oligosaccharides involving 6, 7, or 8 (α , β

or γ -cyclodextrins) repeating glucose units joint by α -(1 \rightarrow 4) glycosidic linkages. Cyclodextrins with well-recognized biocompatibility are a versatile device in pharmaceutical and bioengineering to serve as a vehicle for drug delivery application, supporting cell adhesion, and forming reversible scaffold. The capability of cyclodextrins for hosting the therapeutic components and also tissue-engineering applications opens innovative techniques in addressing the cutting-edge design of 3D printed constructs. In the food industry, cyclodextrins are only being explored as a stabilizing agent for flavoring applications and to minimize unpleasant odor and taste. The multifaceted abilities of cyclodextrins are also finding a place in the rapidly evolving field of 3D printing technology. It should be noted that an applicable limitation of 3D printing is the fabrication of cytocompatible bioinks that can resist the printing processing situations and result in 3D architectures, replicating the shape of the tissue gap. It is reported that using maltodextrin as the binding additive in the printing manufacture of scaffolds caused an issue concerning depowdering, resulting in weak shape accuracy associated with the original 3D design.¹⁸⁴ Conceição et al.¹⁸² used extrusion-based 3D printing to prepare 3D printed hydroxypropyl- β -cyclodextrin with the aim of fast-release printlets of carbamazepine. Allahham et al.¹⁸³ explored the application of the SLS printing system for the construction of an orodispersible printlet including ondansetron, where it was added to cyclodextrin structure. In another work, Andriotis et al.¹⁸¹ manufactured a 3D printable structure including pectin and honey formulated with β -cyclodextrins. Musazzi et al.¹⁸⁵ established the possible preparation of extemporaneous made by maltodextrin orodispersible films using a hot-melt ram-extrusion 3D printer. They reported that the optimal conditions to print a mixture of maltodextrins/glycerine were a ratio of 80/20 w/w and a heating temperature of 85 °C. Diaz et al.⁸² concluded that the binder comprising maltodextrin with a glass-transition temperature of 62 °C, proved outstanding printability in terms of resolution and printing accuracy of 3D printing architectures. Elbl, Gajdziok, and Kolarczyk²²⁵ attempted to develop benzydamine hydrochloride including orodispersible films through modified semisolid extrusion 3D printing technique, where orodispersible films consisted of maltodextrin, as a film-forming matrix, sorbitol as a plasticizer, and hydroxyethyl cellulose as a thickening agent.

3.2.11. Other Polysaccharides. Other kinds of polysaccharides are reported to employ as the printable component in 3D printing applications, such as inulin, gum Arabic, and pullulan. Inulin, as a storage carbohydrate in plants, is naturally occurring fructan formed with β -(2,1)-connected fructosyl residues that ends by a glucose unit.^{226–228} Inulin offers numerous functionalities, accompanied by positive industrial features owing to its gelling properties. By applying 3D printing, Severini and Derossi²²⁹ produced 3D printed food objects where a bulk portion of 15% of fat was replaced by inulin. In the printed food products, inulin acts as a dietary fiber with multifunctionality features stimulating bifidobacteria growth entire intestine, calorie reduction, and fat replacer. Gum Arabic is the most commonly applied amphiphilic polysaccharide in the pharmaceutical and food sector.¹⁴⁰ Some researchers mixed gelling agents with gum Arabic to develop a functional-based printable ink for fabricating 3D printed constructs.^{140,214} Azam et al.²¹⁴ studied the impact of a diverse range of biopolymers, including gum Arabic, on flow behavior and printability of vitamin D-fortified orange concentrate. Pullulan is another biopolymer used in the 3D printing process as a nonionic linear

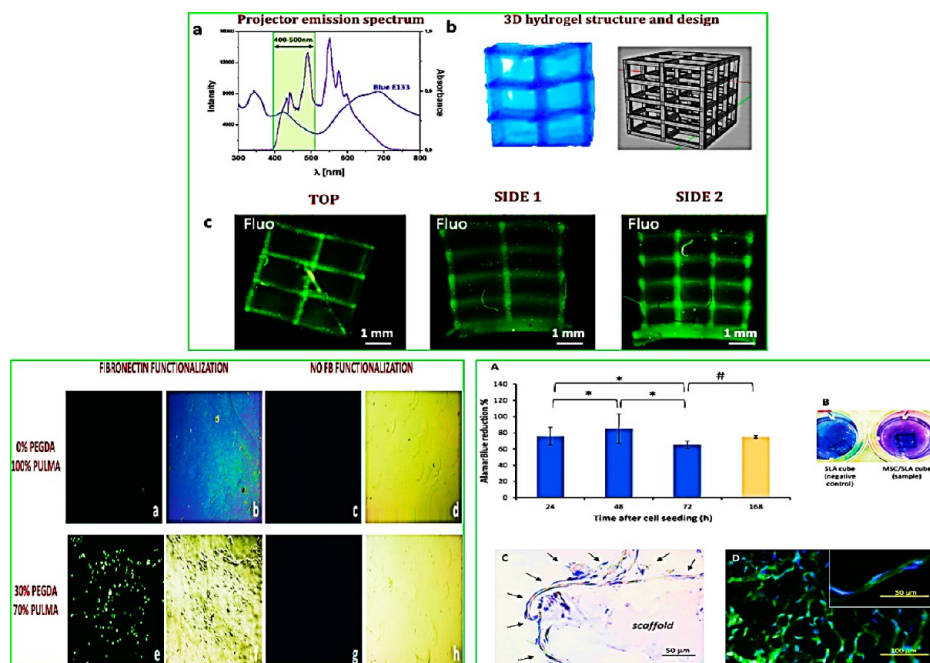


Figure 12. (Top) Hydrogel fabrication by SLA. (a) Emission spectrum of SLA light source, (b) 3D structure fabricated by methacrylated pullulan with 30% PEGDA, and (c) fluorescence micrographs of printed cubical objects. (Bottom-left) Cultured cell array in the two-dimensional matrices of methacrylated pullulan containing 0 (a–d) and 30% (e–h) polyethylene glycol diacrylate, with (a, b, e, f) and without (c, d, g, h) fibronectin functionalization. (Bottom-right) (A) Tendency of metabolic behavior about seeded human MSCs embedded printed scaffolds over time. (B) Change in culture substrate, altering from blue to pink. (C, D) Cryosections of MSCs printed cubical 3D structures after 3 days seeding. Reproduced with permission from ref 230. Copyright 2018 The Authors. Published by Elsevier, Ltd.

polysaccharide, which is obtained by starch upon the action of *Aureobasidium pullulans* (a yeast-like fungus).²¹³ Pullulan shows numerous valuable features, including an edible nontoxic compound, biodegradable, bio- and blood-compatible, biocompatible, nonmutagenic, and noncarcinogenic. Della Giustina et al.²³⁰ fabricated 3D printed methacrylated pullulan constructs of different sizes (millimeters to microns) through a special kind of 3D printing system. They argued that the 3D printed methacrylated pullulan objects could develop multisize printing scaffolds, confirming methacrylated pullulan shows suitable repellence for proteins and cells, and as a biocompatible component is simply functionalized by proteins, offering support for cell adhesion (Figure 12).

4. TUNING BIOPOLYMERS STRUCTURAL PROPERTIES FOR 3D PRINTING APPLICATION

Complex and sometimes opposite requirements of biobased polymeric inks have resulted in a concerted push to develop novel techniques of introducing the best promising qualities into inks. The biobased polymers offer supramolecular functional properties to ink dispersion, which while have frequently poorer rheological characteristics and weaker printing performance than the synthetic polymers.^{12,23,231,232} Therefore, the tuning properties of biopolymers give the way for a desired ink flow property and improved printability, attaining tailored geometry upon the printing process. Unlike the synthetic polymers, difficulty existed in the tuning biopolymer structures through modification techniques, as synthesizing modified biopolymers with prevalent synthetic approaches is challenging. Biopolymer modification processes frequently lack restricted mechanical strength, poor flow behavior, in addition to the elimination of unwanted side components with less than quantitative efficiencies. Early 3D printed products compromised between

rheological parameters, mechanical properties, and cytocompatibility to develop biobased polymeric inks. As the printing process has prolonged, there has been a substantial increase in the fabrication of novel methods to strengthen inks using innovative technologies.²³³ Nowadays, several common modification techniques are widely being applied for enhancement of rheological, mechanical, self-healing, biocompatibility, and thermoreversible properties of biopolymers, achieving enhanced functionality and printability.^{27,143,172,234} To attain desired functional properties, supramolecular biopolymers are tuned with different methods, including biopolymers blending, nanoparticle incorporation, and cross-linking. Cross-linking is an efficient modification technique to improve the flow behavior of ink-containing biopolymers, which can be performed through photo-cross-linking (with the addition of a photocurable group), chemical, enzymatic, and ionic cross-linking treatments. Cross-linking allows the postprinting treatments of biomaterials, leading to an important enhancement of thermal, flow behavior, and mechanical parameters, as well as an improvement of resolution and printing performance.¹² This section emphasizes the innovative trends in biopolymer-based inks strengthening and how the proposed modifications for 3D printed structures affect the crucial functionalities argued as described in the previous sections. Specially, we discuss the main ink strengthening techniques including biomaterial functionalization, supramolecular reinforced 3D structure, and fabrication of nanocomposite, as well as different cross-linking methods (Table 5).

4.1. Chemical Cross-linking Agents and Mechanisms.

Cross-linking methods are a linking reaction of biopolymeric strands using noncovalent or covalent linkages, promoting three-dimensional networks.^{261,262} The reaction process might be intra- or intermolecular linkages, which are

Table 5. Summarize Central Crosslinking Approaches, Described Utilizations, and Conditions

cross-linker/cross-linking mechanism	chemical involved biopolymers groups	protein or polysaccharide printing applications	application conditions/effects and drawbacks
aldehydes	nonprotonated primary amino groups (with proteins); hydroxyl groups (with polysaccharides)	gelatin; ^{23,24} silk fibroin; ^{23,5} collagen; ^{14,3} methylcellulose; ^{14,1,2,3,6} cellulose nanofibril; ^{2,37} hyaluronic acid; ^{23,9,23,9} alginate ^{24,0}	favoured by neutral/alkaline pH (for proteins) and through acidic pH (for polysaccharides); some aldehydes may be toxic; cinnamaldehyde can induce cinnamon flavor
oxidized polysaccharides	ϵ -amino groups	dextran; ^{24,1} gelatin/cellulose; ^{24,2} alginate; ^{24,3,24,4} hyaluronate/chitosan; ^{24,5} cellulose nanofibrils; ^{17,9,24,6} bean starch; ^{24,7} cassava starch ^{24,8}	favoured by neutral/alkaline pH
genipin	amino groups	silk fibroin/gelatin; ^{24,9} collagen; ^{25,1–25,3} gelatin; ^{25,4} alginate/gelatin ^{25,5}	neutral/alkaline pH; development of a dark blue color
transglutaminase	γ -carboxamide groups and ϵ -amino groups	meat paste; ^{7,0} sodium caseinate; ¹⁷ gelatin; ²⁵ gelatin methacrylate ^{26,25,6}	the reaction is developed at temperatures about 50 °C; inactivation of the enzyme should be done with higher temperatures
divalent cations	uronate blocks	alginate; ^{69,25,7} chitosan/polyphosphate; ^{23,4} TEMPO-oxidized cellulose ²⁷	
ionic cross-linking			
polyelectrolyte complexes	cationic groups (e.g., ammonium) and anionic groups (e.g., carboxylate)	gelatin/chitosan; ^{1,64,165} carboxymethyl chitosan/polyphosphate; ^{23,4} glycol oxidized hyaluronate/chitosan; ^{24,4} chitosan/pectin; ^{17,3} chitosan/poly(ϵ -caprolactone)/poly(ethylene glycol)-diacrylate; ^{25,8} gelatin/sodium alginate/carboxymethyl chitosan ^{25,9}	
photo-cross-linking	amino groups	alginate; ^{1,2} collagen; ^{12,2} chitosan; ^{1,68} locust bean; ^{21,7} gelatin ^{26,0}	

the main methods for the improvement of the biopolymeric structure. Chemical cross-linking causes by covalent linking among biopolymeric strands performed through sulfur vulcanization, high-energy radiation, and chemical agents,^{262,263} whereas physical methods include noncovalent linking, that is, cation ionic cross-linking, hydrogen, and hydrophobic interaction.^{263,264} Cross-linking is particularly convenient for proteins or polysaccharides to improve the physicochemical properties of 3D printed constructs. Those classes of biomaterials have been broadly studied because of their biodegradable, renewable features, and extensive cross-linking site suitable for cross-linking.^{23,24,143,235,236}

4.1.1. Aldehyde Cross-linking Agents. The chemical cross-linker contains a responsive group, which is chemically linked with a particular free active group including amine ($-\text{NH}_2$), carboxyl ($-\text{COOH}$), ethylene ($-\text{CH}_2=\text{H}_2\text{C}-$), and thiol ($-\text{SH}$) groups.²³² Chemical cross-linkers promote a covalent linkage to the polymeric backbone, giving the approach to form a firm matrix. Numerous cross-linking agents, differing in mechanisms, have been applied for protein modification. Aldehydes, including glutaraldehyde and formaldehyde, are the most frequently utilized cross-linking agents for protein modification. Formaldehyde comprises only one reactive group, showing the widest reaction specificity.^{143,265} Formaldehyde can be cross-linked proteins through a two-step mechanism, where the initial one is related to developing the methylol product, and the last step is producing methylene linkages among strands (Figure 13a). Glutaraldehyde also has high levels of efficiency in the term of cross-linking reaction due to the existing two reactive moieties;²⁶⁴ however, it shows the local toxicity and consequent calcification in long-term implants for printing process.²³

4.1.2. Cross-linking of Proteins with Aldehydes. Many printable inks including collagen and gelatin have been cross-linked by functionalization to enhance structural strength and stability in vivo conditions.^{23,24,143,235} The structural protein including collagen and its derivatives without a cross-linking process will form mechanically inferior hydrogels upon the 3D printing process. In this regard, chemical cross-linking of collagen and gelatin can be performed by formaldehyde and glutaraldehyde agents.^{23,143} The cross-linked collagen upon acid-soluble collagen neutralization forms an insoluble compound, which lacks the substantial variant suffering multifunctionalities. According to the mentioned disadvantages, and with consideration of considerable collagen molecular weight, it is scarcely considered for additive manufacturing in the single form.²³ As an alternative, collagen derivative, that is, gelatin simplifies printing and developing a complicated three-dimensional matrix, whereas preserving collagen advantages, such as biodegradability and biocompatibility. Gelatin, however, has poor rheological and mechanical characters, making it improper for additive manufacturing applications. Hence, to improve gelatin printability and maintain the geometrical structure of 3D printed constructs, many attempts were performed on the way to tuning the cross-linking types in the gelatin printable ink to modify the lateral functional groups between the chains. Klotz et al.²³ reported a review focusing on gelatin cross-linking methods with the aim of modification of printable gelatin ink by using a variety of chemical modifications. Mechanical strength, resolution, and printing performance of the 3D printed objects prepared by gelatin are considerably improved through glutaraldehyde cross-linking.²³ In an investigation performed with Wang et al.,²⁴ they plotted 20 (w/v)% glutaraldehyde for gelatin cross-linking but had to reduce the temperature of the

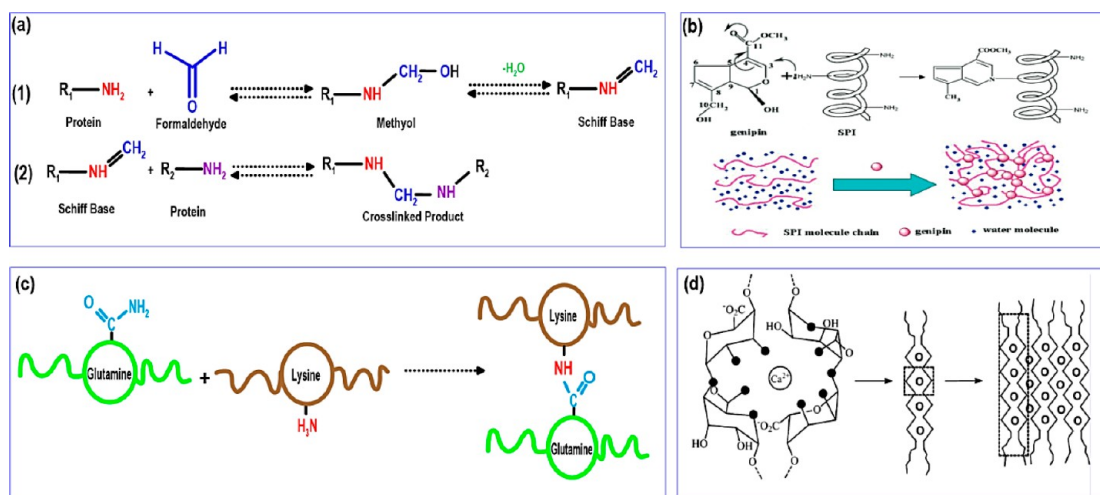


Figure 13. (a) Cross-linking reaction formed among formaldehyde with an amine group. (b) Schematic illustrations for the cross-linking reaction of soy protein isolate (SPI) and genipin, where a cross-linked network is formed. Reproduced with permission from ref 265. Copyright 2009 American Chemical Society. (c) Cross-linking process performed by transglutaminase. (d) Schematic illustration of the hierarchical structure of egg-box junction zones in alginate/calcium gels: (left) coordination of Ca²⁺ in a cavity produced by a pair of guluronate sequences along alginate chains, (middle) egg-box dimer, and (right) laterally associated egg-box multimer. Dark filled circles represent O₂ possibly involved with calcium ions coordination. The open circles represent Ca²⁺ ions. Reproduced with permission from ref 194. Copyright 2007 American Chemical Society.

printable ink solution below 20 °C, leading to a greatly physically gelled solution. The development of 3D printed hepatocyte-gelatin constructs cross-linked with glutaraldehyde was reported to have a viability of 93%.²⁴ In another work by Pitjamit et al.,²³⁵ silk fibroin was cross-linked by using glutaraldehyde (0.0025%) for the FFF printing process.

4.1.3. Carbohydrates Cross-linking with Aldehydes. It is reported that aldehydes can chemically cross-link reactive free groups of carbohydrates for example methylcellulose,²³⁶ cellulose nanofibril,²³⁷ hyaluronic acid,²³⁸ and alginate²⁶² for the 3D printing process. Regarding this type of cross-linking, in contrast to proteins cross-linking by aldehydes, a strict environmental factor including reduced pH with high temperature is required.²³¹ Torres-Rendon et al.²³⁷ manufactured cellulose nanofibril hollow tubes by the 3D printing process. The cellulose nanofibril was cross-linked either with covalently glutaraldehyde linkage or through complexed calcium ions, providing improved structural strength for printed hydrogel objects. An enzymatic degradation allowed the 3D printed cellulose nanofibril scaffold resealed the confluent cell layer, leading to an efficient drug delivery system for macroscale 3D cell architectures.²³⁷ It was reported that modification of hyaluronic acid improves the viscoelastic and rheological parameters of hyaluronic acid-based ink upon extrusion printing in addition to the construct stability upon the printing process. As an instance, hyaluronic acid was treated by aldehyde reactive group and hydrazide, providing self-healing with the shear-thinning character for bioink because of promoting the cross-linking mediated by hydrazine linkages.²³⁸ In another related work, Weis et al.²³⁹ fabricated hydrogels based on oxidized hyaluronic acid, which was cross-linked by adipic acid dihydrazide for their appropriateness as bioinks to produce a mechanically stable hydrogel with good printability. However, cross-linking of biobased materials by aldehydes is fairly used in 3D printing and bioprinting due to the aldehyde residues toxic compound remains in cross-linked objects, which is extremely challenging especially their migration in food and pharmaceutical compounds.²³ Thus, other nontoxic or less toxic cross-linker

materials as better alternatives in the 3D printing process have been widely applied.

4.1.4. Genipin. Genipin is a natural cross-linker that is 10 000 times less cytotoxic than glutaraldehyde, and it can fabricate stable cross-linked printed constructs with resistance against intense mechanical condition (like shear force in the extrusion 3D printing process) and enzymatic degradation.^{231,266} To improve mass retention, enhance mechanical strength, and preserve structural properties of 3D printed objects, genipin can be used to develop an insoluble structure without using the toxic cross-linking approaches (Figure 13b). Regarding the 3D printing process, genipin has been stated to cross-link amino groups in silk fibroin with gelatin,²⁴⁹ collagen,²⁵⁰ chitosan,^{251,252} and gelatin.²⁵⁴ Kim et al.²⁵⁰ developed highly cross-linked collagen hydrogels for 3D printing through the cross-linking via genipin for more support cross-linking and, thus, enhance the mechanical properties. Liu et al.²⁵¹ compared the mechanical property and biological feature between neat chitosan scaffolds with chitosan-based scaffolds cross-linked with genipin and pectin through a 3D plotting technique. They detected that the alternative cross-linking method led to stronger scaffolds with less chance for degradation and improved developed osteoblast cell proliferation. Hafezi et al.²⁵² performed cross-linking of chitosan-based film matrices by genipin as a cross-linker for the 3D printing process. The water uptake character and in vitro medicine releasing model exposed that genipin cross-linked 3D printed film could swell and release the drug, which can be applied to managing wound exudate. Moreover, cytotoxicity assay confirmed that the 3D printed cross-linked films were not toxic. In another study, Montemurro et al.²⁵⁴ used a polymeric system based on gelatin in phosphate-buffered saline with collagen solutions (1:1 weight ratio) as a template and cross-linked it with different genipin concentrations. Rheological analysis exhibited a rather large time window, in which the polymeric system produced by genipin/gelatin/collagen could be applied a range of 0.1–1.5% w/w concerning gelatin for the 3D printing process. Nagiah et al.²⁵⁵ also attempted to cross-link gelatin and sodium alginate through genipin with various geometries for the 3D printing process. They reported that

differences in the contact parts among the strands from adjacent layers of printed constructs resulted in the important difference in compression modulus. They also stated that by taking advantage of genipin cross-linking, the 3D printing gelatin/sodium alginate objects presented well-defined structures with improved geometries. Hafezi et al.²⁵³ developed a novel genipin cross-linked chitosan ink and processed it effectively through an extrusion bioprinter. They proposed that this approach could overcome the current printing limitations with extrusion-based bioprinting.

4.1.5. Oxidized Polysaccharides. Oxidation of biomaterials for the 3D printing process has been stated through oxidizing agents, including sodium periodate,^{241–245} TEMPO-mediated oxidation,^{246,267} ozone gas,^{20,247,248} and hydrogen peroxide,²⁶⁸ which results to improve rheological properties of printable ink to develop a highly complex 3D objective. The oxidation of dextran using sodium periodate is a recognized technique to functionalize dextran with aldehyde part. This modification approach has been extensively used to conjugate N-nucleophiles owing to the fast and almost complete reaction process.²⁴¹ A comparable work regarding dextran oxidation was performed with Du et al.,²⁶⁹ who developed an extrudable hydrogel based on phase separation of oxidized dextran and gelatin with tunable gelation time below physiological pH. Du et al.¹⁵⁶ stated that the oxidized dextran containing aldehyde groups could react with amine side groups of chitosan and gelatin to in situ generate a series of hydrogels for applications in hemostatic agents, tissue adhesives, smart drug delivery vehicles, and antibacterial materials. Jiang et al.²⁷⁰ also fabricated hydrogels based on oxidized dextran, cellulose nanocrystal, and gelatin scaffolds through 3D printing. The printed filaments widths proved the oxidized dextran showed an important impact on the printing performance of 3D printed hydrogels. Lee et al.²⁴³ also oxidized alginate by sodium periodate and produced reversible imine bonds between oxidized alginate and silica nanoparticles, leading to improved rheological parameters and high printing fidelity of printed objects. Similar work was accomplished by Schwarz et al.,²⁴⁴ who oxidized alginate by sodium periodate and then incorporated it into a gelatin system to develop 3D printed grid-like shapes. Jiang et al.²⁴² prepared a blended ink based on gelatin and cellulose nanocrystals and oxidized the obtained mixture by sodium periodate. This blend ink showed a little swelling magnitude with an improved breaking strength in comparison with neat gelatin hydrogel. Furthermore, the flow behavior experiments confirmed that the hydrogel revealed greater elastic modulus with suitable rheological properties for the printing process.

The application of native starch in the printing process suffers from many weaknesses such as weak processability, high flow behavior index, weak self-healing, and thermoreversible features. To obtain a functionalized modified starch suitable for the 3D printing process, it is often modified through different modification methods. The common chemical and physical modifications are oxidation and dry heating treatments, respectively. The ozone treatment approach has found good results for starch modification and led to enhanced functional properties for 3D printing applications.²⁰ Ozone processing can promote starch modification by the cleavage of the glycosidic bonds of amylose and amylopectin, resulting in the replacement of hydroxyl groups with carboxyl and carbonyl groups, primarily in the amorphous areas of the granules. Maniglia et al.²⁴⁸ recently demonstrated that ozone treatment is a related strategy for cassava starch modification intended for 3D printing. The

hydrogels produced by native and ozonated starches presented improved printing performance once gelatinization temperature set at 65 °C; however, a further increase in the temperature led to ozonated starch produced more printable hydrogels. Dry heating treatment (DHT), as a simple physical method for starch modification, includes heating starch at temperatures between 110–150 °C for 1–4 h, keeping moisture content low (<10% w/w).²⁰ Maniglia et al.²⁰ reported the effective DHT method could enlarge the application of cassava starch, especially for the 3D printing technique. They stated that the 4 h heating process generated hydrogel-based inks with enhanced printability, leading to 3D architectures with well-defined shapes and improved resolution.

TEMPO oxidation of cellulose shows a great selectivity for primary alcohol groups on C-6 carbons, in which the amount of oxidation can be precisely controlled. To this effect, TEMPO-oxidized cellulose nanofiber is a favorable reinforcing candidate for the 3D printing process. Cernescu et al.¹⁷⁴ fabricated an innovative ink formulation by using TEMPO-oxidized cellulose nanofibrils and pectin for 3D printing. Such oxidized cellulose nanofibrils/pectin formulations presented the potential to be utilized as hydrogel inks in 3D bioprinting applications. In another study, Wei et al.²⁶⁷ fabricated a multicomponent nanocomposite ink based on TEMPO-oxidized cellulose/alginate/laponite nanoclay. This printing ink showed structural stability with long-term protein releasing behavior. Fiorati et al.²⁷ TEMPO-oxidized cellulose nanofibers and fabricated a well-defined hydrogel with tunable rheological features, which can be applied as an appropriate tool for bioprinted structures. Another oxidation treatment of polysaccharides by using glycol oxidized was recently performed. Ko et al.²⁴⁵ revealed that glycol oxidized hyaluronate and chitosan could be applied to develop a self-healing ferrogel with superparamagnetic iron oxide nanoparticles. The printed constructs were produced through the 3D extrusion printing process, presenting the promising potential for 4D printing with a magnetic field. Weis et al.²³⁹ also oxidized hyaluronic acid using NaIO₄ for 3D printing and used it as a bioink for bioprinting. Their results presented the rheological and mechanical features of tunable 3D printed hydrogels were critically related to concentrations of oxidized hyaluronic acid.

4.2. Enzymatic Cross-linking. There is increased attention for enzymatic cross-linking in 3D printing application as a nontoxic and certain biotechnological means to improve the functional features of biobased materials because of the need to minimize the non-natural components, as well as the increasing demand for protein alternatives that do not depend on the animal basis.^{25,26,256} Although chemical reagents are frequently used to develop the covalent bonds between protein chains, enzyme-mediated cross-linking makes safer and improved control of specificity through selecting a suitable enzyme.²⁷¹ There are different enzymes capable of developing covalent cross-links in proteins, which have been applied in additive manufacturing. In this regard, several efforts have been developed to enzyme-mediated cross-linking of biopolymers for the 3D printing process.^{17,25,26,70,256} Transglutaminase is responsible for certain biological actions containing epidermal keratinization, blood clotting, and controlling erythrocyte membranes (Figure 13c). Enzymatic cross-linking can be induced using transglutaminase in an extrusion-based printing process.¹⁴³ Lipton et al.⁷⁰ described that transglutaminase cross-linking offered the desired functionality of printed meat in terms of printability and stability of 3D structures, in which they

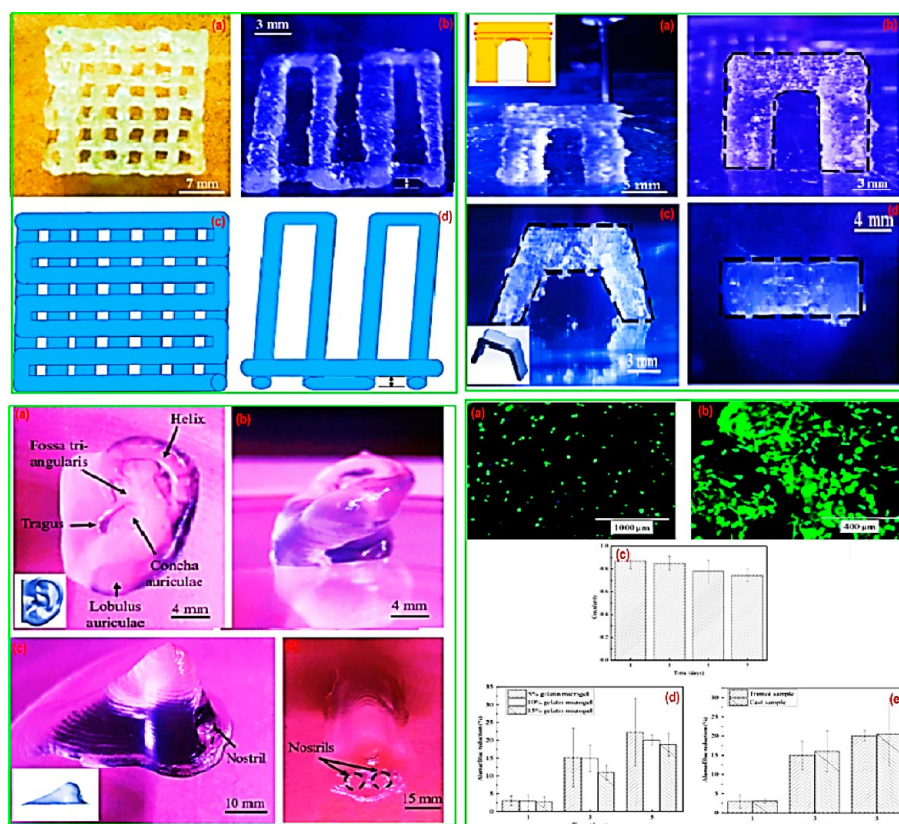


Figure 14. (Top-left): Image of lattice object. (a) Top view and (b) printed two layers' isotropic view. (c) Top view of the finished object and (d) 3D design of printed two layers' isotropic view. (Top-right) (a) Triumphal arch and (b) its front view. (c) Side and (d) top views of printing bridge object. (Bottom-left) Ear design. (a) Top and (b) front views of printing ear object. (c) Nose design and (d) top view of printing nose object. (Bottom-right) Biocompatibility investigations of designing gelatin hydrogel ink. Morphological evaluations of the cell (a) upon finishing printing and (b) upon 2 weeks of culturing. (c) Circularity of cell over the culture period. (d) Decreasing ratio difference of Alamar Blue with diverse gelatin levels in microgels. (e) Decreasing ratio difference of Alamar Blue among printing object and casting object. Reproduced with permission from ref 261. Copyright 2020 American Chemical Society.

produced high resolution and intricate shape of 3D printed meat using transglutaminase as a food additive. Transglutaminase addition to the meat paste before the printing process led to retained rheological properties of materials with the development of a new protein matrix.⁷⁰ This change could be described by the fact that catalyzes protein cross-linking by making the creation of an amide linkage among the carboxylic groups of glutamic acid, as well amine groups of lysine, in a divalent cation ionic process. Therefore, the protein portion in meat paste was enzymatically cross-linked, resulting in self-supporting 3D structures.²⁷² Though, the application of transglutaminase, even though has possibly valuable impacts on final structural strength, which is in contrast with the recent marketplace tendency of returning to more organic products. This insinuates any 3D object fabricated through the mentioned type of cross-linking reaction may be meeting with customer resistance, leave alone regulatory barriers in some countries.²⁷³

Schutyser et al.¹⁷ produced a cross-linked sodium caseinate by transglutaminase to examine its printing performance. It was observed gelation process promoted in caseinate needed higher temperatures upon transglutaminase curing; presenting a positive feature for 3D printing since a low level of caseinate offered an acceptable printability. Irvine et al.²⁵ defined a technique to cross-link gelatin by using transglutaminase for cell printing, which could be considered as healthy products including bioactive cells. Zhou et al.²⁵⁶ presented an approach to adjust the flow behavior of gelatin methacrylate via limited

enzymatic cross-linking of gelatin ink by transglutaminase. They assumed that in contrast to the other enzymatic cross-linking approaches, in which the flow behavior could not be adjusted once the reaction process starts, their method, to a great level, kept the stable rheological features with the introduction of deactivation stage upon gaining adjusted flow behavior. In this regard, calcium ion-independent transglutaminase media were added to partly covalent linkage development among strands of gelatin methacrylate. Upon finishing the printing process, an additional postprinting reinforcing method by using photo-cross-linking was performed. The secondary cross-linking confirmed the longstanding strength of printed constructs aimed at following cell evaluations to enhance the usability of bioink. Basara et al.²⁶ presented a dual cross-linking technique for gelatin methacrylate through cross-linking the methacrylate introduced $-NH_2$ groups, and also transglutaminase to enzymatically cross-link the hydrogels. The data exhibited double cross-linking reaction enhanced rigidity and viscosity of gels with no negative effect on the cell viability in comparison with one-step cross-linking reaction, either by UV irradiation or transglutaminase cross-linking reaction.²⁷⁴

On the other hand, some efforts have been completed to cross-link biobased polymeric inks with other types of enzymatically cross-linking for additive manufacturing. Zhou et al.¹³⁵ assessed the influences of a Maillard product based on enzymatically hydrolyzed pea protein and xylose on the printing performance of 3D printed structures. Reportedly, compared to

the object produced by enzymatic hydrolysate, 3D printed cross-linked object was shown an enhancement in the physico-mechanical features and an improvement in the printability of 3D printed architectures. Besides, 3D printed objects containing enzymatically hydrolyzed pea protein/xylose Maillard product offered greater thermal stability than that of developed by enzymatic hydrolysate, where the cross-linked 3D objects with 6 g xylose showed the best printing performance. In another work conducted by Petta et al.,²⁷⁵ they studied the printability of 3D printed hyaluronic acid-treated by enzymatic- and photo-cross-linking methods. Then, the tyramine-modified hyaluronic acid-treated with dual cross-linking reaction was characterized. The results showed that the tyramine enzymatic cross-linking process produced smooth hydrogel proper for cell encapsulation and extrusion-based printing process. The secondary cross-linking reaction through a visible light process allowed the structural retention of a 3D printing object. Song et al.²⁶¹ improved the printing performance of 3D printed gelatin objects by designing a microgel-based 3D bioprinting ink. An entirely modified biocompatible viscous ink was fabricated using gelatin preprocessing into covalently cross-linked microgel. In presence of curable gelatin sol, two-phase gelatin printable hydrogels were injectable, became stiff rapidly upon extrusion, and enabled the suitable manufacturing of architectures from pure gelatin, without any polymeric supporting system. This method offered a simple printing construction of 3D structures based on the lattice, tube, as well as human anatomic-based shapes. The generated shapes further enzymatically cross-linked once dispersed in transglutaminase solution, creating a stable 3D object. It was reported that besides minimizing the complication of ink design, the cross-linked ink might simplify the conversion of 3D printed architectures to medical sectors (Figure 14).

4.3. Physical Cross-linking. **4.3.1. Ionic Cross-linking.** The ionic cross-linking could be accomplished by incorporating two oppositely charged polymers or directly blending small polyions into polymeric inks.^{27,172,234} The ionic cross-linking reinforces the 3D printed matrix against osmotic pressure and also regulates a dual swelling/deswelling behavior as pH across pK_a and pK_b .^{120,257} Thanks to the stiff and lengthy backbone polymeric matrix of alginate, the 3D printing process of alginate shows several drawbacks.²⁷⁶ Approaches contain tuning its structure, increasing the cross-linking degree of alginate-based ink, and developing a multicomponent system, making it proper for different additive manufacturing methods, such as extrusion and inkjet printing, since the 3D geometrical structure is maintained stably.²⁷⁶ After mixing alginate with Ca^{2+} ions, multivalent coordination was created between carboxylic groups of alginate and metal cations, giving a viscoelastic hydrogel (Figure 13d). A partially Ca^{2+} -cross-linked alginate hydrogel was developed by Li et al.²⁵⁷ using 4 wt % of alginate and 0.4 wt % of $CaCl_2$ for direct ink write printer. The extruded structure was progressively immersed in a solution of $CaCl_2$ upon printing enhancing supramolecular cross-linking density, thus developing a robust self-supportive 3D construct. Kuo et al.¹²⁰ produced 3D printed bioscaffold based on gelatin and alginate using ionic cross-linking. They stated that the soaking period aimed at postprocessing changed scaffold softness, its stability, and mechanical parameters. After immersing printed constructs in an ionic calcium-enriched solution for a longer period, the softness character of the scaffold was greatly enhanced, albeit it led to increasing deformation. Müller et al.²³⁴ described the formulation and construction of multicomponent carboxymethyl chitosan/polyphosphate blends. The binary system was

ionically connected through calcium ions linkages in a thermodynamically stable manner providing a porous matrix, which led to $-OH$ groups linked with primary alcohol and amine groups. The printed hydrogels exhibited good printability, precisely tailored geometry of the printed structures, and improved biocompatibility with fibroblast skin cells. Fiorati et al.²⁷ prepared stable hydrogels with tunable rheological features through introducing Ca^{2+} ions to aqueous dispersions of TEMPO-oxidized and ultrasonicated cellulose nanofibers, which is suitable to manufacture 3D materials with embedded bioprinting cells objects.

Ionic cross-linking in the presence of other cations has also been applied for the 3D printing process. One promising simple alternative method to improve the flow behavior of soy protein isolate gel is salt incorporation. This method then results in quick gelation and aggregation of the protein, where hydrogel rigidity was nonetheless not affected.²⁷⁷ Numerous efforts were indeed applied diverse ionic salt kinds to promote the protein gelation, including KCl ,²⁷⁸ $CaCl_2$,²⁷⁹ $NaCl$,²⁸⁰ $CaSO_4$,²⁸¹ and $MgCl_2$.²⁸² $NaCl$ is of special interest in 3D printing applications as it is a simple salt, which reduces the viscosity and induces gelation of soy protein aggregates. Phuhongsung et al.¹¹⁵ added $NaCl$ in a blend of soy protein and xanthan gum, where 3D printed objects showed excellent resolution and printability. Xu et al.²⁸³ demonstrated that it is possible to obtain bulk chitosan/tripolyphosphate scaffolds with different non-cross-linking primary amine levels. For this, the ionic strength-dependent solubility of chitosan was applied to control the magnitude of reaction between chitosan and tripolyphosphate in the presence of $NaCl$. They argued that the non-cross-linking primary amine in 3D printed chitosan constructs influenced mechanical parameters, protein adsorption, as well as cell behavior. Abouzeid et al.²⁸⁴ printed cross-linked PVA/alginate/reactive cellulose nanofibers scaffolds. The cross-linking was achieved in the presence of Na_2HPO_4 . The cross-linked ink was printed via 3D printing and a consequent in situ mineralization of calcium phosphate upon scaffold cross-linking was performed using soaking in a $CaCl_2$ solution. In another study, Gutierrez et al.²⁸⁵ generated innovative antimicrobial 3D printed hydrogels formulated with alginate, bacterial-cellulose, and in situ-fabricated copper nanostructures with improved printability. Before 3D printing, two approaches were established for the development of the alginate hydrogels. The first one was ionic cross-linking with a solution containing calcium ion afterward ion exchange using copper ions, and the second one was the ionic cross-linking reaction by copper ions. Fischetti et al.²⁸⁶ attempted to blend chitosan with gelatin to form a polyelectrolyte complex to improve printability and shape retention. In this regard, tripolyphosphate was applied as a cross-linking agent for chitosan-based scaffolds. Their results showed the surface morphology and geometrical stability of the 3D printed scaffolds upon cross-linking process were dependent on cross-linking conditions.

4.3.2. Polyelectrolyte Complexes. Polyelectrolyte complexes are simply developed among anionic and cationic polyelectrolytes. The main interaction in polyelectrolyte complexes is the strong electrostatic association, but hydrogen linking, hydrophobic, dipole, or van der Waals interactions could be involved. A recognized case is polyelectrolyte complexes developed through ionic interaction among ammonium group (NH_4^+) in cationic chitosan and carboxylate group of anionic alginate.¹⁶⁵ Ng et al.¹⁶⁴ produced polyelectrolyte gelatin-chitosan hydrogel for 3D printing and stated the addition of

gelatin into chitosan colloidal dispersion made a well-defined polyelectrolyte printed hydrogel for the printing process. Zolfagharian et al.¹⁶⁵ also developed printing adjustment and parameters to produce a 3D construction based on chitosan/gelatin polyelectrolyte hydrogel actuator upon severe analysis condition regarding process parameters. The results revealed the printability enhanced maximum deflection rate, as well as the degree of deflection as compared to intact gelatin and intact chitosan films. Müller et al.²³⁴ studied the manufacture of a blended complex based on carboxymethyl chitosan and polyphosphate, which was associated together with Ca²⁺ bridges and a porous structure. The chitosan modifications were performed by the oppositely charged free reactive group promoting the polyelectrolyte complex, where chitosan-based inks showed improved printability, higher resolution, as well as enhanced object fidelity of 3D printed architectures. Ko et al.²⁴⁵ optimized self-healing ferrogel ink based on glycol oxidized hyaluronate and chitosan containing superparamagnetic iron oxide nanoparticles aimed at printing application. Long et al.¹⁷³ produced 3D printed polyelectrolyte complex prepared by chitosan/pectin blend using in wound dressing. The chitosan/pectin complex presented good printability and the obtained lyophilized 3D printed wound dressings displayed high physical stability and flexibility. Cheng and Chen²⁵⁸ produced a blended complex of chitosan/PCL/PEGDA resin to fabricate printed scaffolds. The 3D printed constructed scaffolds presented that chitosan addition to the baseline resin did not considerably change the processability of the biomaterial. Huang et al.²⁵⁹ also studied the printability of a polyelectrolyte complex made from a ternary blend of gelatin/alginate/carboxymethyl chitosan hydrogel for printing application. Compared to binary gelatin/alginate hydrogel blend, the ternary polyelectrolyte complex hydrogel was revealed outstanding equilibrium water content, improved mechanical parameters, antibacterial activity, and low decomposition rate.²⁵⁹ It was reported that additive manufacturing by using SLA manufactured a desired 3D object in microreplication and photoresin through the chitosan/gelatin casting onto poly(dimethylsiloxane) molds, which allowed the final layer of chitosan/gelatin polyelectrolyte complex to be loaded in a layer-by-layer fashion constructing polyhedral hierarchical objects.¹⁹⁶

4.3.3. Polymer Blending. Another way to overcome poor physicochemical properties and insufficient resolution of printed constructs is biopolymers blending to improve printability and processability. The biopolymer blending techniques employed in additive manufacturing are described in detail in section 3.2.2. Overall, this approach applies two or more biopolymers or mixing a biopolymer with other biodegradable polymers or even synthetic polymers,²⁸⁷ providing a good opportunity for the improvement of functional properties of 3D objects in additive manufacturing. These improvements could be ascribed to the strengthening of the ink rheological properties,¹²⁰ mechanical parameters of 3D printed constructs,^{139,168,242,254} enhancing the resolution of the deposited layers, and printing precision,^{7,67,115,133,285} and inhibiting the geometry instability.⁷ Moreover, for the cost reduction of industrial manufacture of the 3D printing process, it is showed that a blending method using inkjet printing or extrusion is inevitable. In this regard, the balance among rheological properties of multicomponent ink, along with printing performance, physicochemical, and structural features of 3D printing structures must be sensibly performed.^{7,130,161,175}

Although starch has great advantages in the printing application (as previously noted in section 3.2.2), the use of native starch in the printing process showed several drawbacks due to weak flow behavior,¹¹ low solubility,²⁸⁷ and the lack of the stability²⁸⁸ required to develop a stable 3D structure. A unique 3D printable ink hydrogel based on starch mixed with alginate, pectin, carrageenan, and gelatin has been developed for the 3D printing process.^{11,33,80,88} It has been reported that the precise geometries with an improvement in the spatial resolution of the deposited layers obtained by starch blending could be effectively achievable.^{11,80,158} Gelatin systems blended by numerous biomaterials have also been utilized to adjust printing performance and to improve geometrical preservation upon 3D printing. In this sense, gelatin can be blended with soy protein isolate,⁷ alginate,¹²⁰ agar,¹⁰¹ chitosan,¹⁶⁵ xanthan,⁷⁴ carrageenan,¹¹⁹ dextran,²⁸⁹ and hyaluronic acid.¹⁸⁷ A multicomponent system based on gelatin and silk protein was extruded for producing implantable and stable 3D structures. This blending system was reported to be appropriately aimed at the soft rebuilding of precisely controlled properties and improved the spatial resolution of the deposited layers. Kuo et al.¹²⁰ aimed to produce 3D printed objects with diverse levels of gelatin and alginate for pharmaceutical and supplemental compounds delivery systems. They argued that the ratios of gelatin and alginate influenced the rheology properties, which were particularly associated with printability and deformability of the 3D structures. The optimum printing performance and lowest deformation were found in the ratio of gelatin and alginate of 1:1, making it a superior ink for 3D printing purposes.

Chitosan blended inks with other biodegradable polymers, for example, starch, pectin, hyaluronic acid, and cellulose were used for reinforcement of flow behavior and improvement of deposited layers resolution with well-defined geometry.¹⁶⁵ Wu¹⁶⁸ evaluated the structural strength of 3D printed strips from multicomponent systems comprising chitosan and polylactide. The structural properties and printability of the blends were improved by introducing maleic anhydride-grafted polylactide/chitosan. The grafted materials showed better mechanical properties and printing performance than those of the polylactide and chitosan composites owing to greater compatibility between the grafted polyester and chitosan.¹⁶⁸ Cellulose shows the ability for applying as part of a blended biomaterials system of gelatin, collagen, sodium alginate, and konjac gum for the 3D printing process.^{31,98,111,203} Gutierrez et al.²⁸⁵ fabricated an innovative antimicrobial 3D printed hydrogel blend comprising alginate/bacterial-cellulose with in situ-produced copper nanostructures. The printing performance of the alginate inks was further enhanced by adding bacterial-cellulose nanofibrils, allowing the manufacture of novel antimicrobial blend hydrogels that possessed long-term dimensional stability after exposure to CaCl₂ solutions. It has been stated that the addition of xanthan, as a thickening agent, to support the 3D printed architectures can be suitable for the printing process. A printed blend construct has been developed based on xanthan with other biopolymers in additive manufacturing.^{10,31,86,115,158} For example, Phuhongsung et al.¹¹⁵ incorporated xanthan gum into soy protein in the presence of NaCl. This mixture was effectively printed, where the printed xanthan/soy protein objects well-matched following the CAD design model compared to printed hydrogels made by other ink formulations. Gellan gum, in combination with other biomaterials or modified with methacrylate groups, also encourages successful material for the 3D printing process.²⁰¹ A blend of

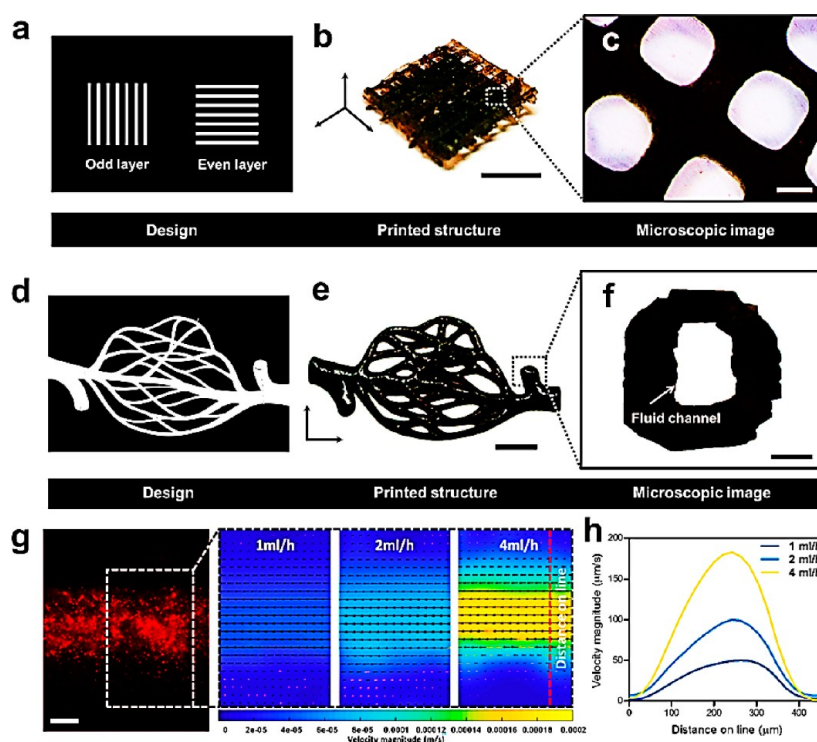


Figure 15. 3D printed PEG4A and SFM blend. (a) Microporous meshed object design. (b) Image for 3D printing structure with patterns of the digital beam. (c) 3D printing object's porous matrix. (d) Intricate blood vessel structure design. (e) Images for 3D printed structure with patterns of a digital beam in panel d. (f) Hollow structure cross-sectional view. Velocity magnitude field (g) and velocity profile (h) based on exterior injection amount in the constructed blood vessel. Reproduced with permission from ref 290. Copyright 2018 American Chemical Society.

gellan gum/alginate reinforced proliferation of mesenchymal stem cells with differentiation subsequent 3D printing process.²⁰¹ Gellan gum and alginate in their native form produced a well-defined hydrogel blend to release several growth parameters stimulating the proliferation of endothelial cells to modify the bone flaws. Shin et al.²⁹⁰ used silk fibroin containing nanoscale melanin particles (SFM) as poly(ethylene glycol)-tetra acrylate (PEG4A) solution transparency modifier. The printability evaluation was studied using comparing the feature sizes of 3D printed objects with the CAD design model. Introducing SFM (1.0% (w/v)) to PEG4A (4% (w/v)) precursor ink efficiently decreased the solution transparency with improving printability through limiting light beam to designed zone, which allowed constructing hard-to-express properties including empty vessels and vacant tubes. Moreover, Young's modulus of 3D printing PEG4A/SFM nanocomposite object increased (about 2.5-fold) compared to PEG4A free SFM sample. Regarding bioink, the PEG4A/SFM blend including cell revealed noncytotoxicity behavior, where reinforced the embedded cells proliferation, proposing great biocompatibility for 3D printed PEG4A/SFM objects (Figure 15).

4.3.4. Photo-cross-linking. There is increased attention to tuning the functional properties of biomaterials using photo-cross-linking methods for additive manufacturing applications. The photo-cross-linking of biopolymers is simply accomplished through UV irradiation,²³² gamma irradiation, and electron beam accelerator.¹² Concerning photo-cross-linking, a photosensitizer or photoinitiator is generally required to be added to printable ink solution producing a reactive radical type, initiating subsequent cross-linking process upon radiation.^{198,232} The combined effects of high-energy radiation with photoinitiator result in a reinforcement of functional features of 3D printed

constructs prepared from locust bean,²¹⁷ collagen,¹²² gelatin,²⁶⁰ alginate,¹² and chitosan.¹⁶⁸ The most common biopolymeric functionalization approaches are promoting a covalent linkage through cross-linking of biopolymeric backbone by methacrylate group. Reportedly, a biopolymer can be subjected to a methacrylic group developing functionalized methacrylated biomaterials, which can then be photo-cross-linked through a photosensitizer. The mentioned procedure is a promising reinforcement to introduce the covalent cross-linking linkage onto gelatin, alginate, hyaluronic acid, and kappa-carrageenan,^{256,260,277,291} which is then physically cross-linked by noncovalent linkages at room temperature (Figure 16). Functionalized gelatin methacryloyl (GelMA) preserves several critical functional features of gelatin and also facilitates the printing application by taking advantage of regulating the rheological properties of polymeric inks.^{189,230} Usually, the reaction of a methacrylic group and free amine groups of gelatin produced photo-cross-linkable functional products, which offers further structural strength to the 3D printed objects following the printing application. The photopolymerization process of gelatin aimed at the 3D printing process coupled with a light-assisted system has been well recognized in comparison with other biomaterials. This is because of developing an efficient approach to amend gelatin via the methacrylic group, making photocurable GelMA. Comprehensive and up-to-date reviews regarding utilizing GelMA are available elsewhere, while a detailed review of gelatin and gelatin blend compounds for additive manufacturing can be found here.²⁶⁰ Bozuyuk et al.²⁹² used a two-photon-assisted printer to produce a double-helical and magnetically powered chitosan-based microswimmer for releasing doxorubicin chemotherapeutic drug. The amino groups in chitosan microswimmers were treated via doxorubicin

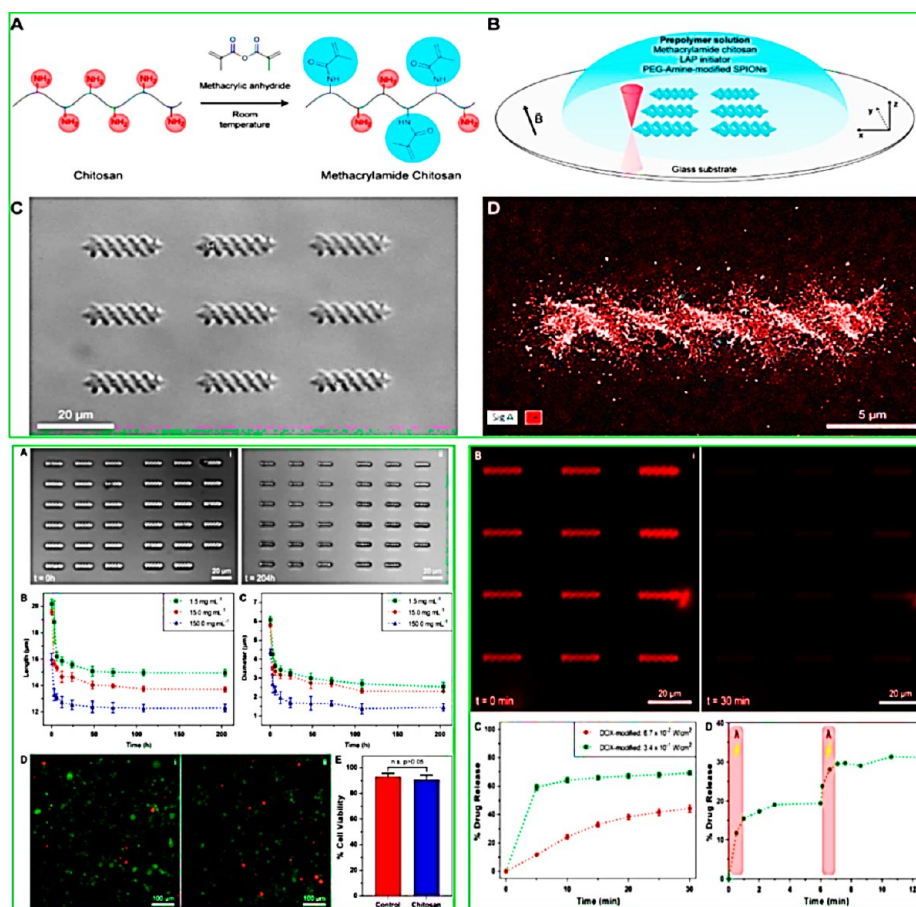


Figure 16. (Top) (A) Synthesis of the photo-cross-linkable methacrylamide chitosan. (B) Printed microswimmer. (C) Micrographs for printing array in microswimmers. (D) Energy-dispersive XRS mapping reveals iron atom existence inside microswimmer (red color). (Bottom-left) (A) Treatment of microswimmer via lysozyme ($15 \mu\text{g mL}^{-1}$): (i) $t = 0 \text{ h}$ and (ii) $t = 204 \text{ h}$. Changes in length (B) and diameter (C) of microswimmer during time having diverse lysozyme contents. (D) Fluorescence micrographs of Live/Dead SKBR3 breast cancer cell (i) without treatment and (ii) treatment via the microswimmer degraded products for 24 h. (E) Quantification of the viability of SKBR3 breast cancer cells treated with the degradation products (Bottom-right) Light-initiated released drug from microswimmer (B) DOX release from the microswimmers: (i) $t = 0 \text{ min}$ and (ii) $t = 30 \text{ min}$. A reduction in fluorescence magnitude specifies DOX degradation from microswimmer releasing its products. (C) Releasing DOX cumulative from microswimmers. (D) Smart DOX dosing from microswimmer. Reproduced with permission from ref 292. Copyright 2018 American Chemical Society.

using a photocleavable linking agent. Chitosan imparted microswimmers by a biodegradability and biocompatibility character for biological setting application. The microswimmer controlled steerability was revealed a rotational magnetic field with less than 10 mT. Using 365 nm wavelength light induction and 0.34 W cm^{-2} magnitude, doxorubicin with a level of 60% was released from microswimmers for 5 min. The releasing character was prevented through light induction controlled patterns, adjusting appropriate releasing amounts in the temporal area. In physiologically applicable circumstances, considerable microswimmers degradation was detected within 204 h of nontoxic degradation material (Figure 16).

To further tuning shape structural retention and precise geometries of the 3D structure made by hyaluronic acid, an effective photo-cross-linking process can be simply applied. In this regard, methacrylated hyaluronan (MeHA) is cross-linked via irradiation upon printing, reinforcing the rheological, self-healing, biocompatibility, and thermoreversible features. It is reported that increasing MeHA from an initial value of 1 to 3% (w/v) before UV irradiation treatment resulted in a rise in storage modulus from 5 to 200 Pa, respectively, whereas upon exposing to UV irradiation, an elastic modulus from 170 reached

2602 Pa. Such development has resulted in photopolymerizable hyaluronic acid-based inks suitable for the printing process in the desired size of $\sim 300 \mu\text{m}$. Hyaluronan was also grafted with methacrylated gelatin and hydroxyethyl acetate developing a printed 3D structure using extrusion-based printing. It was reported the obtained printable inks were printed as scaffold shape with a resolution of $\sim 500 \mu\text{m}$.²⁹¹ Qi et al.²⁹³ fabricated cryogel comprising GelMA, MeHA, and PEGDA through cryopolymerization, in which the printable ink was continually injectable and stretchable with a good printing character. Burdick et al.²⁹⁴ appended cyclodextrin and adamantane to hyaluronic acid, making two side-chain polymers with viscoelastic shear-thinning hydrogel behavior and self-healing features, where stable and freestanding 3D architecture was fabricated through printing direct ink writing.

4.3.5. Incorporation of Nanoparticles. The intrinsic drawbacks of the 3D printed objects produced by biopolymer lie in their poor mechanical properties and weak printing resolution, and also geometrical instability. In recent years, an innovative class of nanoscale filler has been incorporated into the biopolymeric printable inks to produce so-called nanocomposite 3D printed structures with a reinforced and tuned functional

Table 6. Summary of Biopolymers Integrated with Different Nanoparticles and Processed by 3D Printing Techniques

nanomaterials	host polymers	printing technique	functional properties	applications	ref
carbon nanotube	gelatin/alginate	extrusion printing	enhanced mechanical strength; improved printability	vasculature fabrication- printing microvascular conduits	297
montmorillonite nanoclay	alginate	extrusion printing	thermal stability; improved mechanical properties	wastewater treatment	12
graphene oxide	alginate/chondroitin sulfate/gelatin	microextrusion	enhanced printability and anisotropic structures	cartilage tissue engineering	296
titanium dioxide	alginate/gelatin	extrusion printing	enhanced mechanical properties	tissue regeneration	298
zinc oxide	gelatin	melt extrusion (twin-screw extrusion printing)	excellent shape-fidelity; accuracy the printing	tissue regeneration; food packaging	121
silica nanoparticles	oxidized alginate	extrusion printing	enhanced shear-thinning properties; High fidelity; Good mechanical stability	tissue bioprinting	243
cellulose nanocrystals	chitosan; modified CNC; modified pectin		compact network structure; better the resistance to degradation; cell supportive properties	tissue engineering	300
cellulose nanofiber	starch/milk powder/rye bran/oat/faba bean	extrusion printing	softening the samples; reduced the hardness; high water-binding capacity	healthy and structured foods	11
cellulose nanocrystals		extrusion printing	improved rheological and mechanical properties	sustainable materials for 3D printing of cellular architectures	299
cellulose nanofibers/ cellulose nanocrystals	alginate	microextrusion	sufficient shape-fidelity	tissue engineering	201
laponite nanoclay	TEMPO-oxidized bacterial cellulose/ Alginate	extrusion printing	better 3D printability; structural retention	drug release; biomedical devices; tissue engineering	267
iron oxide nanoparticles	oxidized hyaluronate	extrusion bioprinting	enhanced shear-thinning properties; self-healing capability	fabricating drug delivery systems and tissue engineering scaffolds	245
copper nanostructures/ cellulose nanofibers	alginate	extrusion printing	dimensional stability; improved printability; antimicrobial feature	tissue engineering; regenerative medicine	285
nanocellulose	alginate/gelatin	extrusion printing	biobased scaffolds with controlled pore sizes	tissue regeneration	301
nanocellulose	alginate	extrusion bioprinting	shear-thinning property; preserving living cells	cartilage tissue engineering	302
nanocellulose	alginate	extrusion printing	improved tissue compatibility	wound dressing	303
nanocellulose	alginate	SLA	auricular cartilage regeneration	auricular cartilage tissue engineering	200

feature, including structural strength,²⁹⁵ well-defined geometries and biocompatibility,^{11,201,245,296} enhanced printability,^{12,121,243,297} and self-healing properties.²⁴⁵ The introduction of nanoparticles into biopolymeric matrices followed by 3D printing is poised to open new prospects in additive manufacturing by developing customized 3D constructs with improved multifunctionality (Table 6). Several reports in the literature state the utilization of nanoparticles in the ink-based biopolymers as a reinforcing agent for improving functional properties of obtained 3D printed constructs, including nanoclay,¹² graphene oxide,²⁹⁶ carbon nanotube,²⁹⁷ titanium dioxide,²⁹⁸ zinc oxide,¹²¹ silica nanoparticles,²⁴³ and cellulose nanofiber.¹¹ A large number of works in nanocellulose-based materials focus on the 3D printing process for diverse applications. To tune the ink printing performance, flow behavior, and printing shape fidelity, cellulose nanocrystals (CNC) can be added to the polymeric matrix to reinforce the flow behavior of ink. Siqueira et al.²⁹⁹ designed viscoelastic inks based on anisotropic CNC, which allowed suitable printed constructs patterning through direct ink writing. They established a method for 3D printing both intact CNC and CNC-reinforced composite objects by direct writing of concentrated, viscoelastic, and monomer-based CNC inks. This technique produced cellulose-based objects showing a homogeneously dispersed CNC pattern along the 3D printing direction. Ghorbani et al.³⁰⁰ stated a biobased strategy for the fabrication of injectable nanocomposite objects prepared by chitosan, functionalized CNC, as well as modified pectin. The obtained hydrogel was produced in a liquid form through a double-barrel syringe, indicating an improved mechanical feature and enhanced printability. The introduction of modified CNC into the chitosan/pectin hydrogels resulted in a more rigid

network with reduced pore sizes.³⁰⁰ A cellulose nanofiber (CNF) also self-assembles and aggregates into fibrils with reinforced mechanical strength namely tensile strength and storage modulus. The interest in producing advanced 3D printable bioinks formulated with CNF has recently grown because of the appropriateness of improving the printing performance and spatial resolution.³⁰¹ Heggset et al.²⁰¹ studied 3D printing of the CNF and an obtained adequate resolution with improved geometrical structure of printing constructs given that the solid ratio of nanofiller was around 4 wt %. The geometrical retention and printing performance of the printed objects were progressively lost by increasing CNCs volume. Furthermore, substituting the nanofiller with alginate (1.5 wt %) offered acceptable printing performance. In the case of food printing, introducing CNF to printable food inks as a dietary fiber to fabricate 3D printed custom-designed and healthy meals were described in the literature.¹¹ Regarding bioengineering applications, Olate-Moya et al.²⁹⁶ developed bioconjugated hydrogel nanocomposite from photo-cross-linkable alginate containing a blend of gelatin/chondroitin sulfate simulating ECM (cartilage extracellular matrix). In this system, graphene oxide (GO), as a nanofiller, was incorporated into bioconjugated hydrogel ink to reinforce printing performance and cell proliferation. The data showed introducing GO to the hydrogel matrix substantially enhanced the geometrical retention of printing objects owing to quicker recovery of the consistency index postprinting of ink. Furthermore, the bioconjugated composite hydrogel generated anisotropic architectures upon printing due to casting liquid crystals of GO. In vitro proliferation was done in hADMSCs (adipose tissue-derived mesenchymal stem cell), in which the experimental results revealed the printed nanocomposite object had a greater

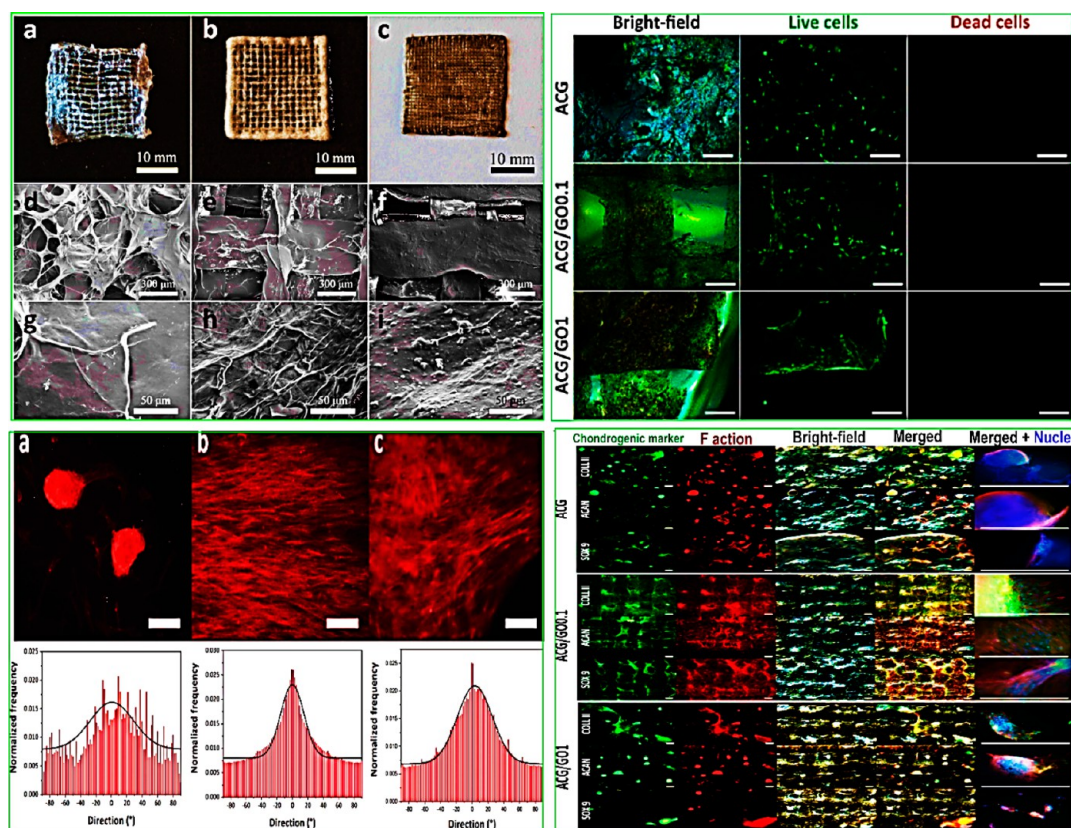


Figure 17. (Top-left) Freeze-dried printing objects prepared by (a) alginate/chondroitin sulfate/gelatin (ACG) ink, (b) the ACG ink with 0.1% GO, and (c) the ACG ink with 1% GO. Thread micrographs: (d, g) 3D printed ACG scaffold, (e, h) 3D printed ACG scaffold with 0.1% GO, and (f, i) 3D printed ACG scaffold with 0.1% GO. (Top-right) Fluorescence live/dead micrographs for hADMSCs seeding on printing object after 1 week. (Bottom-left) Fluorescence images for cytoskeleton F actin (top); Cytoskeleton F actin cell directionality histograms frequency distribution, in which 0° related direction of thread (bottom) in (a) 3D printed objects ACG, (b) 3D printed ACG scaffold with 0.1% GO, and (c) 3D printed ACG scaffold with 1% GO. (Bottom-right): Immunostaining fluorescence micrographs in chondrogenic markers (green) collagen, ACAN (aggrecan), SOX 9 in printing objects: ACG (top), ACG scaffold with 0.1% GO (central), and ACG scaffold with 1% GO (down), upon 4 weeks culture. The red color shows cytoskeleton F actin, the blue color represents nuclei counterstaining. Reproduced with permission from ref 296. Copyright 2020 American Chemical Society.

proliferation of hADMSCs compared to neat alginate. Remarkably, the 3D printed bioconjugated construct could guide hADMSCs proliferation along printing threads direction. Besides, 3D printed architectures promoted chondrogenic differentiation with no obvious factors of exogenous pro-chondrogenesis determined by immunostaining upon 4 weeks of culture. The great chondroinductive and cytocompatibility impact on the cells, in conjunction with improved printing accuracy and 3D anisotropic matrices, offers this printed scaffold to be an effective nominee aimed at 3D printing of tissue engineering of cartilage (Figure 17).

There are other types of nanoparticles that have been applied as a base material or nanoscale filler for additive manufacturing. Ahmed et al.¹²¹ developed a bioactive gelatin/zinc oxide nanocomposite containing clove essential oil for the 3D printing process. They showed a semisolid melt extruder 3D printer was included in a continuously developed platform providing a noticeable advantage, including a lower progress period. It was detected zinc oxide along with clove essential oil introduced gelatin film can be developed using 3D printing. Wei et al.²⁶⁷ developed a multicomponent nanocomposite based on TEMPO-oxidized cellulose/alginate/laponite. The nanocomposite blend showed well 3D printability compared to nanoparticle-free cellulose and alginate. The authors argued that obtained nanocomposite can be applied to develop a drug

delivery vehicle as well as tissue engineering. Lee et al.²⁴³ produced reversible imine bonds between oxidized alginate and silica nanoparticles, which led to considerably enhanced flow behavior and high 3D printing fidelity. In another study, Ko et al.²⁴⁵ demonstrated that glycol oxidized hyaluronate and chitosan could be used to obtain a self-healing ferrogel with superparamagnetic iron oxide nanoparticles without introducing cross-linking agents. Gutierrez et al.²⁸⁵ developed novel antimicrobial 3D printed alginate hydrogel with in situ-synthesized copper nanostructures. The printability of the alginate hydrogel inks was further improved by introducing CNF, allowing the development of innovative antimicrobial nanocomposite that possess long-term shape retention after exposure to CaCl₂ solutions.

4.4. Cellulose Derivation. Pure cellulose is difficult to dissolve in a wide range of solvents because of its inherent chemistry,²⁰³ which consequently limits its printing process. To make neat cellulose desired for employing in 3D printing, it is tuned with physical, mechanical, and chemical approaches. According to the literature, promising outcomes have been attained once cellulose ether-based hydrogel is applied as printable ink. In this regard, modified cellulose derivatives including hydroxypropyl methylcellulose,^{304,305} CMC,^{10,166} methylcellulose,^{86,204} microfibrillated cellulose,¹¹¹ and ethylcellulose³⁰⁴ were employed in 3D printing because of their

improved flow behavior and printing performance. Polamapilly et al.³⁰⁵ used hydroxypropyl methylcellulose (HPMC) and methylcellulose (MC), as supporting 3D printing components, with diverse substitution degrees of $-OH$ groups. The hydrogel formulated with HPMC and MC at a level of 12% (w/v) was effectively processed through an extruder-typed printer. Their work proposed that HPMC and MC once utilized as supporting materials in printing applications could remove the toxic compounds. The MC-based hydrogels were excellently processed through an extrusion-type printer by Negrini et al.²⁰⁴ They optimized the printing temperature of the methylcellulose-based hydrogel at a temperature of 21 °C, obtaining the printed strands reproducing the designed geometry without deficiencies. They also argued that a reduction in sol–gel transition temperature was evidenced, together with an increase in the swelling rate for printed methylcellulose-based hydrogels compared to nonprinted samples. Similar work was performed by Kim et al.,²¹⁰ who used MC as a proper reference compound aimed at its ability for mimicking the printing performance of numerous kinds of 3D structures. They added different biopolymers involving HPMC at concentrations of 9%, 11%, and 13% to produce a well-defined scaffold with 20, 40, and 80 mm heights, respectively, without collapsing. Yu et al.³⁰⁴ also prepared effective drug delivery devices based on printed HPMC and ethylcellulose for realizing the application system. Shao et al.¹¹¹ examined the rheological properties of microfibrillated cellulose/lignosulfonate hydrogel blend and used this multicomponent system to construct the carbon objects with a combination of 3D printing and carbonization. They reported that microfibrillated cellulose at a concentration of 2% offered shear-thinning character and great yield stress value. In another study, the printing performance of the CMC/taro paste multi-component system was performed by Huang et al.¹⁰ Considering the textural attribute of the printed product, appropriate hardness was an important parameter aimed at widespread acceptability. They reported maximum firmness was detected in the 3D printed object containing CMC. Moreover, among all 3D printed constructs, cohesiveness, springiness, as well as gumminess pursued the order: CMC > alginate > gellan gum > xanthan > whey protein > control.¹⁰

5. RHEOLOGICAL PROPERTIES OF BIOBASED INKS

The printing performance of biomaterials employed in additive manufacturing is the most important parameter particularly once one starts producing 3D printed constructs with architectural complexities. The printing performance is considered to be a feature that causes the printable inks to be processed with improved resolution and high shape fidelity able to support the object's weight.^{3,76,96} Thus, printability can be determined by the physicomechanical properties and flow behavior of a printable ink among other parameters.⁸ In this way, ink rheological properties can directly impact the printing shape fidelity and printing performance to dispense the material, which consequently can inhibit geometry instability; however, viscosity alone cannot capture the complex behavior of biobased inks during the printing process. Rheological features as imperative factors in the 3D printing process can undertake the geometrical retention, preventing discontinuities, and the resolution of the deposited layers printing precision, thus inhibiting the geometry instability.^{15–18} The rheological properties of a printable biobased ink measured by fundamental static and dynamic rheological approaches, including oscillatory assays (strain and

frequency sweeps), as well as creep-recovery tests on ink formulations.¹² Oscillatory shear experiments are broadly applied to simultaneously assess the viscoelastic parameters, that is, storage (G') and viscous (G'') moduli.^{7,130,161,175,299} Another important parameter in ink flow behavior determination is creep-recovery assessment, which is valuable to establish links with results from empirical methods. This assessment involves the application of constant stress; once the stress is released, some recovery is observed as the material efforts to return to its original shape.

In this section, we outline the flow behaviors of biobased ink solutions/suspensions that determine printability, including viscosity. Besides, we focus on other rheological features of inks, such as shear-thinning, thixotropic, and yield stress parameters. We also outline the effect of different factors affecting the rheology of the ink, along with discussing rheological models to support characterize the reinforcement impacts.

5.1. Newtonian Model. Biobased polymeric inks that preserve a consistency index over a range of predictable printing circumstances are regularly modeled with Newtonian behavior, in which the viscosity does not change with the deformation rate at constant pressure and temperature.³⁰⁶ This behavior is mostly seen in the ink solutions below the critical concentration of biopolymers, where viscosity is prevailed with the small, isotropic molecule and in actual little deformation magnitudes; in which Brownian motion inhibits the biopolymer alignment.³⁰⁷ At the below critical overlap concentration (c^*), that is, $c < c^*$, the separate coils are disconnected showing slight reciprocal interference, where the system offers Newtonian flow behavior. In practice, most biobased ink dispersions used in 3D printing applications are non-Newtonian fluids presenting substantial more complex rheological behavior, implying the consistency index relates to the deformation history. The non-Newtonian behavior results from the reorientation of entangled polymeric strands and electrostatic interaction discontinuation, which is considered as a general flow behavior that occurs in the printable inks with strengthening functionalized biopolymers. In contrast, the Newtonian behaviors are only dedicated to water, gelatin (in dilute solution), and sugar syrup, where the consistency index does not depend on deformation rate.⁸ It should note that the application of flexible protein (i.e., gelatin) in the printable ink due to the existence of electric charges gives rise to the appropriate impact on the flow properties. In the presence of electric charges, biopolymers are completely precipitated in isoelectric point, in which slight changes in rheological parameters are noticed. Any alteration in the pH (either direction) of polymeric ink changes the functional groups' ionization raising the positive charge or negative charge majority. Reciprocal repulsions of comparable electric charge prolong the molecule structure and increase consistency index or elastic modulus. Though, if alterations of pH are excessively severe, molecule structures accede utmost expansion, in this situation gelatin approves a non-Newtonian behavior (as mentioned earlier, gelatin usually displays Newtonian behavior in dilute solution), excluding once prolonged by charged groups.⁸

5.2. Power-Law Model. Shear stress–deformation rate plots of several fluids convert linear once plotted on double logarithmic coordinates and the Power-law behavior explains the results of shear-thinning and shear-thickening fluid behaviors. Shear-thinning is a valuable rheological character in the 3D printing process since it increases resolution, printability, and shape fidelity of viscous inks and improves viscoelastic

behavior, which is required as the printable inks can simply extrude out from nozzle tip using the utilization of extrusion shear force. Aggregation in the results of the polymeric chain from entanglement contains reptation motion causes an alteration of conformational interaction of polymeric chains.³⁰⁶ Beyond critical coil-overlap point ($c > c^*$), biopolymeric strands are greatly entangled in the network, which moves through reptation among the system. In this sense, macrostructure entanglements of the biopolymers are developed because of the chain–chain interactions. Once the concentrations of biopolymers are identical or greater than the critical coil overlapping point, the separated strands are forced to interpenetrate promoting an entangled structure, which is likely the stiffness, consistency index, and elastic modulus increases.³⁰⁷ Shear-thinning behaviors are more evident in the supramolecular biomaterials with higher molecular weight, especially at higher biopolymeric levels. This is more noticeable in some features of a 3D printed construct, such as mechanical parameters, where a compact or stiff matrix can enhance the structural strength of the printed architectures. The common ways to model shear-thinning behavior are using the Power-law model, in which shear stress is associated with deformation, flow behavior index, and plastic viscosity, where it is considered the consistency index at 1 s^{-1} deformation rate. Regarding the Power-law model, the flow behavior index (n) equal to one suggests a Newtonian behavior, whereas $n < 1$ implies more shear-thinning.³⁰⁶ This model is simply applied for many biopolymer-containing inks in additive manufacturing. It is reported that the Power-law inks presented improved printing features once the consistency index is between 1000 and 3000 Pa s^n and the n is between 0.2 and 0.8 in an experimental 3D printing system. In the 3D printing, a shear-thinning model can be applied to fit the rheological data of biobased polymeric inks based on starch,¹⁶¹ whey protein isolate,¹¹⁰ carrageenan/xanthan/starch,³³ sodium caseinate,¹⁷ gluten-free product,³⁴ egg yolk/rice flour,¹³³ and mashed potato.^{88,89}

5.3. Herschel–Bulkley Model. When the yield stress of a biopolymeric ink is measurable, it can be involved in the Power-law model and it is recognized as the Herschel–Bulkley model. Yield stress is the least force necessary starting the flow, which is an indicator of hardness in the coherent network structure.³⁰⁶ Yield stress variation has been considered as a prominent feature of biopolymeric inks and has been attributed to improving and tuning ink printability and geometrical retention of 3D printed structures.²³³ To determine yield stress, the Herschel–Bulkley model is regularly used in 3D printing applications, which is like a Power-law behavior with an extra parameter for the yield stress. Once shear force surpasses yield stress, printable ink dispersion acts similar to an elastic system. Herschel–Bulkley model specifically detects rheological features of non-Newtonian printable ink showing *pseudoplasticity* and yield stress, as well as is accepted to ink model in numerous printing publications. It is reported Herschel–Bulkley is the appropriate model to predict some 3D printed products, including mashed potato,¹⁵⁹ potato puree,³⁰⁸ orange concentrate,¹⁹⁹ cordyceps flower powder,³⁰⁹ and chocolate.³¹⁰ Print fidelity and mechanical strength can be enhanced by changing the yield stress and the ink dispersion preserves its solid-like character upon the printing process, even with no effective cross-linking modification. Upon the printing process, low values of yield stress are greatly appropriate since the 3D printing process almost is not a consecutive process, but launches and ends regularly thru printing. Great yield stress involves a printing system inducing

larger shear stress for exceeding yield stress, leading to extraordinary force in a controlled manner. Great yield stress induces the printable inks challenging to work with. As an instance, larger yield stress values affect typical colloidal ink dispersion and pipetting approaches, needing replacing methods similar to needles and common blending approaches to be utilized as an alternative way.

5.4. Factors Affecting the Rheology of the Ink. The information about the rheological properties of biopolymeric-based ink formulation and printing variables optimization are important parameters to effectively manufacture advanced 3D architectures. The flow behavior of biopolymeric-based ink has been stated as the decisive feature of 3D printing shape fidelity. The consistency index can have then diverse impacts toward ink-based dispersions performance, in which a larger consistency index does not certainly confer improved printing accuracy or desired mechanical strength.¹¹² Greater consistency index offers printable inks to efficiently maintain their geometrical structures, which reinforces mechanical strength upon printing, especially shows advantageous in 3D printing of intricate architectures. In this sense, materials with a higher viscosity need higher extrusion forces, resulting in higher shear stresses experienced by the bioactive compounds and can, consequently, cause severe structural damage. Moreover, the comparatively excessive resistance against flow results in the extrusion nozzle tip to block, causing uneven and irregular ink deposition.^{3,8,34,96,108} Conversely, a low consistency index level minimizes the ink printability leading to heterogeneous 3D printed construct geometrical alignment and quick sedimentation and/or precipitation. It is specified in the literature that inducing any alteration in ink formulation (such as changes in biomaterial content, molecular weight, ion content, etc.), as well as the change in printing variables (including temperature, flow rate, pressure, etc.) can directly influence ink flow behavior.^{17,52,109,130,208,248}

To enhance ink printing performance for the 3D printing process, a good understanding of the biopolymer's flow behavior is necessary. Two approaches have been suggested for tuning and reinforcing the flow properties of biopolymeric ink. The first one formulates printable ink with reduced consistency index and yield stress to extrude out efficiently and simply from nozzle tip and quickly solid via a gelation method exactly after extruding process, showing desired elastic modulus to withstand deposited structure. The second technique is manufacturing biopolymeric ink with suitable flow parameters (i.e., *pseudoplasticity*), which is required for almost all 3D printing processes to offer adequate mechanical strength, the improved spatial resolution of the deposited layers, and increased geometrical retention.³¹¹ In the 3D printing process, it is widely emphasized the *pseudoplasticity* and thermoreversible behavior of biomaterials' ink are extremely critical.^{8,12,14,33,159,161} The shear-thinning behavior allows the facile extrusion of printable inks, whereas thermoreversible behavior makes inks rapidly attain sufficient viscosity and mechanical strength to be able to self-support 3D printed architectures.^{14,33,159,161} Regarding biomaterials with thermoresponsive behavior, including kappa-carrageenan and methylcellulose thermoreversible hydrogels, the determination of an effective 3D printing process is critically dependent on gelation/solidify temperature.^{33,119,208} Therefore, thoughtful insight into the rheological features of biopolymeric ink-based dispersions is essential to allow efficacious printing. Recently, several researchers have explored the impact of the flow behavior of biopolymeric ink toward the 3D printing process. Reportedly,

the significance of inks' flow factors is contributed to printability, shape fidelity, biocompatibility, and resolution of 3D structure. These rheological parameters includes shear-thinning behavior, *pseudoplasticity*, consistency index, viscosity recovery, elastic, complex, and loss moduli, as well as loss tangent.^{12,14,32,34,88,90,110,139,157–159,256}

The ink composition and additives addition have an important impact on flow properties through changing droplets/particles stability, which is dispersed in the ink system, and also with interfacial interactions between droplets/particles via ink's overall interfacial structure. Garcia-Segovia et al.¹⁷⁵ showed that rheological and textural properties could describe the formulation composition, giving rise to the validation of printing constructs. This facts type supports improving the pattern design provided by 3D CAD models or even a pattern of 3D printer system without the interference of the final operator. As mentioned earlier, to ensure adequate chain entanglement in the biobased inks, concentrated inks, and their flow behavior are of great significance. In this sense, ionic-type surfactant adsorbs at the interfaces and usually produces screened electrostatic repulsion, providing outstanding ink stabilization to any flocculation or coalescence. This is resulted in improving the osmotic pressure and interfering ink droplet/particle interface deformation in viscous systems.³¹² Introducing salts into the ink system changes the electrostatic interaction capacities, leading to important interdroplet attraction. Other modifying agents including stabilizers, emulsifiers, thickening agents, as well gelling promoters can yield aggregation and entanglement of biopolymeric ink via depletion attraction.³¹² Because of effective attractive force, distribution of droplet size of inks behaves working together droplet–droplet interaction, which extremely affects the stability of biopolymeric ink in cooperation with the interfacial matrix. The mentioned situations consecutively, likely affect the flow behavior of the ink system.³⁰⁶ Furthermore, the interfacial and spatial structures of droplets/particles in concentrated systems show an intrinsic association with droplet size by using emulsification; therefore, they have a critical character in flow behavior. The flexibility characters of viscous printable ink dispersion are prominently affected with droplet/particle packing, relating to the volume fraction of droplet/particle.³¹² Once volume fraction rises, droplet/particle crowding is attained upon osmotic force, accordingly, the beginning of flexibility is resulted by droplet interfaces deformation that is related to the utmost random packing of ionic, disordered, and monodisperse ink dispersions.³¹³ Concerning polydispersity, some disordered polymeric ink dispersions with homogeneously droplet/particle distribution are induced to developing ordered alignments in particular deformation, leading to greater volume fraction related to droplet/particle packing in comparison with monodispersed ink dispersions.³⁰⁶ On the contrary, polydispersity is expected to considerably change in the presence of additional emulsification because of the utilization of great deformation in the defined rheological experiments. As a result, without truly altering the droplet size distribution, specific flow parameters are likely to be difficult to detect for some kinds of ink dispersions, especially in higher flow rates.

Structural modifications of printable biopolymeric ink, as mentioned in section 4, develop well-defined 3D constructs with improved functionalities and precise geometries. Thus, all reinforcement methods are likely to impact the rheological features. While the effects of physical, chemical, and enzymatic reinforcements on the flow properties of inks are usually

underappreciated, the strengthening of ink cannot be fully recognized by ignoring these factors. These effects are dependent on the magnitude and period of shear force to which ink dispersion is exposed. During printing, biopolymeric ink is commonly non-cross-linked biopolymer or even prebiopolymer systems. In detail, the shear force has been revealed inducing morphological variations, constructs with enhanced functionalities, precise geometries, improve the spatial resolution of the deposited layers, and increase geometrical retention.

The rheological properties of biopolymeric mixtures comprising dispersed particles in the system are also influenced by powder type, particle size distribution, as well as the swelling degree. Moreover, flow behavior is also meaningfully influenced by volume fractions that consecutively are linked to swelling ratio, which could be adjusted with biopolymer incorporation to prevent swelling.^{7,15–18} In the powdery materials, the water content of components is the main factor affecting the printability, where the moisture regulation approaches are likely to enable the accomplishment of proper flow behavior aimed at the 3D printing process.^{18,314} The utilization of powdery compounds, where water content is reduced by drying approaches, for the formulation of biopolymeric printable inks can improve the printing performance of the 3D printed structures. Another essential criterion for the printability of biobased materials is its extrudability, that is, nozzle diameter and dispensing pressure, where the dispensing pressure is needed to attain extrusion at a sufficient flow rate (or print head speed).⁸ Shearing force also has a considerable impact on the flow behavior of ink, and excessive shear stress induces an irreversible loss in consistency index. From mechanical or structural features of printed materials, optimum defined printing variables will help researchers in the usage of the right 3D printing technique. Because of the different sensitivity of different biopolymers and modification techniques, controlling the shear stress and extrusion shear force upon printing is of critical importance for 3D printing applications. Extensive reviews on the printing parameters in additive manufacturing have been published elsewhere.^{3,8,77}

6. PRINTING BOTTLENECKS AND FUTURE REQUIREMENTS

With the progressively widespread application of the 3D printing process in more challenging sectors, an increased request is placed toward the factors of fabrication technique with consideration of final 3D printed architectures performance. Although, there is still an important subject to defeat before the 3D printing technique is accepted as a popular fabrication method. Commonly, the shortcomings of the 3D printing process can be observed as areas of opportunity, and certainly, printing is in the address to these shortcomings where the innovative signs of progress in additive manufacturing have developed. One of the main concerns is the restricted capabilities of 3D printer systems.^{4,36,37} The printing speed and printing performance in terms of precise geometries with a high spatial resolution of the deposited layers have improved massively in recent years yet still a gap between optimum levels in various cases.⁷⁷ Several 3D printing techniques relate to the mechanism of the nozzle for the fabrication of deposited layers upon developing the 3D printing constructs. This induces the main problem in preserving consistent and reproducible flow on-demand about printing head stops and restarts. Regarding powder-based printer, as an instance, nozzle blocking, migration

of additives, as well as inadequate feeding or bleeding are glitches which must be dealt with.³⁶ This printer also in specific needs appropriate infrastructures for performing the printing process as the elimination of extra powdery materials with possible toxicity and health hazards are necessary.³⁶ The second main concern is the absence of a variety of printable biopolymers.^{3,4,37} The impact of different biopolymers on the functional characteristics of printed objects is recognized to be greatly reliant on raw materials, nature, and concentration of biopolymers, as well as their rheological properties. How to achieve the mentioned required parameters differs somewhat relating to which printer techniques are being applied and the planned end utilization of the instrument.

Although additive manufacturing is used increasingly in pharmaceuticals, complete accomplishment in this domain is attained upon gaining elaborated innovative developed 3D dosage objects toward industrial scales. Additive manufacturing and printing potential for designing and developing 3D medicine objects are regularly under the special attention of regulatory administrations. Though, addressing the present FDA regulatory necessities might be an important obstacle, which prevents the introduction of 3D printed medicines to the marketplace.³⁶ FDA documented novel cases associating with 3D printing fabrication will occur and processes to alteration are already in progress. The working toward developing 3D printed medicine architectures does sound understanding of 3D printing through its research.³¹⁵ Concerning bioengineering as an innovative fabrication paradigm in tissue engineering, it provides spatial 3D structural adjusting among cellular and biopolymers deposition that is important to initiate cell–cell interaction and cell–extracellular matrix relation. As an example, bioprinting is now a reality to apply sophisticated machine-control to generate tissue-engineered skin architectures. Although the final objective of bioprinting a skin equivalent with complete functional performance has yet to be accomplished, bioprinting demonstrates promises in several critical aspects of skin tissue engineering, containing fabricating pigmented and/or aging skin models, hair follicles, and vasculature networks. The potential of bioprinting with promising prospects in advanced biomaterial, biology, as well as design computing finally allows the actualization of fully functional skin constructs or 3D printed functional organs.^{316–319} With regard to food science and technology, the advantages and disadvantages of additive manufacturing usage remain to be investigated. The main part of biomaterials-based printing objects is recently utilized in the food sector because of their functionality, complexity, and intrinsic rigidity of finished 3D printed biopolymers, simulating the textural features and sensory properties of food products, outside of some biobased hydrogel matrix. Moreover, some foods, such as rice, meat, vegetables, and fruit, are generally consumed with consumers daily, but at the moment it is impossible to print them by nature. Furthermore, quality control matters, reproducibility concerns, and regulatory hurdles are required to be addressed before the 3D printing process can reach the food market. Ultimately, a balance among all 3D printing factors must be considered for the fabrication of a suitable printable biopolymeric ink. Descriptions of challenges for biobased inks can be found in previous reviews.^{3,36,37,77} The following are some main of these shortcomings.

6.1. Printability. Although 3D printing techniques provide a pioneering construction platform with flexible processability, flow behavior requirements placed on printable inks are inflexible and strict. Rheological investigation offers to the

speed-up improvement of printable biobased inks and proves valuable characterization methods, as well as involves mathematical models, gaining a profound understanding of the biopolymers' printability according to the rheological investigation. Sarker and Chen³²⁰ and Kraut et al.³²¹ presented outstanding flow behavior analysis of recognized and innovative biopolymeric ink preparation presenting a simple robust and non-Newtonian behavior model adapted by food application and electronics packaging research fields. Though, characterization techniques suffer from transferability and comparability for biomaterials with unidentified printability features. Particularly for scientists switching into the biofabrication area, reproducible, comparable, as well as effective characterization methods regarding printing performance of inks would be an essential benefit.³²² Many printable biobased materials have excellent functional properties for external applications, but the printable polymeric inks need particular characteristics based on both compatibility and rheological features, making progress much more challenging. Generally, the biobased materials should be printable, biocompatible, show suitable rheological and mechanical properties with good degradation kinetics, and produce nontoxic degradation byproducts. Moreover, despite numerous research efforts, 3D objects produced by printing techniques are inferior concerning printing performance in many cases.^{3,4,8,36,37,76}

6.2. Building Speed. Rapid prototyping term is generally applied synonymously to 3D printing application, which is rather equivocal concerning the build speed. The continuing evolution from rapid prototyping to fast construction gives rise to different shortcomings for materials researchers, pharmaceutical and food scientists, as well as mechanical bioengineers in the 3D printing areas. Moreover, although the 3D printing process facilitates a much quicker construct assembly with minimizing the time required to designing proofs, allowing functional prototype assembly at present in the early steps of progression and growth. The 3D printing methods are still slow related to mass-production approaches. So far, it is accepted in many manufacturing applications including custom-designed engineering takes advantage of revolutionary construction and flexible processability of 3D printing. However, the attempts to widen 3D printing scope application have been an important motivator aimed at research works in the future.

6.3. Mechanical Properties. The ink dispersion should not only be simply extruded from the nozzle but also have adequate elastic modulus to reduce possible deformation when being printed. As the utilization of the 3D printing process from (visual) prototyping to the fabrication of finished applicable 3D constructs, functionalities of the 3D printed objects are likely to match the efficiency of constructs prepared by formative or subtractive techniques. Irrespective of a large number of works, the 3D structures developed with the 3D printing process are inferior concerning structural and mechanical strength. Regarding particular applications, the potential shortcoming might be because of restricted compounds selection appropriate aimed at 3D printing (such as photocurable biobased inks in the presence of a photoinitiator for photo-cross-linking), as well as an unavoidable porosity of objects prepared by PBF or extrusion printing. Furthermore, because of layered manufacturing fashion, mechanical features of printed objects tend to behave like an anisotropic network, where the boundary among deposited layers indicating poor areas with extreme residual forces, in which structural stability and geometrical structure alignment are the main concern. Mechanical features and

anisotropy for extrusion-based methods were recognized to be extremely reliant on applied biopolymers and process conditions. Moreover, the anisotropy feature is a weakness concerning SLA printing applications, in which postcuring was reported to offer functional modifications. Any reinforcement in the mechanical strength of 3D printed structures opens cutting-edge procedures for additive manufacturing, where improvement and application of tuned multicomponent objects can be considered as an advantageous strategy.

6.4. Resolution. Spatial resolution is the main problem affected by specific printing processes and the utilized components, which is of great importance in PBF, inkjet printing, and extrusion systems as a substantial drying period are necessary before the 3D object handling.³²³ The gap lines among the deposited layers can also be occurred upon printing with the FDM technique. Furthermore, some authors reported that although the accuracy of the 3D object obtained was good enough for the process, it is significant to consider that some 3D constructs may be too thin for image acquisition and the printing technique.³²⁴ The inadequate resolution also offers a major impact on the printing quality and functionality of a 3D printed construct. However, the manufactured constructs are likely to need great fidelity with virtual design; the restrictions of printing method along with applied biopolymers imply some levels of geometrical instability. Resolution necessities adjusted by innovative applications of 3D printing have caused numerous researches in the fields of biomaterials science and bioengineering application. The resolution of 3D printed objects in extrusion-based printing methods, as an example, is achieved by the deposition of thin layers, which increases the operation time and induces high processing cost, placing the printing technique in unfavorable condition compared to the common engineering methods. In the current scenario of significant progress in the ways of layers deposition, the manufacturing obstacles faced with additive manufacturing techniques are expected to provide commercialization underpinning for the printing system. In this sense, the addition of functionalized biobased polymers improves the geometrical retention, offered a higher resolution, precise geometries, and enhanced structural strength. Biobased polymeric inks viscosity has been reported as the determining factor of printing performance.^{112,231,232,317,319} For a specific 3D printing process, greater nozzle diameter and/or extrusion rate could also considerably decrease the operation time, albeit always triggered a negative impact toward printing accuracy, whereas smaller nozzle diameter enhances the resolution, while leading to a substantial increase in the processing period.

CONCLUSION

This Review focuses specifically on the application progress of biobased polymers (namely, protein and carbohydrate-based materials) and main procedures for biopolymeric structure reinforcements in pharmaceutical, bioengineering, and food printing. A special focus was also paid on the factors affecting the rheology of biopolymeric inks applied in these fields. Going well beyond its common role regarding conceptual modeling, rapid prototyping, as well as end-user customized constructing, 3D printing methods are growing beyond niche marketplaces and introducing into an extensive range of different fields spanning, pharmaceutical, bioengineering, and even food application. Outstanding futurists comprise 3D printing as a central cutting-edge tool in an innovative and custom-designed industrial revolution. The rise to the importance of 3D printing has been

intrinsically tied to developments in thoughtful of the processing of supramolecular biopolymers. Principally, removing the requirement aimed at postprinting treatment has been reported as an essential tool to enhance 3D printing competitiveness. Efforts are progressively shifting on the printability and printing accuracy of 3D printing architectures and as a consequence of structural strength and shape fidelity. The advanced biomaterials and 3D printing techniques can be well merged to offer 3D constructs with enhanced shape retention, self-healing, biocompatibility, and thermoreversible properties. As a fundamental compound, biomaterials are detecting a growing utilization in a large number of printed constructs with improved flow behavior of polymeric ink, enhanced resolution of the deposited layers, and well-defined geometrical of printed structures. The role of each biopolymer in ink preparation and improvement of 3D structures was outlined together with instances, reinforcement approaches, and characterization methods to specify the growing trend in utilizing biomaterials for pharmaceutical, bioengineering, and food printing. In this regard, tuning structural features of biopolymers give the way for the desired flow property and mechanical strength, attaining tailored geometry upon the printing process. It was argued that multifunctionalities through the introduction of different biopolymers affected the resolution and printing performance of finished constructs. This type of information can support the improvement of pattern design offered by virtual CAD models without the involvement of the final user. From mechanical and flow behavior of printed objects, optimum printing variables will be specified serving the final user in the usage of 3D printing. The history of biomaterial reinforcement aimed at 3D printing applications has also been fruitful, and constant invention will be required to guarantee printing development in the future.

AUTHOR INFORMATION

Corresponding Authors

Mahdiyah Shahbazi – *Institute of Food Technology, University of Natural Resources and Life Sciences (BOKU), 1190 Vienna, Austria*; orcid.org/0000-0002-2485-9130;
Email: shahbazim00@yahoo.com

Henry Jäger – *Institute of Food Technology, University of Natural Resources and Life Sciences (BOKU), 1190 Vienna, Austria*; Email: henry.jaeger@boku.ac.at

Complete contact information is available at:
<https://pubs.acs.org/10.1021/acsabm.0c01379>

Funding

Open access funding provided by the University of Natural Resources and Life Sciences Vienna (BOKU).

Notes

The authors declare no competing financial interest.

REFERENCES

- (1) Van Bommel, K. *3D Food Printing*; 2014, pp 255–263.
- (2) Van der Linden, D. *3D Food Printing: Creating Shapes and Textures*; TNO, 2015.
- (3) He, C.; Zhang, M.; Fang, Z. 3D printing of food: Pretreatment and post-treatment of materials. *Crit. Rev. Food Sci. Nutr.* **2020**, *60*, 2379–2392.
- (4) Luo, Y.; Lode, A.; Wu, C.; Chang, J.; Gelinsky, M. Alginate/nanohydroxyapatite scaffolds with designed core/shell structures fabricated by 3D plotting and in situ mineralization for bone tissue engineering. *ACS Appl. Mater. Interfaces* **2015**, *7* (12), 6541–6549.

- (5) Mantihal, S.; Prakash, S.; Godoi, F. C.; Bhandari, B. Optimization of chocolate 3D printing by correlating thermal and flow properties with 3D structure modeling. *Innovative Food Sci. Emerging Technol.* **2017**, *44*, 21–29.
- (6) Huang, M. S.; Zhang, M.; Bhandari, B. Assessing the 3D printing precision and texture properties of brown rice induced by infill levels and printing variables. *Food Bioprocess Technol.* **2019**, *12* (7), 1185–1196.
- (7) Chen, J.; Mu, T.; Goffin, D.; Blecker, C.; Richard, G.; Richel, A.; Haubruge, E. Application of soy protein isolate and hydrocolloids based mixtures as promising food material in 3D food printing. *J. Food Eng.* **2019**, *261*, 76–86.
- (8) Godoi, F. C.; Prakash, S.; Bhandari, B. R. 3D printing technologies applied for food design: Status and prospects. *J. Food Eng.* **2016**, *179*, 44–54.
- (9) Daffner, K.; Vadodaria, S.; Ong, L.; Nöbel, S.; Gras, S.; Norton, I.; Mills, T. Design and characterization of casein-whey protein suspensions via the pH-temperature-route for application in extrusion-based 3D-Printing. *Food Hydrocolloids* **2021**, *112*, 105850.
- (10) Huang, M. S.; Zhang, M.; Bhandari, B.; Liu, Y. Improving the three-dimensional printability of taro paste by the addition of additives. *J. Food Process Eng.* **2020**, *43* (5), e13090.
- (11) Lille, M.; Nurmela, A.; Nordlund, E.; Metsä-Kortelainen, S.; Sozer, N. Applicability of protein and fiber-rich food materials in extrusion-based 3D printing. *J. Food Eng.* **2018**, *220*, 20–27.
- (12) Shahbazi, M.; Jäger, H.; Ahmadi, S. J.; Lacroix, M. Electron beam crosslinking of alginate/nanoclay ink to improve functional properties of 3D printed hydrogel for removing heavy metal ions. *Carbohydr. Polym.* **2020**, *240*, 116211.
- (13) Liu, L.; Ciftci, O. N. Effects of high oil compositions and printing parameters on food paste properties and printability in a 3D printing food processing model. *J. Food Eng.* **2021**, *288*, 110135.
- (14) Chameettachal, S.; Midha, S.; Ghosh, S. Regulation of chondrogenesis and hypertrophy in silk fibroin-gelatin-based 3D bioprinted constructs. *ACS Biomater. Sci. Eng.* **2016**, *2* (9), 1450–1463.
- (15) Yang, X.; Lu, Z.; Wu, H.; Li, W.; Zheng, L.; Zhao, J. Collagen-alginate as bioink for three-dimensional (3D) cell printing based cartilage tissue engineering. *Mater. Sci. Eng., C* **2018**, *83*, 195–201.
- (16) Mazzocchi, A.; Devarasetty, M.; Huntwork, R.; Soker, S.; Skardal, A. Optimization of collagen type I-hyaluronan hybrid bioink for 3D bioprinted liver microenvironments. *Biofabrication* **2019**, *11* (1), 015003.
- (17) Schutyser, M. A. I.; Houlder, S.; de Wit, M.; Buijsse, C. A. P.; Alting, A. C. Fused deposition modelling of sodium caseinate dispersions. *J. Food Eng.* **2018**, *220*, 49–55.
- (18) Zhang, L.; Lou, Y.; Schutyser, M. A. 3D printing of cereal-based food structures containing probiotics. *Food structure* **2018**, *18*, 14–22.
- (19) Zheng, L.; Yu, Y.; Tong, Z.; Zou, Q.; Han, S.; Jiang, H. The characteristics of starch gels molded by 3D printing. *J. Food Process. Preserv.* **2019**, *43* (7), e13993.
- (20) Maniglia, B. C.; Lima, D. C.; Matta, M. D., Jr.; Le-Bail, P.; Le-Bail, A.; Augusto, P. E.D. Preparation of cassava starch hydrogels for application in 3D printing using dry heating treatment (DHT): A prospective study on the effects of DHT and gelatinization conditions. *Food Res. Int.* **2020**, *128*, 108803.
- (21) Pekkanen, A. M.; Mondschein, R. J.; Williams, C. B.; Long, T. E. 3D printing polymers with supramolecular functionality for biological applications. *Biomacromolecules* **2017**, *18* (9), 2669–2687.
- (22) Theagarajan, R.; Moses, J. A.; Anandharamkrishnan, C. 3D Extrusion Printability of Rice Starch and Optimization of Process Variables. *Food Bioprocess Technol.* **2020**, *13*, 1048.
- (23) Klotz, B. J.; Gawlitta, D.; Rosenberg, A. J.; Malda, J.; Melchels, F. P. Gelatin-methacryloyl hydrogels: towards biofabrication-based tissue repair. *Trends Biotechnol.* **2016**, *34* (5), 394–407.
- (24) Wang, X.; Yan, Y.; Pan, Y.; Xiong, Z.; Liu, H.; Cheng, J.; Liu, F.; Lin, F.; Wu, R.; Zhang, R.; Lu, Q. Generation of three-dimensional hepatocyte/gelatin structures with rapid prototyping system. *Tissue Eng.* **2006**, *12* (1), 83–90.
- (25) Irvine, S. A.; Agrawal, A.; Lee, B. H.; Chua, H. Y.; Low, K. Y.; Lau, B. C.; Machluf, M.; Venkatraman, S. Printing cell-laden gelatin constructs by free-form fabrication and enzymatic protein crosslinking. *Biomed. Microdevices* **2015**, *17* (1), 16.
- (26) Basara, G.; Yue, X.; Zorlutuna, P. Dual crosslinked gelatin methacryloyl hydrogels for photolithography and 3D printing. *Gels* **2019**, *5* (3), 34.
- (27) Fiorati, A.; Contessi Negrini, N.; Baschenis, E.; Altomare, L.; Faré, S.; Giacometti Schieroni, A.; Piovani, D.; Mendichi, R.; Ferro, M.; Castiglione, F.; Mele, A.; et al. TEMPO-nanocellulose/Ca²⁺ hydrogels: Ibuprofen drug diffusion and in vitro cytocompatibility. *Materials* **2020**, *13* (1), 183.
- (28) Fan, H.; Zhang, M.; Liu, Z.; Ye, Y. Effect of microwave-salt synergetic pre-treatment on the 3D printing performance of SPI-strawberry ink system. *LWT* **2020**, *122*, 109004.
- (29) Jing, L.; Wang, X.; Liu, H.; Lu, Y.; Bian, J.; Sun, J.; Huang, D. Zein Increases the cytoaffinity and biodegradability of scaffolds 3D-printed with zein and poly (ϵ -caprolactone) composite ink. *ACS Appl. Mater. Interfaces* **2018**, *10* (22), 18551–18559.
- (30) Oliveira, S. M.; Fasolin, L. H.; Vicente, A. A.; Fuciños, P.; Pastrana, L. M. Printability, microstructure, and flow dynamics of phase-separated edible 3D inks. *Food Hydrocolloids* **2020**, *109*, 106120.
- (31) Holland, S.; Foster, T.; MacNaughtan, W.; Tuck, C. Design and characterisation of food grade powders and inks for microstructure control using 3D printing. *J. Food Eng.* **2018**, *220*, 12–19.
- (32) Liu, Y.; Zhang, W.; Wang, K.; Bao, Y.; Regenstein, J. M.; Zhou, P. Fabrication of gel-like emulsions with whey protein isolate using microfluidization: Rheological properties and 3D printing performance. *Food Bioprocess Technol.* **2019**, *12* (12), 1967–1979.
- (33) Liu, Z.; Bhandari, B.; Prakash, S.; Mantihal, S.; Zhang, M. Linking rheology and printability of a multicomponent gel system of carrageenan-xanthan-starch in extrusion based additive manufacturing. *Food Hydrocolloids* **2019**, *87*, 413–424.
- (34) Marchetti, L.; Andrés, S. C.; Cerruti, P.; Califano, A. N. Effect of bacterial nanocellulose addition on the rheological properties of gluten-free muffin batters. *Food Hydrocolloids* **2020**, *98*, 105315.
- (35) Li, J.; Wu, C.; Chu, P. K.; Gelinsky, M. 3D printing of hydrogels: Rational design strategies and emerging biomedical applications. *Mater. Sci. Eng., R* **2020**, *140*, 100543.
- (36) Alhnan, M. A.; Okwuosa, T. C.; Sadia, M.; Wan, K. W.; Ahmed, W.; Arafa, B. Emergence of 3D printed dosage forms: opportunities and challenges. *Pharm. Res.* **2016**, *33* (8), 1817–1832.
- (37) Jamróz, W.; Szafraniec, J.; Kurek, M.; Jachowicz, R. 3D printing in pharmaceutical and medical applications—recent achievements and challenges. *Pharm. Res.* **2018**, *35* (9), 176.
- (38) Ursan, I. D.; Chiu, L.; Pierce, A. Three-dimensional drug printing: a structured review. *Journal of the American Pharmacists Association* **2013**, *53* (2), 136–144.
- (39) Allahham, N.; Fina, F.; Marcuta, C.; Kraschew, L.; Mohr, W.; Gaisford, S.; Basit, A. W.; Goyanes, A. Selective laser sintering 3D printing of orally disintegrating printlets containing ondansetron. *Pharmaceutics* **2020**, *12* (2), 110.
- (40) Fina, F.; Madla, C. M.; Goyanes, A.; Zhang, J.; Gaisford, S.; Basit, A. W. Fabricating 3D printed orally disintegrating printlets using selective laser sintering. *Int. J. Pharm.* **2018**, *541* (1–2), 101–107.
- (41) Salmoria, G. V.; Klauss, P.; Kanis, L. A. Laser Printing of PCL/Progesterone Tablets for Drug Delivery Applications in Hormone Cancer Therapy. *Lasers in Manufacturing and Materials Processing* **2017**, *4* (3), 108–120.
- (42) Salmoria, G. V.; Cardenuto, M. R.; Roesler, C. R. M.; Zepon, K. M.; Kanis, L. A. PCL/ibuprofen implants fabricated by selective laser sintering for orbital repair. *Procedia CIRP* **2016**, *49*, 188–192.
- (43) Goyanes, A.; Chang, H.; Sedough, D.; Hatton, G. B.; Wang, J.; Buanz, A.; Gaisford, S.; Basit, A. W. Fabrication of controlled-release budesonide tablets via desktop (FDM) 3D printing. *Int. J. Pharm.* **2015**, *496* (2), 414–420.
- (44) Chai, X.; Chai, H.; Wang, X.; Yang, J.; Li, J.; Zhao, Y.; Cai, W.; Tao, T.; Xiang, X. Fused deposition modeling (FDM) 3D printed

- tablets for intragastric floating delivery of domperidone. *Sci. Rep.* **2017**, *7* (1), 2829.
- (45) Goyanes, A.; Buanz, A. B.; Hatton, G. B.; Gaisford, S.; Basit, A. W. 3D printing of modified-release aminosalicylate (4-ASA and 5-ASA) tablets. *Eur. J. Pharm. Biopharm.* **2015**, *89*, 157–162.
- (46) Sadia, M.; Sośnicka, A.; Arafat, B.; Isreb, A.; Ahmed, W.; Kellarakis, A.; Alhnan, M. A. Adaptation of pharmaceutical excipients to FDM 3D printing for the fabrication of patient-tailored immediate release tablets. *Int. J. Pharm.* **2016**, *513* (1–2), 659–668.
- (47) Li, Q.; Guan, X.; Cui, M.; Zhu, Z.; Chen, K.; Wen, H.; Jia, D.; Hou, J.; Xu, W.; Yang, X.; Pan, W. Preparation and investigation of novel gastro-floating tablets with 3D extrusion-based printing. *Int. J. Pharm.* **2018**, *535* (1–2), 325–332.
- (48) Yu, D. G.; Branford-White, C.; Ma, Z. H.; Zhu, L. M.; Li, X. Y.; Yang, X. L. Novel drug delivery devices for providing linear release profiles fabricated by 3DP. *Int. J. Pharm.* **2009**, *370* (1–2), 160–166.
- (49) Wu, B. M.; Borland, S. W.; Giordano, R. A.; Cima, L. G.; Sachs, E. M.; Cima, M. J. Solid free-form fabrication of drug delivery devices. *J. Controlled Release* **1996**, *40* (1–2), 77–87.
- (50) Xiong, R.; Zhang, Z.; Chai, W.; Chrisey, D. B.; Huang, Y. Study of gelatin as an effective energy absorbing layer for laser bioprinting. *Biofabrication* **2017**, *9* (2), 024103.
- (51) Wang, Y.; Wu, S.; Kuss, M. A.; Streubel, P. N.; Duan, B. Effects of hydroxyapatite and hypoxia on chondrogenesis and hypertrophy in 3D bioprinted ADMSC laden constructs. *ACS Biomater. Sci. Eng.* **2017**, *3* (5), 826–835.
- (52) Yeo, M.; Lee, J. S.; Chun, W.; Kim, G. H. An innovative collagen-based cell-printing method for obtaining human adipose stem cell-laden structures consisting of core–sheath structures for tissue engineering. *Biomacromolecules* **2016**, *17* (4), 1365–1375.
- (53) Zhou, Y.; Gui, Q.; Yu, W.; Liao, S.; He, Y.; Tao, X.; Yu, Y.; Wang, Y. Interfacial Diffusion Printing: An Efficient Manufacturing Technique for Artificial Tubular Grafts. *ACS Biomater. Sci. Eng.* **2019**, *5* (11), 6311–6318.
- (54) Zhou, Y.; Liao, S.; Tao, X.; Xu, X. Q.; Hong, Q.; Wu, D.; Wang, Y. Spider-inspired multicomponent 3D printing technique for next-generation complex biofabrication. *ACS Applied Bio Materials* **2018**, *1* (2), 502–510.
- (55) Bredt, J. F.; Anderson, T. U.S. Patent US5,902,441, 1999.
- (56) Yang, J.; Wu, L. W.; Liu, J. U.S. Patent US6,280,785, 2001.
- (57) Electrolux. *Interview with Nico Kläber (Moléculaire) Electrolux-Design Lab finalist*, 2009. <http://group.electrolux.com/en/interview-with-nico-klaber-moleculaire-electrolux-design-lab-finalist-2040/> (accessed Dec 2014).
- (58) CandyFab. *The CandyFab Project*, 2007. http://wiki.candyfab.org/Main_Page (accessed Dec 2014).
- (59) Philips Design. *New design probe explores the future of food*, 2010. www.design.philips.com/philips/sites/philipsdesign/about/design/designnews/pressreleases/foodprobes.page (accessed 22 March 2010).
- (60) Liu, Z.; Zhang, M.; Bhandari, B.; Wang, Y. 3D printing: Printing precision and application in food sector. *Trends Food Sci. Technol.* **2017**, *69*, 83–94.
- (61) Wohlers, T.; Gornet, T. History of additive manufacturing. *Wohlers Report* **2014**, *24*, 118.
- (62) Zhou, X.; Liu, C. J. Three-dimensional printing of porous carbon structures with tailorable pore sizes. *Catal. Today* **2020**, *347*, 2.
- (63) Paggi, R. A.; Salmoria, G. V.; Ghizoni, G. B.; de Medeiros Back, H.; de Mello Gindri, I. Structure and mechanical properties of 3D-printed cellulose tablets by fused deposition modeling. *International Journal of Advanced Manufacturing Technology* **2019**, *100* (9–12), 2767–2774.
- (64) Portanguen, S.; Tournayre, P.; Sicard, J.; Astruc, T.; Mirade, P. S. Toward the design of functional foods and biobased products by 3D printing: A review. *Trends Food Sci. Technol.* **2019**, *86*, 188–198.
- (65) Oyinloye, T. M.; Yoon, W. B. Stability of 3D printing using a mixture of pea protein and alginate: Precision and application of additive layer manufacturing simulation approach for stress distribution. *J. Food Eng.* **2021**, *288*, 110127.
- (66) Severini, C.; Derossi, A.; Ricci, I.; Caporizzi, R.; Fiore, A. Printing a blend of fruit and vegetables. New advances on critical variables and shelf life of 3D edible objects. *J. Food Eng.* **2018**, *220*, 89–100.
- (67) Dankar, I.; Pujolà, M.; El Omar, F.; Sepulcre, F.; Haddarah, A. Impact of mechanical and microstructural properties of potato puree-food additive complexes on extrusion-based 3D printing. *Food Bioprocess Technol.* **2018**, *11* (11), 2021–2031.
- (68) Chang, C.; Chen, S.; Delgado, V.; Hsu, T.; Huang, S.; Kuo, C.; Mao, C.; Olive, X.; Rodriguez, L.; Sepulveda, E. *Additive Manufacturing Printer System for Printing Eg Food Product, Has Processor That Provides Controller with Position Coordinates for Movement of Tool, Instructions for Exchange of Capsule Holders, and Adjustment of Heating Device*; Natural Machines, LLC (NATU-Nonstandard), 2014.
- (69) Kuo, C. J.; Huang, S. H.; Hsu, T. H.; Rodriguez, L.; Olivé, X.; Mao, C. Y.; Chang, C. T.; Chen, S. C.; Sepulveda, E.; Delgado, V. *Manufacturing Food Using 3D Printing Technology*; Natural Machines, LLC, 2014.
- (70) Lipton, J.; Arnold, D.; Nigl, F.; Lopez, N.; Cohen, D. L.; Norén, N.; Lipson, H. Multi-material food printing with complex internal structure suitable for conventional post-processing. *Solid Free-Form Fabrication Symposium* **2010**, 809–815.
- (71) Periard, D.; Schaal, N.; Schaal, M.; Malone, E.; Lipson, H. Printing food. In *2007 International Solid Freeform Fabrication Symposium*, 2007.
- (72) Hao, L.; Mellor, S.; Seaman, O.; Henderson, J.; Sewell, N.; Sloan, M. Material characterisation and process development for chocolate additive layer manufacturing. *Virtual and Physical Prototyping* **2010**, *5* (2), 57–64.
- (73) Schaal, N. *Printing Chocolate*; Du Pont Manual High, 2007.
- (74) Cohen, D. L.; Lipton, J. I.; Cutler, M.; Coulter, D.; Vesco, A.; Lipson, H. Hydrocolloid printing: A novel platform for customized food production. In *Solid Freeform Fabrication Symposium*, Austin, TX, 2009.
- (75) FoodJet *FoodJet Printing Systems*, 2015. <https://www.foodjet.com/>.
- (76) Sher, D.; Tutó, X. Review of 3D Food Printing. *Temas de Disseny* **2015**, No. 31, 104–117.
- (77) Sun, J.; Zhou, W.; Huang, D.; Fuh, J. Y.; Hong, G. S. An overview of 3D printing technologies for food fabrication. *Food Bioprocess Technol.* **2015**, *8* (8), 1605–1615.
- (78) Grood, J. P. W.; Grood, P. J. Method and device for dispensing a liquid. US Patent US20110121016A1, (2011).
- (79) 3D Systems. *3D Systems Previews New Chocolate 3D Printer CocoJet™ at 430 2015 InternationalCES*, 2015. <http://www.3dsystems.com/de/node/7563>.
- (80) Diaz, J. V.; Noort, M. W. J.; Van Bommel, K. J. C. U.S. Patent US15/116,048, 2017.
- (81) Von Hasseln, K. W.; Von Hasseln, E. M.; Williams, D. X.; Gale, R. R. *Making an Edible Component, Comprises Depositing Successive Layers of Food Material According to Digital Data That Describes the Edible Component, and Applying Edible Binders to Regions of the Successive Layers of the Food Material*; 3d Systems, Inc. (Thde-C), 2014.
- (82) Diaz, J. V.; Van Bommel, K. J. C.; Noort, M. W. J.; Henket, J.; Briër, P. Method for the production of edible objects using sls and food products. Patent WO2014193226A1, 2014.
- (83) Diaz, J. V.; Van Bommel, K. J. C.; Noort, M. W.; Henket, J.; Briër, P. *Preparing Edible Product, Preferably Food Product Including Bakery Product, and Confectionary Product, Involves Providing Edible Powder Composition, and Subjecting Composition to Selective Laser Sintering*; Nederlandse Org. Toegepast Natuurwetensch (Nede-C), 2014.
- (84) Forgacs, G.; Marga, F.; Jakab, K. R. U.S. Patent US8,703,216, 2014.
- (85) Marga, F. S. *Engineered Comestible Meat*; National Institute of Food and Agriculture, 2012.
- (86) Kim, H. W.; Lee, I. J.; Park, S. M.; Lee, J. H.; Nguyen, M. H.; Park, H. J. Effect of hydrocolloid addition on dimensional stability in post-processing of 3D printable cookie dough. *Lwt* **2019**, *101*, 69–75.

- (87) Pulatsu, E.; Su, J. W.; Lin, J.; Lin, M. Factors affecting 3D printing and post-processing capacity of cookie dough. *Innovative Food Sci. Emerging Technol.* **2020**, *61*, 102316.
- (88) Liu, Z.; Zhang, M.; Bhandari, B. Effect of gums on the rheological, microstructural and extrusion printing characteristics of mashed potatoes. *Int. J. Biol. Macromol.* **2018**, *117*, 1179–1187.
- (89) Liu, Z.; Zhang, M.; Ye, Y. Indirect prediction of 3D printability of mashed potatoes based on LF-NMR measurements. *J. Food Eng.* **2020**, *287*, 110137.
- (90) Kern, C.; Weiss, J.; Hinrichs, J. Additive layer manufacturing of semi-hard model cheese: Effect of calcium levels on thermo-rheological properties and shear behavior. *J. Food Eng.* **2018**, *235*, 89–97.
- (91) Le Tohic, C.; O'Sullivan, J. J.; Drapala, K. P.; Chartrin, V.; Chan, T.; Morrison, A. P.; Kerry, J. P.; Kelly, A. L. Effect of 3D printing on the structure and textural properties of processed cheese. *J. Food Eng.* **2018**, *220*, 56–64.
- (92) Adediran, A.; Oyedele, A. Operational aspects and regulatory gaps in additive manufacturing. *Additive Manufacturing Handbook: Product Development for the Defense Industry* **2017**, 129.
- (93) Guvendiren, M.; Molde, J.; Soares, R. M.; Kohn, J. Designing biomaterials for 3D printing. *ACS Biomater. Sci. Eng.* **2016**, *2* (10), 1679–1693.
- (94) Zhang, H.; Fang, M.; Yu, Y.; Liu, Q.; Hu, X.; Zhang, L.; Hu, H.; Zhang, C.; Huang, F.; Tian, F.; Zhang, N. Application prospect of 3D printing technology in the food intelligent manufacturing. In *International Conference on Mechatronics and Intelligent Robotics*; Springer: Cham, 2018; pp 974–984.
- (95) Shen, X.; Naguib, H. E. A robust ink deposition system for binder jetting and material jetting. *Additive Manufacturing* **2019**, *29*, 100820.
- (96) Sun, J.; Peng, Z.; Zhou, W.; Fuh, J. Y.; Hong, G. S.; Chiu, A. A review on 3D printing for customized food fabrication. *Procedia Manufacturing* **2015**, *1*, 308–319.
- (97) Southerland, D.; Walters, P.; Huson, D. Edible 3D printing. In *NIP & Digital Fabrication Conference*; Society for Imaging Science and Technology, 2011; Vol. 2011, No. 2, pp 819–822.
- (98) Holland, S.; Tuck, C.; Foster, T. Selective recrystallization of cellulose composite powders and microstructure creation through 3D binder jetting. *Carbohydr. Polym.* **2018**, *200*, 229–238.
- (99) Izdebska, J.; Zolek-Tryznowska, Z. 3D food printing—facts and future. *Agro FOOD Industry Hi Tech* **2016**, *27* (2), 33–37.
- (100) Willcocks, N. A.; Shastry, A.; Collins, T. M.; Camporini, A. V.; Suttle, J. M. U.S. Patent US7,884,953, 2011.
- (101) Serizawa, R.; Shitara, M.; Gong, J.; Makino, M.; Kabir, M. H.; Furukawa, H. 3D jet printer of edible gels for food creation. In *Behavior and Mechanics of Multifunctional Materials and Composites 2014*; International Society for Optics and Photonics, 2014; Vol. 9058, p 90580A.
- (102) Severini, C.; Derossi, A.; Azzollini, D. Variables affecting the printability of foods: Preliminary tests on cereal-based products. *Innovative Food Sci. Emerging Technol.* **2016**, *38*, 281–291.
- (103) Caser, C. They've got a golden ticket. *IEEE Potentials* **2009**, *28* (4), 42–44.
- (104) Zoran, A.; Coelho, M. Cornucopia: the concept of digital gastronomy. *Leonardo* **2011**, *44* (5), 425–431.
- (105) Golding, M.; Archer, R.; Gupta, G.; Wegrzyn, T.; Kim, S.; Millen, C. *Design and Development of a 3-D Food Printer*; Centre of Research Excellence, Massey University, 2011.
- (106) Molitch-Hou, M. *The 3d Fruit Printer and the Raspberry That Tasted Like a Strawberry*, 2014. <https://3dprintingindustry.com/news/3d-fruit-printer-raspberry-tasted-like-strawberry-27713/>.
- (107) Yang, F.; Zhang, M.; Bhandari, B.; Liu, Y. Investigation on lemon juice gel as food material for 3D printing and optimization of printing parameters. *Lwt* **2018**, *87*, 67–76.
- (108) Kim, H. W.; Bae, H.; Park, H. J. Classification of the printability of selected food for 3D printing: Development of an assessment method using hydrocolloids as reference material. *J. Food Eng.* **2017**, *215*, 23–32.
- (109) Liu, L.; Meng, Y.; Dai, X.; Chen, K.; Zhu, Y. 3D printing complex egg-white protein objects: Properties and optimization. *Food Bioprocess Technol.* **2019**, *12* (2), 267–279.
- (110) Liu, Y.; Yu, Y.; Liu, C.; Regenstein, J. M.; Liu, X.; Zhou, P. Rheological and mechanical behavior of milk protein composite gel for extrusion-based 3D food printing. *Lwt* **2019**, *102*, 338–346.
- (111) Shao, Y.; Chaussy, D.; Grosseau, P.; Beneventi, D. Use of microfibrillated cellulose/lignosulfonate blends as carbon precursors: impact of hydrogel rheology on 3D printing. *Ind. Eng. Chem. Res.* **2015**, *54* (43), 10575–10582.
- (112) Panwar, A.; Tan, L. P. Current status of bioinks for micro-extrusion-based 3D bioprinting. *Molecules* **2016**, *21* (6), 685.
- (113) Jungst, T.; Smolan, W.; Schacht, K.; Scheibel, T.; Groll, J. Strategies and molecular design criteria for 3D printable hydrogels. *Chem. Rev.* **2016**, *116* (3), 1496–1539.
- (114) Truby, R. L.; Lewis, J. A. Printing soft matter in three dimensions. *Nature* **2016**, *540* (7633), 371–378.
- (115) Phuhongsung, P.; Zhang, M.; Devahastin, S. Investigation on 3D printing ability of soybean protein isolate gels and correlations with their rheological and textural properties via LF-NMR spectroscopic characteristics. *LWT* **2020**, *122*, 109019.
- (116) Stein, N.; Saathoff, T.; Antoni, S. T.; Schlaefer, A. Creating 3D gelatin phantoms for experimental evaluation in biomedicine. *Current Directions in Biomedical Engineering* **2015**, *1* (1), 331–334.
- (117) Stevenson, M.; Long, J.; Guerrero, P.; de la Caba, K.; Seyfoddin, A.; Etxabide, A. Development and characterization of ribose-cross-linked gelatin products prepared by indirect 3D printing. *Food Hydrocolloids* **2019**, *96*, 65–71.
- (118) Nijdam, J. J.; LeCorre-Bordes, D.; Delvart, A.; Schon, B. S. A rheological test to assess the ability of food inks to form dimensionally stable 3D food structures. *J. Food Eng.* **2021**, *291*, 110235.
- (119) Warner, E. L.; Norton, I. T.; Mills, T. B. Comparing the viscoelastic properties of gelatin and different concentrations of kappa-carrageenan mixtures for additive manufacturing applications. *J. Food Eng.* **2019**, *246*, 58–66.
- (120) Kuo, C. C.; Qin, H.; Acuña, D. F.; Cheng, Y.; Jiang, X. Printability of Hydrogel Composites Using Extrusion-Based 3D Printing and Post-Processing with Calcium Chloride. *J. Food Sci. Nutr* **2019**, *5*, 051.
- (121) Ahmed, J.; Mulla, M.; Joseph, A.; Ejaz, M.; Maniruzzaman, M. Zinc oxide/clove essential oil incorporated type B gelatin nanocomposite formulations: A proof-of-concept study for 3D printing applications. *Food Hydrocolloids* **2020**, *98*, 105256.
- (122) Madaghiele, M.; Marotta, F.; Demitri, C.; Montagna, F.; Maffezzoli, A.; Sannino, A. Development of semi-and grafted interpenetrating polymer networks based on poly (ethylene glycol) diacrylate and collagen. *J. Appl. Biomater. Funct. Mater.* **2014**, *12* (3), 183–192.
- (123) Duarte Campos, D. F.; Blaeser, A.; Buellbach, K.; Sen, K. S.; Xun, W.; Tillmann, W.; Fischer, H. Bioprinting organotypic hydrogels with improved mesenchymal stem cell remodeling and mineralization properties for bone tissue engineering. *Adv. Healthcare Mater.* **2016**, *5* (11), 1336–1345.
- (124) Chien, K. B.; Makridakis, E.; Shah, R. N. Three-dimensional printing of soy protein scaffolds for tissue regeneration. *Tissue Eng., Part C* **2013**, *19* (6), 417–426.
- (125) Chaunier, L.; Leroy, E.; Valle, G. D.; Dalgalarondo, M.; Bakan, B.; Marion, D.; Madec, B.; Lourdin, D. 3D printing of maize protein by fused deposition modeling. In *AIP Conference Proceedings*; AIP Publishing, LLC, 2017; Vol. 1914, No. 1, p 190003.
- (126) Chaunier, L.; Della Valle, G.; Lourdin, D.; Réguerre, A. L.; Cochet, K.; Leroy, E. Viscous sintering kinetics of biopolymer filaments extruded for 3D printing. *Polym. Test.* **2019**, *77*, 105873.
- (127) Ru, J.; Wei, Q.; Yang, L.; Qin, J.; Tang, L.; Wei, J.; Guo, L.; Niu, Y. Zein regulating apatite mineralization, degradability, in vitro cells responses and in vivo osteogenesis of 3D-printed scaffold of n-MS/ZN/PCL ternary composite. *RSC Adv.* **2018**, *8* (34), 18745–18756.
- (128) Fahmy, A. R.; Becker, T.; Jekle, M. 3D printing and additive manufacturing of cereal-based materials: Quality analysis of starch-

based systems using a camera-based morphological approach. *Innovative Food Sci. Emerging Technol.* **2020**, *63*, 102384.

(129) Zhang, Y.; Yu, W.; Ba, Z.; Cui, S.; Wei, J.; Li, H. 3D-printed scaffolds of mesoporous bioglass/gliadin/polycaprolactone ternary composite for enhancement of compressive strength, degradability, cell responses and new bone tissue ingrowth. *Int. J. Nanomed.* **2018**, *13*, 5433.

(130) Liu, Z.; Chen, H.; Zheng, B.; Xie, F.; Chen, L. Understanding the structure and rheological properties of potato starch induced by hot-extrusion 3D printing. *Food Hydrocolloids* **2020**, *105*, 105812.

(131) Liu, Y.; Liu, D.; Wei, G.; Ma, Y.; Bhandari, B.; Zhou, P. 3D printed milk protein food simulant: Improving the printing performance of milk protein concentration by incorporating whey protein isolate. *Innovative Food Sci. Emerging Technol.* **2018**, *49*, 116–126.

(132) Xu, L.; Gu, L.; Su, Y.; Chang, C.; Wang, J.; Dong, S.; Liu, Y.; Yang, Y.; Li, J. Impact of thermal treatment on the rheological, microstructural, protein structures and extrusion 3D printing characteristics of egg yolk. *Food Hydrocolloids* **2020**, *100*, 105399.

(133) Anukiruthika, T.; Moses, J. A.; Anandharamakrishnan, C. 3D printing of egg yolk and white with rice flour blends. *J. Food Eng.* **2020**, *265*, 109691.

(134) Chuanxing, F.; Qi, W.; Hui, L.; Quancheng, Z.; Wang, M. Effects of pea protein on the properties of potato starch-based 3D printing materials. *Int. J. Food Eng.* **2018**, DOI: 10.1515/ijfe-2017-0297.

(135) Zhou, Q.; Wang, M.; Li, H.; Wang, S.; Sun, W.; Chen, X.; Dong, L.; Ruan, Z. Application of Maillard reaction product of xylose–pea protein enzymatic hydrolysate in 3D printing. *J. Sci. Food Agric.* **2020**, *100* (7), 2982–2990.

(136) Mu, X.; Wang, Y.; Guo, C.; Li, Y.; Ling, S.; Huang, W.; Cebe, P.; Hsu, H. H.; De Ferrari, F.; Jiang, X.; Xu, Q.; et al. 3D Printing of Silk Protein Structures by Aqueous Solvent-Directed Molecular Assembly. *Macromol. Biosci.* **2020**, *20* (1), 1900191.

(137) Zhao, S.; Guo, C.; Kumarasena, A.; Omenetto, F. G.; Kaplan, D. L. 3D Printing of Functional Microalgal Silk Structures for Environmental Applications. *ACS Biomater. Sci. Eng.* **2019**, *5* (9), 4808–4816.

(138) Zhang, J.; Allardyce, B. J.; Rajkhowa, R.; Zhao, Y.; Dilley, R. J.; Redmond, S. L.; Wang, X.; Liu, X. 3D printing of silk particle-reinforced chitosan hydrogel structures and their properties. *ACS Biomater. Sci. Eng.* **2018**, *4* (8), 3036–3046.

(139) Zhang, R.; Tao, Y.; Xu, Q.; Liu, N.; Chen, P.; Zhou, Y.; Bai, Z. Rheological and ion-conductive properties of injectable and self-healing hydrogels based on xanthan gum and silk fibroin. *Int. J. Biol. Macromol.* **2020**, *144*, 473–482.

(140) Gholamipour-Shirazi, A.; Norton, I. T.; Mills, T. Designing hydrocolloid based food-ink formulations for extrusion 3D printing. *Food Hydrocolloids* **2019**, *95*, 161–167.

(141) Tamura, T.; Akiyama, R.; Tanaka, R. I.; Kawamoto, H.; Umez, S. Groove fabrication on surface of soft gelatin gel utilizing micro-electrical discharge machining (Micro-EDM). *J. Food Eng.* **2020**, *277*, 109919.

(142) Park, S. M.; Kim, H. W.; Park, H. J. Callus-based 3D printing for food exemplified with carrot tissues and its potential for innovative food production. *J. Food Eng.* **2020**, *271*, 109781.

(143) Włodarczyk-Biegun, M. K.; del Campo, A. 3D bioprinting of structural proteins. *Biomaterials* **2017**, *134*, 180–201.

(144) Ma, Q.; Mohawk, D.; Jahani, B.; Wang, X.; Chen, Y.; Mahoney, A.; Zhu, J. Y.; Jiang, L. UV-Curable Cellulose Nanofiber-Reinforced Soy Protein Resins for 3D Printing and Conventional Molding. *ACS Applied Polymer Materials* **2020**, *2*, 4666.

(145) Severini, C.; Azzollini, D.; Albenzio, M.; Derossi, A. On printability, quality and nutritional properties of 3D printed cereal based snacks enriched with edible insects. *Food Res. Int.* **2018**, *106*, 666–676.

(146) Chien, K. B.; Shah, R. N. U.S. Patent US14/980,132, 2016.

(147) Bhatnagar, S.; Chawla, S. R.; Kulkarni, O. P.; Venuganti, V. V. K. Zein microneedles for transcutaneous vaccine delivery: fabrication, characterization, and in vivo evaluation using ovalbumin as the model antigen. *ACS omega* **2017**, *2* (4), 1321–1332.

(148) Tomasula, P. M.; Sousa, A. M.; Liou, S. C.; Li, R.; Bonnaillie, L. M.; Liu, L. S. Electrospinning of casein/pullulan blends for food-grade applications. *J. Dairy Sci.* **2016**, *99* (3), 1837–1845.

(149) Xie, J.; Hsieh, Y. L. Ultra-high surface fibrous membranes from electrospinning of natural proteins: casein and lipase enzyme. *J. Mater. Sci.* **2003**, *38* (10), 2125–2133.

(150) Sol, I. E. J.; Van der Linden, D.; Van Bommel, K. J. C. *3D food printing: The barilla collaboration*, 2015.

(151) Keerthana, K.; Anukiruthika, T.; Moses, J. A.; Anandharamakrishnan, C. Development of fiber-enriched 3D printed snacks from alternative foods: A study on button mushroom. *J. Food Eng.* **2020**, *287*, 110116.

(152) Krishnaraj, P.; Anukiruthika, T.; Choudhary, P.; Moses, J. A.; Anandharamakrishnan, C. 3D extrusion printing and post-processing of fibre-rich snack from indigenous composite flour. *Food Bioprocess Technol.* **2019**, *12* (10), 1776–1786.

(153) Gelinsky, M. Biopolymer hydrogel bioinks. In *3D Bioprinting for Reconstructive Surgery*; Woodhead Publishing, 2018; pp 125–136.

(154) Liu, S.; Zhang, H.; Hu, Q.; Shen, Z.; Rana, D.; Ramalingam, M. Designing vascular supportive albumen-rich composite bioink for organ 3D printing. *Journal of the Mechanical Behavior of Biomedical Materials* **2020**, *104*, 103642.

(155) Charbonneau, A. M.; Kinsella, J. M.; Tran, S. D. 3D Cultures of Salivary Gland Cells in Native or Gelled Egg Yolk Plasma, Combined with Egg-white and 3D-Printing of Gelled Egg Yolk Plasma. *Materials* **2019**, *12* (21), 3480.

(156) Du, X.; Wei, D.; Huang, L.; Zhu, M.; Zhang, Y.; Zhu, Y. 3D printing of mesoporous bioactive glass/silk fibroin composite scaffolds for bone tissue engineering. *Mater. Sci. Eng., C* **2019**, *103*, 109731.

(157) Karavasili, C.; Tsongas, K.; Andreadis, I. I.; Andriotis, E. G.; Papachristou, E. T.; Papi, R. M.; Tzetzis, D.; Fatouros, D. G. Physico-mechanical and finite element analysis evaluation of 3D printable alginate-methylcellulose inks for wound healing applications. *Carbohydr. Polym.* **2020**, *247*, 116666.

(158) Bom, S.; Santos, C.; Barros, R.; Martins, A. M.; Paradiso, P.; Cláudio, R.; Pinto, P. C.; Ribeiro, H. M.; Marto, J. Effects of Starch Incorporation on the Physicochemical Properties and Release Kinetics of Alginate-Based 3D Hydrogel Patches for Topical Delivery. *Pharmaceutics* **2020**, *12* (8), 719.

(159) Liu, Z.; Zhang, M.; Bhandari, B.; Yang, C. Impact of rheological properties of mashed potatoes on 3D printing. *J. Food Eng.* **2018**, *220*, 76–82.

(160) Mendes, A. C.; Stephansen, K.; Chronakis, I. S. Electrospinning of food proteins and polysaccharides. *Food Hydrocolloids* **2017**, *68*, 53–68.

(161) Chen, H.; Xie, F.; Chen, L.; Zheng, B. Effect of rheological properties of potato, rice and corn starches on their hot-extrusion 3D printing behaviors. *J. Food Eng.* **2019**, *244*, 150–158.

(162) Wu, Q.; Maire, M.; Lerouge, S.; Therriault, D.; Heuzey, M. C. 3D printing of microstructured and stretchable chitosan hydrogel for guided cell growth. *Advanced Biosystems* **2017**, *1* (6), 1700058.

(163) Wu, Q.; Therriault, D.; Heuzey, M. C. Processing and properties of chitosan inks for 3D printing of hydrogel microstructures. *ACS Biomater. Sci. Eng.* **2018**, *4* (7), 2643–2652.

(164) Ng, W. L.; Yeong, W. Y.; Naing, M. W. Polyelectrolyte gelatin-chitosan hydrogel optimized for 3D bioprinting in skin tissue engineering. *International Journal of Bioprinting* **2016**, *2* (1), 53–62.

(165) Zolfagharian, A.; Kaynak, A.; Khoo, S. Y.; Kouzani, A. Z. Polyelectrolyte soft actuators: 3D printed chitosan and cast gelatin. *3D Printing and Additive Manufacturing* **2018**, *5* (2), 138–150.

(166) Janarthanan, G.; Tran, H. N.; Cha, E.; Lee, C.; Das, D.; Noh, I. 3D printable and injectable lactoferrin-loaded carboxymethyl cellulose-glycol chitosan hydrogels for tissue engineering applications. *Mater. Sci. Eng., C* **2020**, *113*, 111008.

(167) Robinson, T. M.; Talebian, S.; Foroughi, J.; Yue, Z.; Fay, C.; Wallace, G. G. Fabrication of Aligned Biomimetic Gellan Gum-Chitosan Microstructures Through 3D Printed Microfluidic Channels and Multiple In-Situ Crosslinking Mechanisms. *ACS Biomater. Sci. Eng.* **2020**, *6*, 3638.

- (168) Wu, C. S. Modulation, functionality, and cytocompatibility of three-dimensional printing materials made from chitosan-based polysaccharide composites. *Mater. Sci. Eng., C* **2016**, *69*, 27–36.
- (169) Singh, S.; Singh, G.; Prakash, C.; Ramakrishna, S.; Lamberti, L.; Pruncu, C. I. 3D printed biodegradable composites: An insight into mechanical properties of PLA/chitosan scaffold. *Polym. Test.* **2020**, *89*, 106722.
- (170) Erkok, P.; Uvak, I.; Nazeer, M. A.; Batool, S. R.; Odeh, Y. N.; Akdogan, O.; Kizilel, S. 3D Printing of Cytocompatible Gelatin-Cellulose-Alginate Blend Hydrogels. *Macromol. Biosci.* **2020**, *20*, 2000106.
- (171) Vancauwenberghe, V.; Verboven, P.; Lammertyn, J.; Nicolai, B. Development of a coaxial extrusion deposition for 3D printing of customizable pectin-based food simulant. *J. Food Eng.* **2018**, *225*, 42–52.
- (172) Vancauwenberghe, V.; Katalagianakis, L.; Wang, Z.; Meerts, M.; Hertog, M.; Verboven, P.; Moldenaers, P.; Hendrickx, M. E.; Lammertyn, J.; Nicolai, B. Pectin based food-ink formulations for 3-D printing of customizable porous food simulants. *Innovative Food Sci. Emerging Technol.* **2017**, *42*, 138–150.
- (173) Long, J.; Etxeberria, A. E.; Nand, A. V.; Bunt, C. R.; Ray, S.; Seyfoddin, A. A 3D printed chitosan-pectin hydrogel wound dressing for lidocaine hydrochloride delivery. *Mater. Sci. Eng., C* **2019**, *104*, 109873.
- (174) Cernencu, A. I.; Lungu, A.; Stancu, I. C.; Serafim, A.; Heggset, E.; Syverud, K.; Iovu, H. Bioinspired 3D printable pectin-nanocellulose ink formulations. *Carbohydr. Polym.* **2019**, *220*, 12–21.
- (175) García-Segovia, P.; García-Alcaraz, V.; Balasch-Parisi, S.; Martínez-Monzó, J. 3D printing of gels based on xanthan/konjac gums. *Innovative Food Sci. Emerging Technol.* **2020**, *64*, 102343.
- (176) Huang, C. Y. Extrusion-Based 3D Printing and Characterization of Edible Materials. Master's thesis, University of Waterloo, 2018.
- (177) Strother, H.; Moss, R.; McSweeney, M. B. Comparison of 3D printed and moulded carrots produced with gelatin, guar gum and xanthan gum. *J. Texture Stud.* **2020**, *51*, 852.
- (178) Dick, A.; Bhandari, B.; Dong, X.; Prakash, S. Feasibility study of hydrocolloid incorporated 3D printed pork as dysphagia food. *Food Hydrocolloids* **2020**, *107*, 105940.
- (179) Caroway, B.; Malo, S.; Parsons, F. The Effectiveness of a 3D Printed Hydrogel Membrane to Sustain Algal Growth. *ChemRxiv*, 2020. https://chemrxiv.org/articles/preprint/The_Effectiveness_of_a_3D_Printed_Hydrogel_Membrane_to_Sustain_Algal_Growth/12567680/1.
- (180) Bakarich, S. E.; Balding, P.; Gorkin, R., III; Spinks, G. M.; et al. Printed ionic-covalent entanglement hydrogels from carrageenan and an epoxy amine. *RSC Adv.* **2014**, *4* (72), 38088–38092.
- (181) Andriotis, E. G.; Monou, P. K.; Louka, A.; Papaefstathiou, E.; Eleftheriadis, G. K.; Fatouros, D. G. Development of food grade 3D printable ink based on pectin containing cannabidiol/cyclodextrin inclusion complexes. *Drug Dev. Ind. Pharm.* **2020**, *46* (10), 1569–1577.
- (182) Conceição, J.; Farto-Vaamonde, X.; Goyanes, A.; Adeoye, O.; Concheiro, A.; Cabral-Marques, H.; Sousa Lobo, J. M. S.; Alvarez-Lorenzo, C. Hydroxypropyl- β -cyclodextrin-based fast dissolving carbamazepine printlets prepared by semisolid extrusion 3D printing. *Carbohydr. Polym.* **2019**, *221*, 55–62.
- (183) Allahham, N.; Fina, F.; Marcuta, C.; Kraschew, L.; Mohr, W.; Gaisford, S.; Basit, A. W.; Goyanes, A. Selective laser sintering 3D printing of orally disintegrating printlets containing ondansetron. *Pharmaceutics* **2020**, *12* (2), 110.
- (184) Zhou, Z. X.; Buchanan, F.; Lennon, A.; Dunne, N. Investigating approaches for three-dimensional printing of hydroxyapatite scaffolds for bone regeneration. In *Key Engineering Materials*; Trans Tech Publications, Ltd.: 2015; Vol. 631, pp 306–311.
- (185) Musazzi, U. M.; Selmin, F.; Ortenzi, M. A.; Mohammed, G. K.; Franzé, S.; Minghetti, P.; Cilirzo, F. Personalized orodispersible films by hot melt ram extrusion 3D printing. *Int. J. Pharm.* **2018**, *551* (1–2), 52–59.
- (186) Ouyang, L.; Highley, C. B.; Rodell, C. B.; Sun, W.; Burdick, J. A. 3D printing of shear-thinning hyaluronic acid hydrogels with secondary crosslinking. *ACS Biomater. Sci. Eng.* **2016**, *2* (10), 1743–1751.
- (187) Gaetani, R.; Feyen, D. A.; Verhage, V.; Slaats, R.; Messina, E.; Christman, K. L.; Giacomello, A.; Doevendans, P. A.; Sluijter, J. P. Epicardial application of cardiac progenitor cells in a 3D-printed gelatin/hyaluronic acid patch preserves cardiac function after myocardial infarction. *Biomaterials* **2015**, *61*, 339–348.
- (188) Sun, A. X.; Lin, H.; Beck, A. M.; Kilroy, E. J.; Tuan, R. S. Projection stereolithographic fabrication of human adipose stem cell-incorporated biodegradable scaffolds for cartilage tissue engineering. *Front. Bioeng. Biotechnol.* **2015**, *3*, 115.
- (189) Schuurman, W.; Levett, P. A.; Pot, M. W.; van Weeren, P. R.; Dhert, W. J.; Huttmacher, D. W.; Melchels, F. P.; Klein, T. J.; Malda, J. Gelatin-methacrylamide hydrogels as potential biomaterials for fabrication of tissue-engineered cartilage constructs. *Macromol. Biosci.* **2013**, *13* (5), 551–561.
- (190) Pescosolido, L.; Schuurman, W.; Malda, J.; Matricardi, P.; Alhaique, F.; Coviello, T.; van Weeren, P. R.; Dhert, W. J.; Hennink, W. E.; Vermonden, T. Hyaluronic acid and dextran-based semi-IPN hydrogels as biomaterials for bioprinting. *Biomacromolecules* **2011**, *12* (5), 1831–1838.
- (191) Shie, M. Y.; Chang, W. C.; Wei, L. J.; Huang, Y. H.; Chen, C. H.; Shih, C. T.; Chen, Y. W.; Shen, Y. F. 3D printing of cytocompatible water-based light-cured polyurethane with hyaluronic acid for cartilage tissue engineering applications. *Materials* **2017**, *10* (2), 136.
- (192) Shahbazi, M.; Ettelaie, R.; Rajabzadeh, G. Physico-mechanical analysis data in support of compatibility of chitosan/ κ -carrageenan polyelectrolyte films achieved by ascorbic acid, and the thermal degradation theory of κ -carrageenan influencing the properties of its blends. *Data in brief* **2016**, *9*, 648–660.
- (193) Shahbazi, M.; Rajabzadeh, G.; Ahmadi, S. J. Characterization of nanocomposite film based on chitosan intercalated in clay platelets by electron beam irradiation. *Carbohydr. Polym.* **2017**, *157*, 226–235.
- (194) Fang, Y.; Al-Assaf, S.; Phillips, G. O.; Nishinari, K.; Funami, T.; Williams, P. A.; Li, L. Multiple steps and critical behaviors of the binding of calcium to alginate. *J. Phys. Chem. B* **2007**, *111* (10), 2456–2462.
- (195) Shahbazi, M.; Rajabzadeh, G.; Ettelaie, R.; Rafe, A. Kinetic study of κ -carrageenan degradation and its impact on mechanical and structural properties of chitosan/ κ -carrageenan film. *Carbohydr. Polym.* **2016**, *142*, 167–176.
- (196) Jiankang, H.; Dichen, L.; Yaxiong, L.; Bo, Y.; Bingheng, L.; Qin, L. Fabrication and characterization of chitosan/gelatin porous scaffolds with predefined internal microstructures. *Polymer* **2007**, *48* (15), 4578–4588.
- (197) Hospodiuk, M.; Dey, M.; Sosnoski, D.; Ozbolat, I. T. The bioink: a comprehensive review on bioprintable materials. *Biotechnol. Adv.* **2017**, *35* (2), 217–239.
- (198) Morris, V. B.; Nimbalkar, S.; Younesi, M.; McClellan, P.; Akkus, O. Mechanical properties, cytocompatibility and manufacturability of chitosan: PEGDA hybrid-gel scaffolds by stereolithography. *Ann. Biomed. Eng.* **2017**, *45* (1), 286–296.
- (199) Azam, S. R.; Zhang, M.; Mujumdar, A. S.; Yang, C. Study on 3D printing of orange concentrate and material characteristics. *J. Food Process Eng.* **2018**, *41* (5), e12689.
- (200) Martínez Avila, H. M.; Schwarz, S.; Rotter, N.; Gatenholm, P. 3D bioprinting of human chondrocyte-laden nanocellulose hydrogels for patient-specific auricular cartilage regeneration. *Bioprinting* **2016**, *1*–2, 22–35.
- (201) Heggset, E. B.; Strand, B. L.; Sundby, K. W.; Simon, S.; Chinga-Carrasco, G.; Syverud, K. Viscoelastic properties of nanocellulose based inks for 3D printing and mechanical properties of CNF/alginate biocomposite gels. *Cellulose* **2019**, *26* (1), 581–595.
- (202) Liu, Y.; Hamid, Q.; Snyder, J.; Wang, C.; Sun, W. Evaluating fabrication feasibility and biomedical application potential of in situ 3D printing technology. *Rapid Prototyping Journal* **2016**, *22*, 947.
- (203) Lindman, B.; Karlström, G.; Stigsson, L. On the mechanism of dissolution of cellulose. *J. Mol. Liq.* **2010**, *156* (1), 76–81.

- (204) Contessi Negrini, N. C.; Bonetti, L.; Contili, L.; Farè, S. 3D printing of methylcellulose-based hydrogels. *Bioprinting* **2018**, *10*, e00024.
- (205) Vancauwenberghe, V.; Baiye Mfortaw Mbong, V.; Vanstreels, E.; Verboven, P.; Lammertyn, J.; Nicolai, B. 3D printing of plant tissue for innovative food manufacturing: Encapsulation of alive plant cells into pectin based bio-ink. *J. Food Eng.* **2019**, *263*, 454–464.
- (206) Liu, S.; Li, L. Ultrastretchable and self-healing double-network hydrogel for 3D printing and strain sensor. *ACS Appl. Mater. Interfaces* **2017**, *9* (31), 26429–26437.
- (207) Shahbazi, M.; Rajabzadeh, G.; Rafe, A.; Ettelaie, R.; Ahmadi, S. J. The physico-mechanical and structural characteristics of blend film of poly (vinyl alcohol) with biodegradable polymers as affected by disorder-to-order conformational transition. *Food Hydrocolloids* **2016**, *60*, 393–404.
- (208) Yang, L.; Zeng, X.; Ditta, A.; Feng, B.; Su, L.; Zhang, Y. Preliminary 3D printing of large inclined-shaped alumina ceramic parts by direct ink writing. *J. Adv. Ceram.* **2020**, *9* (3), 312–319.
- (209) Tan, C.; Chua, C. K.; Li, L.; Wong, G. Enhancing 3D printability of pureed food by addition of hydrocolloids. *Proceedings of the 3rd International Conference on Progress in Additive Manufacturing (Pro-AM 2018)* **2018**, 662–666, DOI: 10.25341/D42C7V.
- (210) Kim, H. W.; Lee, J. H.; Park, S. M.; Lee, M. H.; Lee, I. W.; Doh, H. S.; Park, H. J. Effect of hydrocolloids on rheological properties and printability of vegetable inks for 3D food Printing. *J. Food Sci.* **2018**, *83* (12), 2923–2932.
- (211) Rapisarda, M.; Valenti, G.; Carbone, D. C.; Rizzarelli, P.; Recca, G.; La Carta, S.; Paradisi, R.; Finchiario, S. Strength, fracture and compression properties of gelatins by a new 3D printed tool. *J. Food Eng.* **2018**, *220*, 38–48.
- (212) Rycerz, K.; Stepien, K. A.; Czapiewska, M.; Arafat, B. T.; Habashy, R.; Isreb, A.; Peak, M.; Alhnan, M. A. Embedded 3D printing of novel bespoke soft dosage form concept for pediatrics. *Pharmaceutics* **2019**, *11* (12), 630.
- (213) Glicksman, M. *Food Hydrocolloids*; CRC Press, 2020; Vol. 1.
- (214) Azam, R. S.; Zhang, M.; Bhandari, B.; Yang, C. Effect of different gums on features of 3D printed object based on vitamin-D enriched orange concentrate. *Food Biophysics* **2018**, *13* (3), 250–262.
- (215) Nida, S.; Anukiruthika, T.; Moses, J. A.; Anandharamkrishnan, C. 3D printing of grinding and milling fractions of rice husk. *Waste Biomass Valorization* **2020**, DOI: 10.1007/s12649-020-01000-w.
- (216) Pan, X.; Wang, Q.; Ning, D.; Dai, L.; Liu, K.; Ni, Y.; Chen, L.; Huang, L. Ultraflexible self-healing guar gum-glycerol hydrogel with injectable, antifreeze, and strain-sensitive properties. *ACS Biomater. Sci. Eng.* **2018**, *4* (9), 3397–3404.
- (217) Palem, R. R.; Madhusudana Rao, K.; Kang, T. J. Self-healable and dual-functional guar gum-grafted-polyacrylamidoglycolic acid-based hydrogels with nano-silver for wound dressings. *Carbohydr. Polym.* **2019**, *223*, 115074.
- (218) Wu, D.; Yu, Y.; Tan, J.; Huang, L.; Luo, B.; Lu, L.; Zhou, C. 3D bioprinting of gellan gum and poly (ethylene glycol) diacrylate based hydrogels to produce human-scale constructs with high-fidelity. *Mater. Des.* **2018**, *160*, 486–495.
- (219) Lozano, R.; Stevens, L.; Thompson, B. C.; Gilmore, K. J.; Gorkin, R., III; Stewart, E. M.; in het Panhuis, M.; Romero-Ortega, M.; Wallace, G. G. 3D printing of layered brain-like structures using peptide modified gellan gum substrates. *Biomaterials* **2015**, *67*, 264–273.
- (220) Yu, I.; Kaonis, S.; Chen, R. A study on degradation behavior of 3D printed gellan gum scaffolds. *Procedia CIRP* **2017**, *65*, 78–83.
- (221) Akkineni, A. R.; Ahlfeld, T.; Funk, A.; Waske, A.; Lode, A.; Gelinsky, M. Highly concentrated alginate-gellan gum composites for 3D plotting of complex tissue engineering scaffolds. *Polymers* **2016**, *8* (5), 170.
- (222) Petta, D.; D'Amora, U.; Ambrosio, L.; Grijpma, D. W.; Eglin, D.; D'Este, M. Hyaluronic acid as a bioink for extrusion-based 3D printing. *Biofabrication* **2020**, *12* (3), 032001.
- (223) Skardal, A.; Devarasetty, M.; Kang, H. W.; Mead, I.; Bishop, C.; Shupe, T.; Lee, S. J.; Jackson, J.; Yoo, J.; Soker, S.; Atala, A. A hydrogel bioink toolkit for mimicking native tissue biochemical and mechanical properties in bioprinted tissue constructs. *Acta Biomater.* **2015**, *25*, 24–34.
- (224) Xia, H.; Zhao, D.; Zhu, H.; Hua, Y.; Xiao, K.; Xu, Y.; Liu, Y.; Chen, W.; Liu, Y.; Zhang, W.; Liu, W.; et al. Lyophilized scaffolds fabricated from 3D-printed photocurable natural hydrogel for cartilage regeneration. *ACS Appl. Mater. Interfaces* **2018**, *10* (37), 31704–31715.
- (225) Elbl, J.; Gajdziok, J.; Kolarczyk, J. 3D printing of multilayered orodispersible films with in-process drying. *Int. J. Pharm.* **2020**, *575*, 118883.
- (226) Kiumarsi, M.; Majchrzak, D.; Yeganehzad, S.; Jäger, H.; Shahbazi, M. Comparative study of instrumental properties and sensory profiling of low-calorie chocolate containing hydrophobically modified inulin. Part I: Rheological, thermal, structural and external preference mapping. *Food Hydrocolloids* **2020**, *104*, 105698.
- (227) Kiumarsi, M.; Majchrzak, D.; Jäger, H.; Song, J.; Lieleg, O.; Shahbazi, M. Comparative study of instrumental properties and sensory profiling of low-calorie chocolate containing hydrophobically modified inulin. Part II: Proton mobility, topological, tribological and dynamic sensory properties. *Food Hydrocolloids* **2021**, *110*, 106144.
- (228) Kiumarsi, M.; Shahbazi, M.; Yeganehzad, S.; Majchrzak, D.; Lieleg, O.; Winkeljann, B. Relation between structural, mechanical and sensory properties of gluten-free bread as affected by modified dietary fibers. *Food Chem.* **2019**, *277*, 664–673.
- (229) Severini, C.; Derossi, A. Could the 3D printing technology be a useful strategy to obtain customized nutrition. *J. Clin. Gastroenterol.* **2016**, *50* (1), S175–S178.
- (230) Della Giustina, G.; Gandin, A.; Brigo, L.; Panciera, T.; Giullitti, S.; Sgarbossa, P.; D'Alessandro, D.; Trombi, L.; Danti, S.; Brusatin, G. Polysaccharide hydrogels for multiscale 3D printing of pullulan scaffolds. *Mater. Des.* **2019**, *165*, 107566.
- (231) Hennink, W. E.; van Nostrum, C. F. Novel crosslinking methods to design hydrogels. *Adv. Drug Delivery Rev.* **2012**, *64*, 223–236.
- (232) Shahbazi, M.; Ahmadi, S. J.; Seif, A.; Rajabzadeh, G. Carboxymethyl cellulose film modification through surface photocrosslinking and chemical crosslinking for food packaging applications. *Food Hydrocolloids* **2016**, *61*, 378–389.
- (233) Chimene, D.; Kaunas, R.; Gaharwar, A. K. Hydrogel bioink reinforcement for additive manufacturing: a focused review of emerging strategies. *Adv. Mater.* **2020**, *32* (1), 1902026.
- (234) Müller, W. E.; Tolba, E.; Schröder, H. C.; Neufurth, M.; Wang, S.; Link, T.; Al-Nawas, B.; Wang, X. A new printable and durable N, O-carboxymethyl chitosan–Ca²⁺–polyphosphate complex with morphogenetic activity. *J. Mater. Chem. B* **2015**, *3* (8), 1722–1730.
- (235) Pitjamt, S.; Thunsiri, K.; Nakkiew, W.; Wongwichai, T.; Pothacharoen, P.; Wattanutchariya, W. The possibility of interlocking nail fabrication from FFF 3D printing PLA/PCL/HA composites coated by local silk fibroin for canine bone fracture treatment. *Materials* **2020**, *13* (7), 1564.
- (236) López De Dicastillo, C. L.; Rodríguez, F.; Guarda, A.; Galotto, M. J. Antioxidant films based on cross-linked methyl cellulose and native Chilean berry for food packaging applications. *Carbohydr. Polym.* **2016**, *136*, 1052–1060.
- (237) Torres-Rendon, J. G.; Köpf, M.; Gehlen, D.; Blaeser, A.; Fischer, H.; Laporte, L. D.; Walther, A. Cellulose nanofibril hydrogel tubes as sacrificial templates for freestanding tubular cell constructs. *Biomacromolecules* **2016**, *17* (3), 905–913.
- (238) Wang, L. L.; Highley, C. B.; Yeh, Y. C.; Galarraga, J. H.; Uman, S.; Burdick, J. A. Three-dimensional extrusion bioprinting of single- and double-network hydrogels containing dynamic covalent crosslinks. *J. Biomed. Mater. Res., Part A* **2018**, *106* (4), 865–875.
- (239) Weis, M.; Shan, J.; Kuhlmann, M.; Jungst, T.; Tessmar, J.; Groll, J. Evaluation of hydrogels based on oxidized hyaluronic acid for bioprinting. *Gels* **2018**, *4* (4), 82.
- (240) Chan, L. W.; Heng, P. W. Effects of aldehydes and methods of crosslinking on properties of calcium alginate microspheres prepared by emulsification. *Biomaterials* **2002**, *23* (5), 1319–1326.

- (241) Maia, J.; Ribeiro, M. P.; Ventura, C.; Carvalho, R. A.; Correia, I. J.; Gil, M. H. Ocular injectable formulation assessment for oxidized dextran-based hydrogels. *Acta Biomater.* **2009**, *5* (6), 1948–1955.
- (242) Jiang, Y.; Zhou, J.; Yang, Z.; Liu, D.; Xu, X.; Zhao, G.; Shi, H.; Zhang, Q. Dialdehyde cellulose nanocrystal/gelatin hydrogel optimized for 3D printing applications. *J. Mater. Sci.* **2018**, *53* (16), 11883–11900.
- (243) Lee, M.; Bae, K.; Levinson, C.; Zenobi-Wong, M. Nanocomposite bioink exploits dynamic covalent bonds between nanoparticles and polysaccharides for precision bioprinting. *Biofabrication* **2020**, *12* (2), 025025.
- (244) Schwarz, S.; Kuth, S.; Distler, T.; Gögele, C.; Stölzel, K.; Detsch, R.; Boccaccini, A. R.; Schulze-Tanzil, G. 3D printing and characterization of human nasoseptal chondrocytes laden dual crosslinked oxidized alginate-gelatin hydrogels for cartilage repair approaches. *Mater. Sci. Eng., C* **2020**, *116*, 111189.
- (245) Ko, E. S.; Kim, C.; Choi, Y.; Lee, K. Y. 3D printing of self-healing ferrogel prepared from glycol chitosan, oxidized hyaluronate, and iron oxide nanoparticles. *Carbohydr. Polym.* **2020**, *245*, 116496.
- (246) Rees, A.; Powell, L. C.; Chinga-Carrasco, G.; Gethin, D. T.; Syverud, K.; Hill, K. E.; Thomas, D. W. 3D bioprinting of carboxymethylated-periodate oxidized nanocellulose constructs for wound dressing applications. *BioMed Res. Int.* **2015**, *2015*, 1.
- (247) Simsek, S.; Ovando-Martínez, M.; Whitney, K.; Bello-Pérez, L. A. Effect of acetylation, oxidation and annealing on physicochemical properties of bean starch. *Food Chem.* **2012**, *134* (4), 1796–1803.
- (248) Maniglia, B. C.; Lima, D. C.; Matta, M. D., Jr.; Le-Bail, P.; Le-Bail, A.; Augusto, P. E. D. Hydrogels based on ozonated cassava starch: Effect of ozone processing and gelatinization conditions on enhancing 3D-printing applications. *Int. J. Biol. Macromol.* **2019**, *138*, 1087–1097.
- (249) Shi, W.; Sun, M.; Hu, X.; Ren, B.; Cheng, J.; Li, C.; Duan, X.; Fu, X.; Zhang, J.; Chen, H.; Ao, Y. Structurally and functionally optimized silk-fibroin–gelatin scaffold using 3D printing to repair cartilage injury in vitro and in vivo. *Adv. Mater.* **2017**, *29* (29), 1701089.
- (250) Kim, Y. B.; Lee, H.; Kim, G. H. Strategy to achieve highly porous/biocompatible macroscale cell blocks, using a collagen/genipin-bioink and an optimal 3D printing process. *ACS Appl. Mater. Interfaces* **2016**, *8* (47), 32230–32240.
- (251) Liu, I. H.; Chang, S. H.; Lin, H. Y. Chitosan-based hydrogel tissue scaffolds made by 3D plotting promotes osteoblast proliferation and mineralization. *Biomedical Materials* **2015**, *10* (3), 035004.
- (252) Hafezi, F.; Scoutaris, N.; Douroumis, D.; Boateng, J. 3D printed chitosan dressing crosslinked with genipin for potential healing of chronic wounds. *Int. J. Pharm.* **2019**, *560*, 406–415.
- (253) Hafezi, F.; Shorter, S.; Tabriz, A. G.; Hurt, A.; Elmes, V.; Boateng, J.; Douroumis, D. Bioprinting and Preliminary Testing of Highly Reproducible Novel Bioink for Potential Skin Regeneration. *Pharmaceutics* **2020**, *12* (6), 550.
- (254) Montemurro, F.; De Maria, C.; Orsi, G.; Ghezzi, L.; Tinè, M. R.; Vozzi, G. Genipin diffusion and reaction into a gelatin matrix for tissue engineering applications. *J. Biomed. Mater. Res., Part B* **2017**, *105* (3), 473–480.
- (255) Nagiah, N.; Bhattacharjee, M.; Murdock, C. J.; Kan, H. M.; Barajaa, M.; Laurencin, C. T. Spatial alignment of 3D printed scaffolds modulates genotypic expression in pre-osteoblasts. *Mater. Lett.* **2020**, *276*, 128189.
- (256) Zhou, M.; Lee, B. H.; Tan, Y. J.; Tan, L. P. Microbial transglutaminase induced controlled crosslinking of gelatin methacryloyl to tailor rheological properties for 3D printing. *Biofabrication* **2019**, *11* (2), 025011.
- (257) Li, L.; Lin, Q.; Tang, M.; Duncan, A. J.; Ke, C. Advanced Polymer Designs for Direct-Ink-Write 3D Printing. *Chem. - Eur. J.* **2019**, *25* (46), 10768–10781.
- (258) Cheng, Y. L.; Chen, F. Preparation and characterization of photocured poly (*ε*-caprolactone) diacrylate/poly (ethylene glycol) diacrylate/chitosan for photopolymerization-type 3D printing tissue engineering scaffold application. *Mater. Sci. Eng., C* **2017**, *81*, 66–73.
- (259) Huang, J.; Fu, H.; Wang, Z.; Meng, Q.; Liu, S.; Wang, H.; Zheng, X.; Dai, J.; Zhang, Z. BMSCs-laden gelatin/sodium alginate/carboxymethyl chitosan hydrogel for 3D bioprinting. *RSC Adv.* **2016**, *6* (110), 108423–108430.
- (260) Wang, X.; Ao, Q.; Tian, X.; Fan, J.; Tong, H.; Hou, W.; Bai, S. Gelatin-based hydrogels for organ 3D bioprinting. *Polymers* **2017**, *9* (9), 401.
- (261) Song, K.; Compaan, A. M.; Chai, W.; Huang, Y. Injectable Gelatin Microgel-Based Composite Ink for 3D Bioprinting in Air. *ACS Appl. Mater. Interfaces* **2020**, *12* (20), 22453–22466.
- (262) Maitra, J.; Shukla, V. K. Crosslinking in hydrogels—a review. *Am. J. Polym. Sci.* **2014**, *4* (2), 25–31.
- (263) Bhattacharya, A.; Rawlins, J. W.; Ray, P. *Polimer Grafting and Crosslinking*; John Wiley & Sons, 2009.
- (264) Hoffman, A. S. Hydrogels for biomedical applications. *Adv. Drug Delivery Rev.* **2012**, *64*, 18–23.
- (265) Song, F.; Zhang, L. M. Gelation modification of soy protein isolate by a naturally occurring cross-linking agent and its potential biomedical application. *Ind. Eng. Chem. Res.* **2009**, *48* (15), 7077–7083.
- (266) Tacias-Pascacio, V. G.; García-Parra, E.; Vela-Gutiérrez, G.; Virgen-Ortiz, J. J.; Berenguer-Murcia, A.; Alcántara, A. R.; Fernandez-Lafuente, R. Genipin as an emergent tool in the design of biocatalysts: mechanism of reaction and applications. *Catalysts* **2019**, *9* (12), 1035.
- (267) Wei, J.; Wang, B.; Li, Z.; Wu, Z.; Zhang, M.; Sheng, N.; Liang, Q.; Wang, H.; Chen, S. A 3D-printable TEMPO-oxidized bacterial cellulose/alginate hydrogel with enhanced stability via nanoclay incorporation. *Carbohydr. Polym.* **2020**, *238*, 116207.
- (268) Park, S. J.; Lee, J. E.; Park, J. H.; Lee, N. K.; Lyu, M. Y.; Park, K.; Koo, M. S.; Cho, S. H.; Son, Y.; Park, S. H. Enhanced solubility of the support in an FDM-based 3D printed structure using hydrogen peroxide under ultrasonication. *Adv. Mater. Sci. Eng.* **2018**, *2018*, 3018761.
- (269) Du, Z.; Li, N.; Hua, Y.; Shi, Y.; Bao, C.; Zhang, H.; Yang, Y.; Lin, Q.; Zhu, L. Physiological pH-dependent gelation for 3D printing based on the phase separation of gelatin and oxidized dextran. *Chem. Commun.* **2017**, *53* (97), 13023–13026.
- (270) Jiang, Y.; Zhou, J.; Shi, H.; Zhao, G.; Zhang, Q.; Feng, C.; Xu, X. Preparation of cellulose nanocrystal/oxidized dextran/gelatin (CNC/OD/GEL) hydrogels and fabrication of a CNC/OD/GEL scaffold by 3D printing. *J. Mater. Sci.* **2020**, *55* (6), 2618–2635.
- (271) Heck, T.; Faccio, G.; Richter, M.; Thöny-Meyer, L. Enzyme-catalyzed protein crosslinking. *Appl. Microbiol. Biotechnol.* **2013**, *97* (2), 461–475.
- (272) Davis, N. E.; Ding, S.; Forster, R. E.; Pinkas, D. M.; Barron, A. E. Modular enzymatically crosslinked protein polymer hydrogels for in situ gelation. *Biomaterials* **2010**, *31* (28), 7288–7297.
- (273) Rachel, N. M.; Pelletier, J. N. Biotechnological applications of transglutaminases. *Biomolecules* **2013**, *3* (4), 870–888.
- (274) Martins, I. M.; Matos, M.; Costa, R.; Silva, F.; Pascoal, A.; Estevinho, L. M.; Choupina, A. B. Transglutaminases: recent achievements and new sources. *Appl. Microbiol. Biotechnol.* **2014**, *98* (16), 6957–6964.
- (275) Petta, D.; Armiento, A. R.; Grijpma, D.; Alini, M.; Eglin, D.; D'Este, M. 3D bioprinting of a hyaluronan bioink through enzymatic and visible light-crosslinking. *Biofabrication* **2018**, *10* (4), 044104.
- (276) Reddy, N.; Yang, Y. Introduction to Chitin, Chitosan, and Alginate Fibers. In *Innovative Biofibers from Renewable Resources*; Springer: Berlin, 2015; pp 93–94.
- (277) Chen, N.; Zhao, M.; Chassenieux, C.; Nicolai, T. The effect of adding NaCl on thermal aggregation and gelation of soy protein isolate. *Food Hydrocolloids* **2017**, *70*, 88–95.
- (278) Braga, A. L. M.; Azevedo, A.; Marques, M. J.; Menossi, M.; Cunha, R. L. Interactions between soy protein isolate and xanthan in heat-induced gels: The effect of salt addition. *Food Hydrocolloids* **2006**, *20* (8), 1178–1189.
- (279) Speroni, F.; Añón, M. C. Cold-set gelation of high pressure-treated soybean proteins. *Food Hydrocolloids* **2013**, *33* (1), 85–91.
- (280) Chen, N.; Chassenieux, C.; Nicolai, T. Kinetics of NaCl induced gelation of soy protein aggregates: Effects of temperature, aggregate size, and protein concentration. *Food Hydrocolloids* **2018**, *77*, 66–74.

- (281) Hu, H.; Li-Chan, E. C.; Wan, L.; Tian, M.; Pan, S. The effect of high intensity ultrasonic pre-treatment on the properties of soybean protein isolate gel induced by calcium sulfate. *Food Hydrocolloids* **2013**, *32* (2), 303–311.
- (282) Wang, X.; Luo, K.; Liu, S.; Adhikari, B.; Chen, J. Improvement of gelation properties of soy protein isolate emulsion induced by calcium cooperated with magnesium. *J. Food Eng.* **2019**, *244*, 32–39.
- (283) Xu, Y.; Han, J.; Chai, Y.; Yuan, S.; Lin, H.; Zhang, X. Development of porous chitosan/tripolyphosphate scaffolds with tunable uncrosslinking primary amine content for bone tissue engineering. *Mater. Sci. Eng., C* **2018**, *85*, 182–190.
- (284) Abouzeid, R. E.; Khiari, R.; Salama, A.; Diab, M.; Beneventi, D.; Dufresne, A. In situ mineralization of nano-hydroxyapatite on bifunctional cellulose nanofiber/polyvinyl alcohol/sodium alginate hydrogel using 3D printing. *Int. J. Biol. Macromol.* **2020**, *160*, 538.
- (285) Gutierrez, E.; Burdiles, P. A.; Quero, F.; Palma, P.; Olate-Moya, F.; Palza, H. 3D Printing of Antimicrobial Alginate/Bacterial-Cellulose Composite Hydrogels by Incorporating Copper Nanostructures. *ACS Biomater. Sci. Eng.* **2019**, *5* (11), 6290–6299.
- (286) Fischetti, T.; Celikkin, N.; Contessi Negrini, N.; Farè, S.; Swieszkowski, W. Tripolyphosphate-Crosslinked Chitosan/Gelatin Biocomposite Ink for 3D Printing of Uniaxial Scaffolds. *Front. Bioeng. Biotechnol.* **2020**, *8*, 400.
- (287) Shahbazi, M.; Majzoobi, M.; Farahnaky, A. Physical modification of starch by high-pressure homogenization for improving functional properties of κ -carrageenan/starch blend film. *Food Hydrocolloids* **2018**, *85*, 204–214.
- (288) Shahbazi, M.; Majzoobi, M.; Farahnaky, A. Impact of shear force on functional properties of native starch and resulting gel and film. *J. Food Eng.* **2018**, *223*, 10–21.
- (289) Lam, C. X. F.; Mo, X. M.; Teoh, S. H.; Hutmacher, D. W. Scaffold development using 3D printing with a starch-based polymer. *Mater. Sci. Eng., C* **2002**, *20* (1–2), 49–56.
- (290) Shin, S.; Kwak, H.; Hyun, J. Melanin nanoparticle-incorporated silk fibroin hydrogels for the enhancement of printing resolution in 3d-projection stereolithography of poly (ethylene glycol)-tetraacrylate bio-ink. *ACS Appl. Mater. Interfaces* **2018**, *10* (28), 23573–23582.
- (291) Fan, D.; Stauffer, U.; Accardo, A. Engineered 3D Polymer and Hydrogel Microenvironments for Cell Culture Applications. *Bioengineering* **2019**, *6* (4), 113.
- (292) Bozuyuk, U.; Yasa, O.; Yasa, I. C.; Ceylan, H.; Kizilel, S.; Sitti, M. Light-triggered drug release from 3D-printed magnetic chitosan microswimmers. *ACS Nano* **2018**, *12* (9), 9617–9625.
- (293) Qi, D.; Wu, S.; Kuss, M. A.; Shi, W.; Chung, S.; Deegan, P. T.; Kamenskiy, A.; He, Y.; Duan, B. Mechanically robust cryogels with injectability and bioprinting supportability for adipose tissue engineering. *Acta Biomater.* **2018**, *74*, 131–142.
- (294) Burdick, J. A.; Chung, C.; Jia, X.; Randolph, M. A.; Langer, R. Controlled degradation and mechanical behavior of photopolymerized hyaluronic acid networks. *Biomacromolecules* **2005**, *6* (1), 386–391.
- (295) Shahbazi, M.; Rajabzadeh, G.; Sotoodeh, S. Functional characteristics, wettability properties and cytotoxic effect of starch film incorporated with multi-walled and hydroxylated multi-walled carbon nanotubes. *Int. J. Biol. Macromol.* **2017**, *104*, 597–605.
- (296) Olate-Moya, F.; Arens, L.; Wilhelm, M.; Mateos-Timoneda, M. A.; Engel, E.; Palza, H. Chondroinductive alginate-based hydrogels having graphene oxide for 3D printed scaffold fabrication. *ACS Appl. Mater. Interfaces* **2020**, *12* (4), 4343–4357.
- (297) Li, L.; Qin, S.; Peng, J.; Chen, A.; Nie, Y.; Liu, T.; Song, K. Engineering gelatin-based alginate/carbon nanotubes blend bioink for direct 3D printing of vessel constructs. *Int. J. Biol. Macromol.* **2020**, *145*, 262–271.
- (298) Urruela-Barríos, R.; Ramírez-Cedillo, E.; Díaz de León, A.; Alvarez, A. J.; Ortega-Lara, W. Alginate/Gelatin Hydrogels Reinforced with TiO₂ and β -TCP Fabricated by Microextrusion-based Printing for Tissue Regeneration. *Polymers* **2019**, *11* (3), 457.
- (299) Siqueira, G.; Kokkinis, D.; Libanori, R.; Hausmann, M. K.; Gladman, A. S.; Neels, A.; Tingaut, P.; Zimmermann, T.; Lewis, J. A.; Studart, A. R. Cellulose nanocrystal inks for 3D printing of textured cellular architectures. *Adv. Funct. Mater.* **2017**, *27* (12), 1604619.
- (300) Ghorbani, M.; Roshangar, L.; Soleimani Rad, J. Development of reinforced chitosan/pectin scaffold by using the cellulose nanocrystals as nanofillers: An injectable hydrogel for tissue engineering. *Eur. Polym. J.* **2020**, *130*, 109697.
- (301) Sultan, S.; Siqueira, G.; Zimmermann, T.; Mathew, A. P. 3D printing of nano-cellulosic biomaterials for medical applications. *Current Opinion in Biomedical Engineering* **2017**, *2*, 29–34.
- (302) Markstedt, K.; Mantas, A.; Tournier, I.; Martínez Ávila, H.; Hägg, D.; Gatenholm, P. 3D bioprinting human chondrocytes with nanocellulose–alginate bioink for cartilage tissue engineering applications. *Biomacromolecules* **2015**, *16* (5), 1489–1496.
- (303) Leppiniemi, J.; Lahtinen, P.; Paajanen, A.; Mahlberg, R.; Metsä-Kortelainen, S.; Pinomaa, T.; Pajari, H.; Vikholm-Lundin, I.; Pursula, P.; Hytönen, V. P. 3D-printable bioactivated nanocellulose–alginate hydrogels. *ACS Appl. Mater. Interfaces* **2017**, *9* (26), 21959–21970.
- (304) Yu, D. G.; Branford-White, C.; Ma, Z. H.; Zhu, L. M.; Li, X. Y.; Yang, X. L. Novel drug delivery devices for providing linear release profiles fabricated by 3DP. *Int. J. Pharm.* **2009**, *370* (1–2), 160–166.
- (305) Polamapally, P.; Cheng, Y.; Shi, X.; Manikandan, K.; Zhang, X.; Kremer, G. E.; Qin, H. 3D printing and characterization of hydroxypropyl methylcellulose and methylcellulose for biodegradable support structures. *Polymer* **2019**, *173*, 119–126.
- (306) Doi, M.; Edwards, S. F.; Edwards, S. F. *The Theory of Polymer Dynamics*; Oxford University Press, 1988; Vol. 73.
- (307) Shahbazi, M.; Rajabzadeh, G.; Rafe, A.; Ettelaie, R.; Ahmadi, S. J. Physico-mechanical and structural characteristics of blend film of poly (vinyl alcohol) with biodegradable polymers as affected by disorder-to-order conformational transition. *Food Hydrocolloids* **2017**, *71*, 259–269.
- (308) Martínez-Monzó, J.; Cárdenas, J.; García-Segovia, P. Effect of temperature on 3D printing of commercial potato puree. *Food Biophysics* **2019**, *14* (3), 225–234.
- (309) Teng, X.; Zhang, M.; Bhandri, B. 3D printing of Cordyceps flower powder. *J. Food Process Eng.* **2019**, *42* (6), e13179.
- (310) Mantihal, S.; Prakash, S.; Bhandari, B. Textural modification of 3D printed dark chocolate by varying internal infill structure. *Food Res. Int.* **2019**, *121*, 648–657.
- (311) M'barki, A.; Bocquet, L.; Stevenson, A. Linking rheology and printability for dense and strong ceramics by direct ink writing. *Sci. Rep.* **2017**, *7* (1), 6017.
- (312) Datta, S. S.; Gerrard, D. D.; Rhodes, T. S.; Mason, T. G.; Weitz, D. A. Rheology of attractive emulsions. *Phys. Rev. E* **2011**, *84* (4), 041404.
- (313) Torquato, S.; Truskett, T. M.; Debenedetti, P. G. Is random close packing of spheres well defined? *Phys. Rev. Lett.* **2000**, *84* (10), 2064.
- (314) Majzoobi, M.; Shahbazi, M.; Farahnaky, A.; Rezvani, E.; Schleining, G. Effects of high pressure homogenization on the physicochemical properties of corn starch. *InsideFood Symposium* **2013**, 33–35.
- (315) Sparrow, N. FDA tackles opportunities, challenges of 3D-printed medical devices. *Plastics Today: Medicine* **2014**.
- (316) Ng, W. L.; Wang, S.; Yeong, W. Y.; Naing, M. W. Skin bioprinting: impending reality or fantasy? *Trends Biotechnol.* **2016**, *34* (9), 689–699.
- (317) Wang, S.; Lee, J. M.; Yeong, W. Y. Smart hydrogels for 3D bioprinting. *International Journal of Bioprinting* **2015**, *1* (1), 3–14.
- (318) Koch, L.; Deiwick, A.; Schlie, S.; Michael, S.; Gruene, M.; Coger, V.; Zychlinski, D.; Schambach, A.; Reimers, K.; Vogt, P. M.; Chichkov, B. Skin tissue generation by laser cell printing. *Biotechnol. Bioeng.* **2012**, *109* (7), 1855–1863.
- (319) Kim, B. S.; Gao, G.; Kim, J. Y.; Cho, D. W. 3D cell printing of perfusable vascularized human skin equivalent composed of epidermis, dermis, and hypodermis for better structural recapitulation of native skin. *Adv. Healthcare Mater.* **2019**, *8* (7), 1801019.
- (320) Sarker, M.; Chen, X. B. Modeling the flow behavior and flow rate of medium viscosity alginate for scaffold fabrication with a three-

dimensional bioplotter. *Journal of Manufacturing Science and Engineering* **2017**, DOI: [10.1115/1.4036226](https://doi.org/10.1115/1.4036226).

(321) Kraut, G.; Yenchsky, L.; Prieto, F.; Tovar, G. E.; Southan, A. Influence of shear-thinning and material flow on robotic dispensing of poly (ethylene glycol) diacrylate/poloxamer 407 hydrogels. *J. Appl. Polym. Sci.* **2017**, *134* (29), 45083.

(322) Melchels, F. P.; Domingos, M. A.; Klein, T. J.; Malda, J.; Bartolo, P. J.; Huttmacher, D. W. Additive manufacturing of tissues and organs. *Prog. Polym. Sci.* **2012**, *37* (8), 1079–1104.

(323) Gaylo, C. M.; Pryor, T. J.; Fairweather, J. A.; Weitzel, D. E. U.S. Patent No. US7,027,887, 2006.

(324) Martelli, N.; Serrano, C.; van den Brink, H.; Pineau, J.; Prognon, P.; Borget, I.; El Batti, S. Advantages and disadvantages of 3-dimensional printing in surgery: a systematic review. *Surgery* **2016**, *159* (6), 1485–1500.